universität wien

DISSERTATION

Titel der Dissertation

„Synthesis of potentially bioactive compounds and tools for biological studies“

Verfasserin

Federica Cappa

angestrebter akademischer Grad

Doktorin der Naturwissenschaften (Dr. rer. nat.)

Wien, 2014

Studienkennzahl lt. Studienblatt:	A 791 419
Dissertationsgebiet lt. Studienblatt:	Chemie
Betreuer:	Univ.-Prof. Mag. Dr. Walther Schmid

...Ai mie genitori, Silvia e Roberto.

Acknowledgements

This project has been supported by the University of Vienna and the multidisciplinary graduate training program (Initiativkolleg, IK) "Functional Molecules".

First of all, I would like to thank my supervisor, Univ.-Prof. Dr. Walther Schmid for having believed in me and therefore given me the opportunity to work in his group and as well the opportunity to expand and improve my knowledge about a really fascinating field of study, bio-organic chemistry.

I would like to thank my colleagues in the AG-Schmid, Tina Nowikow, Michael Fischer, Christoph Schmölzer, Christopher Albler, Manuel Gintner and in particular Roman Lichtenecker, for their help, for the interesting chemical discussions and in general for providing a nice working atmosphere.

I want to thank Gerlinde Benesch for always running to "save us" with our technical problems in the lab and for guiding me through the Austrian bureaucracy.

I also would like to thank Ass.-Prof. Hanspeter Kählig and Susanne Felsinger for the help given to me with NMR measurements.

Special Thanks go to Bettina Riedl to have spent a super funny year with me in the lab also thanks to her baking skills.

Particular thanks go to Ingrid Malene Apeland for being an important friend and for having shared with me almost every working and non-working day, every good and bad moment, during my studies. Thank you for all the crazy moments we had together.

Last, but definitely not least important, I want to thank my family and my parents for all the support they gave me. Without them being so amazing I am sure I would not have achieved so much in my life!

Abstract

NMR spectroscopy is one of the most versatile tools for studying structural parameters of organic and bioorganic compounds. It became a highly suitable method to achieve spectra simplification of macromolecules in combination with isotope labeling techniques. This technique is used to study protein structures, folding properties and mechanisms of chemical and biochemical reactions.

Proteins typically feature a high molecular mass showing a high number of spin systems, being responsible for increasingly difficult to interpret NMR spectra, which is why it is essential to introduce ^{13}C- and ^{15}N- isotopes to obtain reasonable signal intensities.

The development of a new synthetic route towards ^{13}C-isotope labeled Phenylalanine or precursors thereof, starting from inexpensive and easily accessible labeled starting materials, is the main purpose of this work. Label sources such as [^{13}C]-acetic acid, [^{13}C]-formaldehyde, [^{13}C]-allyl alcohol and [^{13}C]-glycine will be used. The synthetic pathway will be carried out in a way where the position-selective incorporation of labeled isotopes can be performed. This important feature of the synthesis may open access towards newly designed NMR-experiments.

Key steps for the tested route are ring closing metatheses as well as indium mediated reactions.

The second part of this work focuses on the field of sugar chemistry, in particular on the family of deoxy sugars, components of many natural products, found in different plants, fungi and bacteria. Deoxy sugars also participate in a wide range of biological processes.

Special focus is given to 3-deoxy sugars and the research of a versatile and flexible synthetic route for their preparation starting from the easily accessible D-glyceraldehyde. These sugars are found on Gram-negative bacteria where they are a key component of the lipopolysaccharides, or where they can take place in the biosynthesis of aromatic amino acids in bacteria and plants.

Being able to perform this synthesis on a preparative scale may potentially increase the specificity and biological activity of these carbohydrates and deepen the understanding of glycobiology in the research of new medicines.

Zusammenfassung

NMR-Spektroskopie gehört zu einer der vielseitigsten Methoden um Strukturen und strukturelle Parameter organischer und bioorganischer Stoffe zu untersuchen. In Kombination mit Labeling-Methoden ist sie eine äußerst geeignete Technik um NMR-Spektren von Makromolekülen zu vereinfachen. NMR-Spektroskopie wird unter anderem zur Untersuchung von Proteinen, sowie deren Falteigenschaften und chemischen und biochemischen Reaktionen benutzt.

Proteine haben typischerweise eine hohe Molekülmasse sowie eine hohe Anzahl an Spin-Systemen, die für schwer interpretierbare NMR Spektren verantwortlich sind, weshalb es notwendig ist ^{13}C- und ^{15}N- Isotope in das Molekül zu integrieren um die jeweiligen Spektren zu vereinfachen.

Die Entwicklung einer neuen synthetischen Route, ausgehend von wirtschaftlich tragbaren und einfach zugänglichen Ausgangsprodukten, hin zu ^{13}C Isotopen-markiertem Phenylalanin, ist der Hauptfokus dieser Arbeit. Zur Markierung wurden [^{13}C]-Essigsäure, [^{13}C]-Formaldehyd, [^{13}C]-Allylalkohol und [^{13}C]-Glycine verwendet. Die Synthesestrategie muss den regioselektiven Einbau von markierten Isotopen erlauben und so möglicherweise die Durchführung völlig neuer NMR-Experimente erlauben.

Schlüsselschritte der Strategie sind vor allem die Ringschluß-Metatheses sowie eine Indium-unterstützte Allylierungsmethode.

Der zweite Teil dieser Arbeit beschäftigt sich mit Kohlenhydratchemie, im speziellen mit Desoxyzuckern, Bestandteile vieler Naturprodukte. Desoxyzucker können unter anderem in Pflanzen, Pilzen und Bakterien gefunden werden und sind Bestandteil einer breiten Anzahl von biologischen Prozessen.

Besondere Beachtung wird 3-Desoxyzucker und einer vielseitigen und flexiblen Synthesestrategie für die Vorbereitung dieses Zuckers, ausgehend von D-Glyceraldehyd, zuteil. Diese Zucker sind ein Hauptbestandteil der Lipopolysaccharide in Gram-negativen Bakterien und sind ebenfalls in die Biosynthese aromatischer Aminosäuren in Bakterien und Pflanzen involviert.

Die Möglichkeit diese Synthese in einem präparativen Ausmaß durchzuführen, erlaubt es möglicherweise die Forschung in diesem Bereich zu vertiefen und zu intensivieren, sowie das Verständnis der Glycobiologie im Bereich neuer Medikamente zu erweitern.

Table of contents

List of abbreviations

DMF	dimethylformamide
DCM	dichloromethane
DMP	dimethoxypropane
Et_2O	diethyl ether
EtOAc	ethyl acetate
EtOH	ethanol
MeOH	methanol
m- CPBA	meta-chloroperbenzoic acid
PCC	pyridinium chlorochromate
PhSH	thiophenol
rt	room temperature
THF	tetrahydrofuran
t-BuSH	*tert*-butylthiol
TLC	thin layer chromatography
DIBAL	diisobutylaluminum hydride
p-TSOH	4-methylbenzenesulfonic acid
TfOH	triflic acid
TEA	triethylamine
Ac_2O	acetic anhydride
LHMDS	lithium bis(trimethylsilyl)azanide
$LiALH_4$	lithiumaluminiumhydrid
DMAP	4-dimethylaminopyridine
TMSCl	trimethylsilyl chloride
$TMSCHN_2$	trimethylsilyldiazomethane
2D	two dimentional
3D	three dimentional
PE	hexane

EE	ethyl acetate
Eq	equivalent
DDQ	2,3-Dichloro-5,6-dicyano-p-benzoquinone
CAN	cerium (IV) ammonium nitrate
Mol. Wt.	molecular weight

Part A

Towards the synthesis of specifically ^{13}C-ring labeled phenylalanine

1. Introduction and aim of the project

1.1. Aim of the project

Due to severe signal overlapping and line broadening in protein NMR spectra, caused by the high molecular mass of the examined macromolecule, structure determination of proteins proofs to be highly complex. Sophisticated and selective isotope labeling strategies for proteins with NMR-active nuclei have been developed in order to increase the number of restrains for accurate protein structure calculation, as well as to study protein dynamics and dynamic interactions (1). Specifically labeled aromatic amino acids are of special interest in this context, since they are preferentially located in hydrophobic cores and ligand binding interfaces of proteins (2). The goal of the approach, presented in this work is to lead to a variety of Phenylalanine labeling patterns, which significantly increase protein NMR spectra resolution.

The presented approach focuses on developing synthetic routes towards ^{13}C and ^{2}H isotope labeled Phenylalanine and Tyrosine or precursors thereof, which fulfill the following requirements:

- the labeled (precursor) compound should be accessible on a preparative scale,
- a broad variety of labeling patterns within the aromatic amino acids should be accessible enabling "tailor-made" experiments for structural and dynamic protein investigations (Figure 17) and
- the synthetic route should start with a limited number of labeled synthons, preferably commercially available or easily accessible, inexpensive isotope labeled starting materials.

1.2. Nuclear Magnetic Resonance as an effective tool for protein studies

Nuclear Magnetic Resonance (NMR) is one of the most effective tools for the study of macromolecules. Thermodynamic and kinetic information of the interaction between diverse molecules at the atomic level can be obtained and therefore be studied through NMR studies. NMR data additionally enables one to investigate the three-dimensional structure of proteins, protein-protein interactions, as well as interactions with DNA or RNA (3). This gave way to understand and clarify the inhibitor or activation mechanisms of drugs in medicinal chemistry (4). The determination of NMR protein spectra is based on the application of diverse NMR experiments which allow studying different parameters. Fundamental parameters studied by NMR techniques are the chemical shift and the relaxation time. The chemical shift provides information about the chemical surrounding of the studied nucleus and therefore the bonds of such a nucleus with its neighboring atoms can be understood. The *relaxation time* instead regulates the relaxation process. Two major relaxation mechanisms are known: *spin-lattice* (T_1) and *spin-spin* relaxation (T_2). *T* indicates the relaxation time which can be of two kinds: T_1 expresses the *longitudinal relaxation time,* stating how fast the magnetization relaxes back along the z-axis, and T_2, the *transversal relaxation time,* which measures how fast the spin exchanges energy in the x-y-plane (Figure 1) (5).

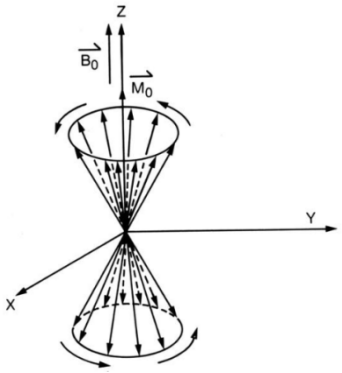

Figure 1: Orientation and precession of nuclear spins (I = 1/2) at thermal equilibrium (5).

By combining the values of the relaxation times and the chemical shifts, the interaction of a protein with other molecules can be studied. NMR measurements can be used not only to better understand the structure of proteins but can also help to investigate protein´s folding (6).

NMR experiments also allow the estimation of interatomic distances (7). Two phenomena play an important role in this case: *scalar coupling* and the *nuclear Overhauser effect* (NOE). *Scalar coupling* occurs between nuclear spins and leads to the splitting of spectral lines. This is an important phenomenon as it provides information about the distances between nuclei. The *nuclear Overhauser effect* (NOE) instead enables the measurements of internuclear distances based on the prediction that nuclear polarization depends on the spin state of nearby (in space) unpaired electrons or nuclei. If the distance is close enough, usually less than 5 Á, magnetization between the nuclei is transferred through space resulting in a signal intensity change (8) (9). The NOE not only provides important information about the three dimensional structure of a protein but also about the assignment of amino acids (10) (11). An example of possible NOE between amino acids is shown in (Figure 2).

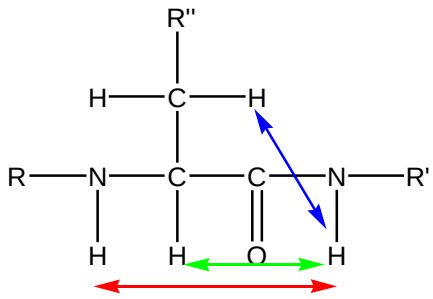

Figure 2: Example of NOE of two neighboring amino acids.

Performing bond correlating experiments provides information about the J-coupling constants, which further helps to better understand the orientation of the protein backbones. The amino group of an amino acid bonded, by the peptide bond, to the carboxyl group of the preceding amino acid can be visualized as a plane that can rotate at the Cα-position. The same applies to the carboxyl group of the given amino acid and its bond to the amino group of the subsequent amino acid. Additionally the peptide bond can take two different angles, depending on its configuration. Due to the previously

described planar form, the peptide bonds' angles are restricted to 0° and 180°, depending on whether the peptide has a *cis*- or a *trans*-configuration. These three rotational angles, as can be seen in Figure 3, are identified as ω, Φ and Ψ and are important for the understanding of the backbone-atoms rotation of the Cα-C, C-N´ and N´-Cα-bonds (12).

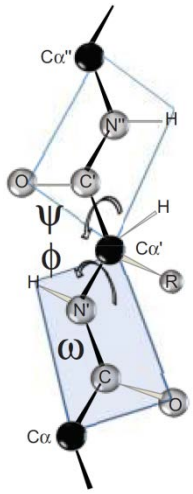

Figure 3: ω, φ and ψ backbone dihedral angles (12).

Investigations of a protein's function require foremost an understanding of the three-dimensional (3D) structure of a protein. The two main techniques used for this purpose are X-ray crystallography and Nuclear Magnetic Resonance spectroscopy, which both provide information at the atomic level. X-ray crystallography is a powerful tool for the determination of the crystal structure of a protein, it however has the disadvantage that obtaining crystals from proteins may present difficulties since in most cases obtaining crystals from proteins requires the introduction of a suitable heavy-atom derivative in order to determine reflections with good resolution (13) (14). Therefore spectroscopic methods are preferred in this case although the combination of both of the described methods gives an optimal overview of the results. The cumulated data obtained can then be analyzed to produce the structural model of the examined macromolecule as the below Figure 4 shows.

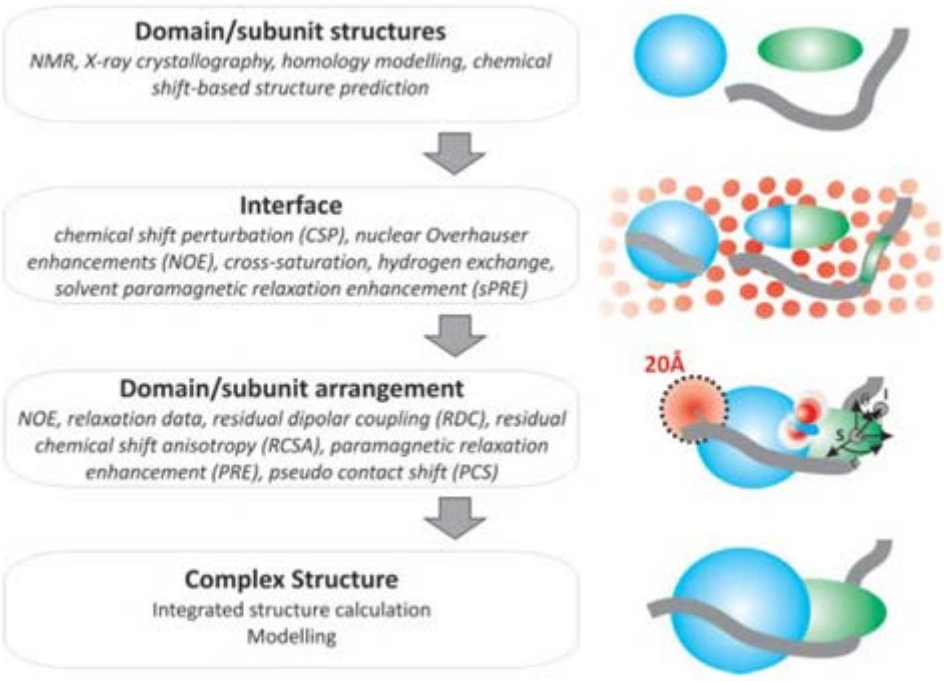

Figure 4: Steps for the development of a complete structure of a protein starting from the three-dimensional structure (7).

In order to obtain a high-resolution 3D image of the structure, further refining steps have to be carried out. These involve gathering of residual dipolar coupling, diffusion anisotropy as well as conformational database potential data (15).

Structure determination of large molecules through NMR spectroscopy has been difficult due to overcrowded spectral regions. Proteins typically have a high molecular mass, which is responsible for increasingly difficult to interpret NMR spectra., representing the major limitation of NMR spectroscopy.

A common approach to prevent these problems is to label proteins in order to simplify the spectra in combination with multidimensional and triple-resonance techniques that allow the distribution of signals in three-dimensional space, therefore avoiding the problem of overlapping peaks (16). These proteins are commonly enriched with ^{13}C or ^{15}N due to the fact that not all isotopes have NMR active spin. Isotopes such as ^{2}H, ^{13}C, ^{15}N or ^{31}P do have magnetic spins but others like ^{12}C or ^{16}O do not present any activity in NMR spectroscopy (17).

NMR spectroscopy relies on the density of NMR-active nuclei. The isotope's natural abundance determines the signal intensity. ^{2}H, ^{13}C or ^{15}N are the used isotopes in protein

NMR spectroscopy due to their low sensitivity, due to the small gyromagnetic ratio values and the low natural abundance, as reported in Table 1.

Table 1 shows the above mentioned NMR-active nuclei as well as the natural abundance.

nucleus	I_n	γ [10^7 rad $T^{-1}s^{-1}$]	$\gamma_{rel.}$	$S_{abs.}$	nat. abd. (%)
^{1}H	½	26.75	1	1	99.99
^{2}H	1	4.11	0.15	0.00000145	0.01
^{13}C	½	6.73	0.25	0.000176	1.07
^{19}F	½	25.18	1	0.83	100
^{15}N	½	-2.71	0.1	0.00000385	0.37
^{31}P	½	10.84	0.41	0.0663	100

Table 1: Spin quantum numbers (I_N), gyromagnetic ratios (γ and $\gamma_{rel.}$), natural abundances (nat.abd.) and absolute sensitivity ($S_{abs.}$) for some NMR active nuclei and deuterium (18). $S_{abs.}$ is given by the product of the sensitivity at a constant magnetic field (equal number of nuclei) with the natural abundance (19).

Structure determination, performed by NMR, breaks down into four main steps: carrying out the sequential resonance assignment, the determination of the torsion angles, identification of the through-space connectivities between protons separated by less than 5 Å and the calculation of the 3D structure based on the NMR restrains data (15).

In the early 1980s important improvements in the 2D NMR technique enabled new possibilities in the determination of a great number of small proteins (20). Nowadays, with new developments in NMR labeling strategies, the structure of bigger macromolecules can be determined. As reported in literature, the upper limit of applicable amounts went from 60-70 kDa to far beyond 100 kDa (13) (21) (22).

1.2.1. Uniform and Selective labeling strategies

Two forms of labeling can be distinguished:

- *Uniform labeling*, in which a specific isotope is chosen to label the whole structure and
- *Selective labeling*, in which the desired isotopes are introduced selectively in precise positions with the purpose to investigate these positions or possible transformations of the examined structure.

An example of uniform labeling is growing bacteria for expression in a medium containing ^{13}C-glucose, $^{15}NH_4Cl$ or ^{15}N-glutamic acid as well as a carbon or nitrogen, as a source of label. The isotopes enrichment obtainable by this method can be up to 98% (23) (24). This technique shows all the possible peaks with enhanced intensity and all the possible couplings. As a result of this process the protein will be uniformly labeled. The NMR-active isotopes can be found in protein backbones and in the side chains of the simple amino acids.

Selective labeling, on the other hand, is commonly used to study biochemical or enzymological pathways due to its advantage of choosing which positions are visible in a spectrum. As a consequence, disturbing coupling effects can be avoided (24). Selective labeling allows introducing the mentioned NMR-active nuclei into one or more amino acids in specific positions. These amino acids are then introduced into a protein by growing the host bacteria in a medium containing the labeled amino acid.

1.2.2. Protein isotope labeling: incorporation of labeled amino acids

The cell-based approach and the cell-free expression technique are two common methods for introducing labeled isotopes into proteins without modifying their structure.

The cell-based approach is an overexpression method where corresponding isotopes are contained in an amino acid precursor which is usually used as carbon or nitrogen source. These precursors are then used for the synthesis of the amino acids and are subsequently introduced into the overexpression system for the incorporation into the protein. For that, two different cell types may be used, eukaryotic and prokaryotic cells. The choice of cell type used for the incorporation is based on three main parameters: the structure complexity of the protein, the amount of protein needed and the type of cell which can overexpress the gene that encodes the desired protein (25).

Cell-based expression has the advantage that bigger amounts of protein can be produced. The disadvantages however are possibly incomplete labeling, a metabolic scrambling of label as well as purification issues (25).

The cell-free expression on the other hand is the preferred method for the expression of aromatic amino acids, for which lysates are the translation system. Produced by the destructive process of lysis, lysates are prepared by centrifugation of the crude lysates of cells. Cells commonly used for the extraction of lysates are *E.Coli* or wheat germ from which the so-called S30 fraction may be obtained, containing the protein synthetic machinery (including for example t-RNA, RNA polymerase or translation factors). In addition to the cellular extract, small molecules such as amino acids or ions are present in the system. (25).

The two possible and optimized cell-free expression techniques are the continuous flow cell-free mode (CFCF) and the continuous exchange cell-free mode (CEFC) (26).

In the CFCF mode the continuous flow of the feeding solution is introduced directly into the system while the by-product is simultaneously removed constantly, making the volume of the whole reaction constant.

The CECF mode however requires the reaction to take place on two different reaction sites. An osmotic membrane separates the feeding and the reaction chamber from each other. Only small molecules (e.g. amino acids) can selectively pass through this

membrane whereas large molecules (e.g. DNA, enzymes) remain in the reaction chamber. This device ensures that fresh suppliers can pass into and inhibitory by-product may escape out of the reaction chamber through the membrane (25).

Advantages of CECF are the possibility to upscale the reaction to magnitudes of milligrams of protein as well as the possibility of avoiding cross labeling. CECF can furthermore be applied to proteins that are toxic to normal bacterial hosts and it is the most used method for the expression of membrane proteins. Non-natural amino acids may be applied as well (e.g. fluorescent labeling).

1.2.3. Synthetic methods for the introduction of isotopes into amino acids

Two strategies are known for labeling proteins, the introduction of active nuclei (which was previously described in chapter 1.2.1) and the introduction of deuterium into the amino acids.

The perdeuteration method is one of the most common ways of isotope labeling, focusing on exchanging hydrogen atoms with deuterium. The scope of this method is the reduction of ^{1}H-^{1}H NOEs that increase linearly with the molecular weight of the macromolecule. In addition, a high number of proton resonances in a fixed chemical-shift range might cause resonance-overcrowding problems resulting in difficulties in spectra interpretation (27). By incorporating deuterium nuclei in proteins, it is possible to eliminate the spectral signals of the replaced nucleus, making deuterium incorporation an important tool for protein-protein studies as well as protein ligand interaction studies. To obtain deuterated proteins, host bacteria cultures such as *E. Coli* as well as yeast or fungi are grown in D_2O. By addition of deuterium sources such as ^{2}H-glucose or ^{2}H-amino acids it is possible to achieve a high level of deuteration (<75%) (28) (29).

1.2.3.1. Aliphatic amino acids as source of label

Aliphatic amino acids such as Valin, Leucin and Isoleucine are characterized by hydrophobic side chains and they occur in the active center of proteins (30) (31). As the biosynthesis of these amino acids is stereoselective, it is possible to distinguish the two diastereotopic CH_3 groups from each other, which is an important feature in terms of protein studies. Two carbon fragments, that are themselves derived from two different units of pyruvate, form an isopropyl group. Pro-S and Pro-R are the two forms of the above mentioned CH_3 groups. Expressing the protein in media containing 10% $^{13}C6$ glucose and 90% $^{12}C6$ glucose allows to see the different coupling patterns between the neighboring atoms, making it therefore possible to distinguish between these two groups (27).

Concerning the synthetical approach, Kainosho (32) developed a new technique, called SAIL (stereo-array isotope labeling), using synthesized amino acids with deuterated methylene and methyl groups, which were subsequently used as labeling source in a cell

free expression sequence (as described in chapter 1.2.2). Methyl groups can be introduced into an amino acids as CHD_2 as an example.

Furthermore, Kay et.al. (33) (34) showed the selective protonation of Isoleucin (Ile), Leucin (Leu) and Valin (Val) residues by specific α-keto acid precursors (30). These three amino acid residues build the three essential branched-chain amino acids and sum up to approximately 21% of all residues.

1.2.3.2. Aromatic amino acids as source of label

1.2.3.2.1. Overview of biosynthesis of the aromatic amino acids

Aromatic amino acids such as L-phenylalanine, L-tryptophan and L-tyrosine are found in the hydrophobic cores and ligand binding interfaces of proteins. The shikimate pathway is the aromatic biosynthetic pathway for the synthesis of aromatic amino acids which have two precursors: phosphoenolpyruvate and erythrose 4-phospate. Phosphoenolpyruvate derives from the glycolysis pathway while the latter is derived from the pentose phosphate pathway. The shikimate pathway, starting with the two described precursors, proceeds through seven steps to chorismate via shikimate to yield the intermediate prephenate for the synthesis of the three mentioned aromatic amino acids as well as other different metabolites (35) (36).

Although studies on bacteria, such as the well-known *E.Coli,* provide the information that shikimate is the most important metabolic intermediate in this pathway, being responsible for the inhibition of the shikimate dehydrogenase, another crucial key step of the pathway is the formation of 3-deoxy-D-*arabino*-heptulosonate 7-phosphate (DAHP). DAHP is catalyzed by the three synthase related enzymes AroF, AroG and AroH and it is the only reaction in the pathway that is controlled by non-homologous enzymes (37).

Similarly important are the inhibitions of the two enzymes responsible for the production of phenylpyruvate and 4-deoxyphenylpyruvate, chorismate mutase and prephenate / cyclohexadienyl dehydratase by L-Phe and L-Tyr respectively (38).

The chemistry of the shikimate pathways is illustrated in Figure 5 in more detail. The initial condensation reaction of PEP and E4P yields DAHP which is subsequently followed by six enzymatic reaction steps yielding the intermediate branch point chorismate. An intramolecular rearrangement converts chorismate to prephenate which

may yield the two desired amino acids via another intermediate. Tyrosine might be acquired through 4-hydroxyphenylpyruvate or arogenate while phenylalanine is yielded via arogenate or phenylpyruvate, making arogenate the only intermediate through which both final amino acids can be accomplished. While Tyr can be synthesized by an enzymatic reaction from 4-hydroxyphenylpyruvate or the oxidative decarboxylation of arogenate, Phe can be obtained from dehydration and decarboxylation of arogenate as well as from phenylpyruvate by an enzymatic reaction (39).

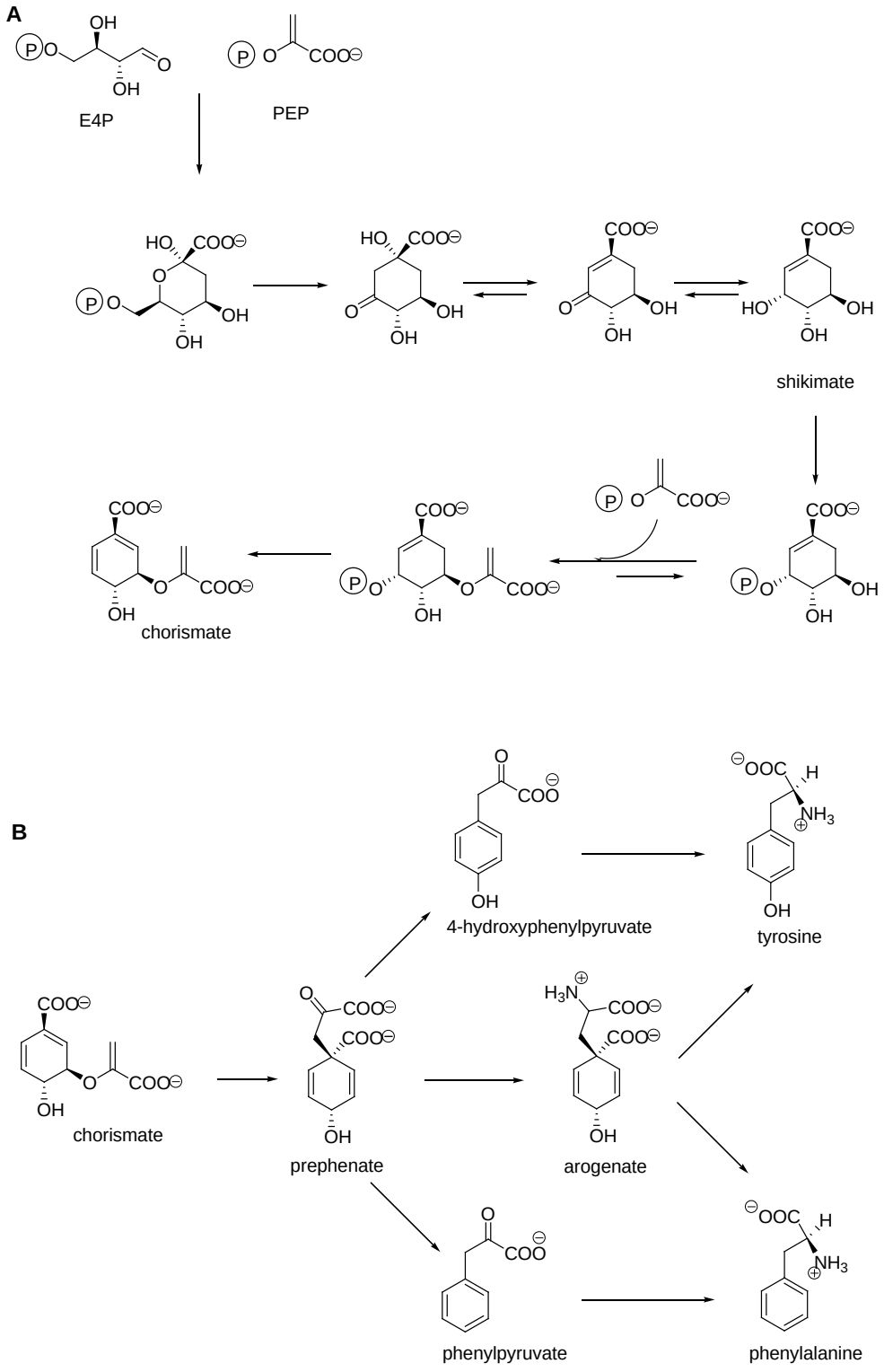

Figure 5: A) Shikimate pathway towards chorismate intermediate, B)from chorismate to the aromatic amino acids.

As the shikimate pathway occurs in fungi, bacteria and plants but not in mammals, the amino acids, called essential amino acids, produced by the pathway must be introduced into a mammals system through nutrients (human diet). One of the differences between microorganisms and plants is the regulation of the shikimate pathway, where in microorganisms the pathway is regulated by feedback inhibition and repression of the initial enzyme while in higher plants the pathway is regulated at a genetic level only (40).

1.2.3.2.2. Synthetic strategies for the preparation of aromatic amino acids

Labeling of aromatic residues is an important approach used in NMR spectroscopy particularly for molecular recognition (41) (42). Different positions of an aromatic amino acid such as the aromatic moiety or the side chain may be labeled individually or as a whole.

Wand et.al. (43) presented labeling strategies for aromatic side chains in Calmodulin in a recent publication. Calmodulin is a small regulating protein, activated by calcium. The interaction of this protein with Ca^{++} provokes an important conformational modification that converts the protein into its active form. In this form the protein can interact with different types of protein kinases (4).

Wand et.al's (43) strategy aims to perform a new synthetic route for the production of predeuterated proteins containing isolated ^{1}H-^{13}C pairs. The biosynthesis, shown in Figure 6, starts with a condensation reaction of erythrose 4-phosphate and phosphoenolpyruvate.

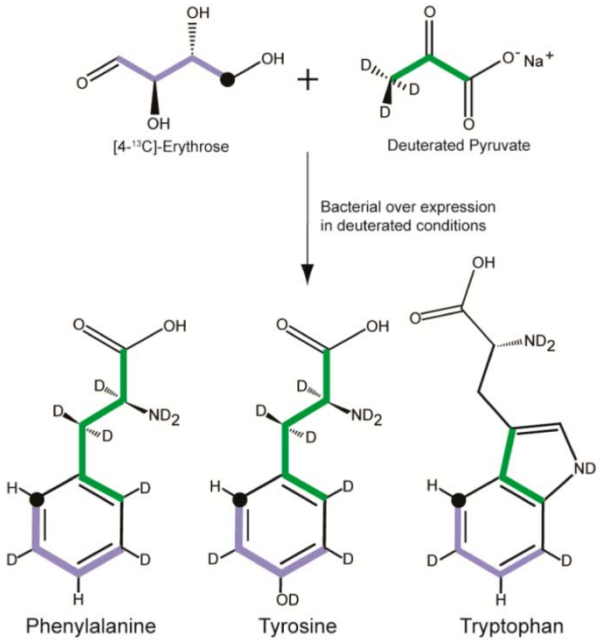

Figure 6: Aromatic pathways of labeled aromatic side chains (43).

Synthetic approaches for the synthesis of aromatic amino acids and their precursors with ^{13}C- or ^{14}C-labeled patterns aim to perform short and powerful routes in which the labeling sources are preferably inexpensive and easily available.

Another method towards the synthesis of labeled phenylalanine and its aromatic precursors is shown in Figure 7. This synthesis allows the incorporation of labeled patterns in specific positions in the molecule. The key reaction step is the ring-closure of compound **4c** (44).

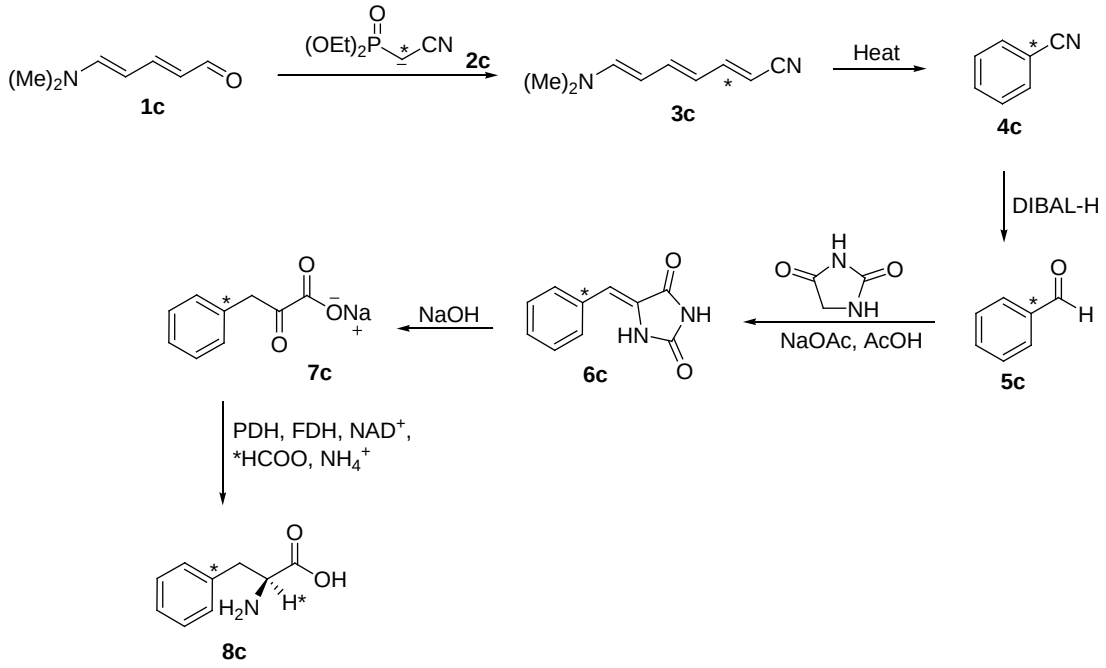

Figure 7: Synthesis of L-[1-^{13}C] phenylalanine (44). With * the possible ^{13}C positions are indicated.

The synthesis starts with labeled [2-^{13}C] acetonitrile, representing the first source of label. This precursor is further treated to obtain the labeled anion **2c**. Reaction of **2c** with 5-(dimethylamino)pentadienal **1c** yields the labeled intermediate **3c**, which easily generates the desired aromatic ring in form of benzonitrile **4c**, in which the label ^{13}C shows at position C1 of the ring. A DIBAL reduction yields the [1-^{13}C] benzaldehyde **5c**, used as aromatic precursor for the reaction to introduce the chiral labeled side chain, performed with hydantoin. Transformation of hydantoin derivative **6c** into the chiral precursor sodium phenyl pyruvate **7c**, followed by an enzymatic reaction with the commercially available L-phenylalanine dehydrogenase (E.C. 1.4.1.20) (45) and NADH as coenzyme, results in the chemically pure L-[1-^{13}C] phenyl alanine **8c**.

The synthesis towards phenylalanine shown in Figure 8 allows the introduction of ^{13}C labeled atoms in every position of the intermediate benzaldehyde **16d** on the other hand. The labeled, non-aromatic precursors are commercially available, labeled acetic acid **1d** and the triethyl phosphonoacetate **6d** however can easily be synthetized in its labeled form starting from acetic acid (44).

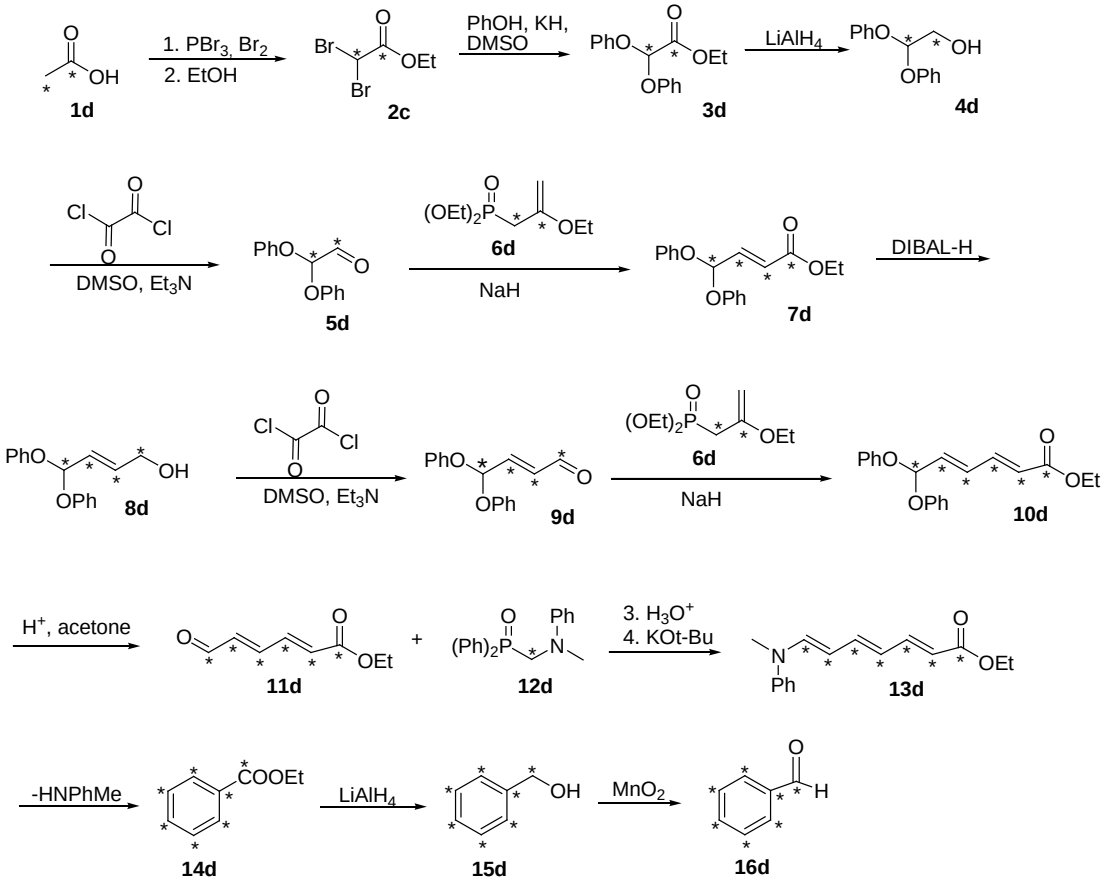

Figure 8: Synthesis of the fully ^{13}C labeled intermediate benzaldehyde (44). With * the possible ^{13}C positions are indicated.

A reaction sequence of four steps transforms the ^{13}C-acetic acid into the intermediate alcohol **4d** which, after Swern oxidation, yielded the intermediate 2,2-diphenyloxy-1-ethanal **5d**.

Reaction of **5d** with the labeled triethyl phosphonoacetate **6d** will yield ester **7d** which, after DIBAL reduction and a second Swern oxidation, is converted into compound **9d**. The coupling of aldehyde **9d** with the labeled source **6d** by a HWE-reaction, followed by acidic deprotection, gave the 5-carbethyloxy-2,4-pentadienal **11d**.

An HWE reaction of aldehyde **11d** with diphenylphosphane oxide labeled derivative **12d** yields compound **13d**. The labeled compound **12d** can be synthetized starting from paraformaldehyde, which is commercially available in its ^{13}C-labeled form.

Final cyclization of intermediate **13d**, followed by reduction and oxidation steps, resulted in the desired precursor benzaldehyde **16d**. As described in the previous synthesis (Figure

7), compound **16d** can be converted via enzymatic reaction into the L-[*ring*-^{13}C] phenylalanine (45).

Another alternative method for the synthesis of phenylalanine is shown in Figure 9. A carboxylation reaction performed with ^{13}C-carbon monoxide and bromobenzene followed by reduction and bromination reactions, yield the intermediate labeled benzyl bromide **3j**, on which the labeled source is introduced in Cα position. Further treatment with oxazinone **5j** gives access to the introduction of the chiral center. Oxazinone was prepared from (S)-2-phenylglycinol and phenyl bromoacetate. Acidic deprotection and cleavage of the C-N bond at the benzyl position of compound **7j** yields the L-[3-^{13}C] phenylalanine ethyl ester **8j**, which can be converted into the desired amino acid (46).

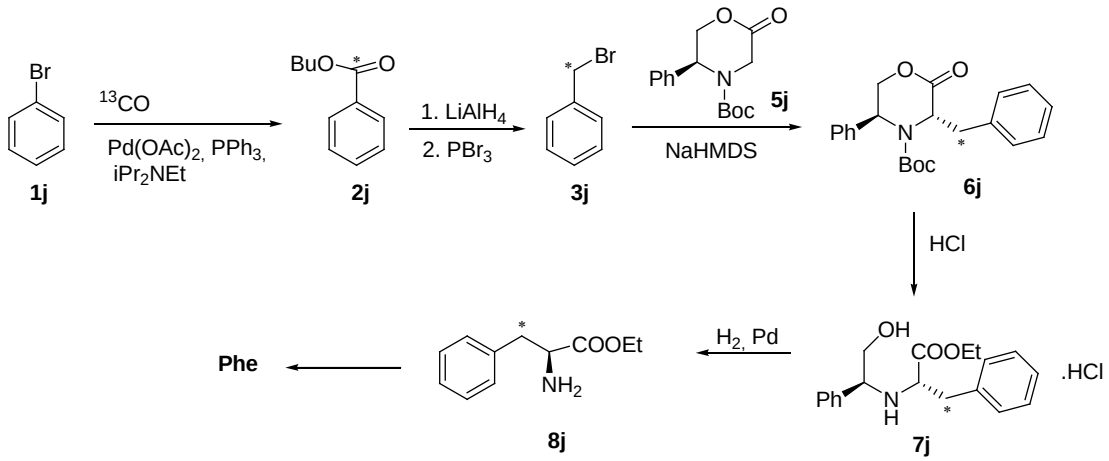

Figure 9: Asymmetric synthesis of L-[3-^{13}C] phenylalanine from ^{13}C-carbon monoxide (46). With * the possible 13C positions are indicated.

1.3. Background theory for the key steps of the synthesis

1.3.1. Synthetic approaches towards $^{14}C/^{13}C$ labeled arenes starting from non-aromatic precursors

Different methods are described in literature for the preparation of labeled aromatic rings. Early attempts were based on Grignard reactions. Figure 15 shows the preparation of labeled toluene and benzoic acid.

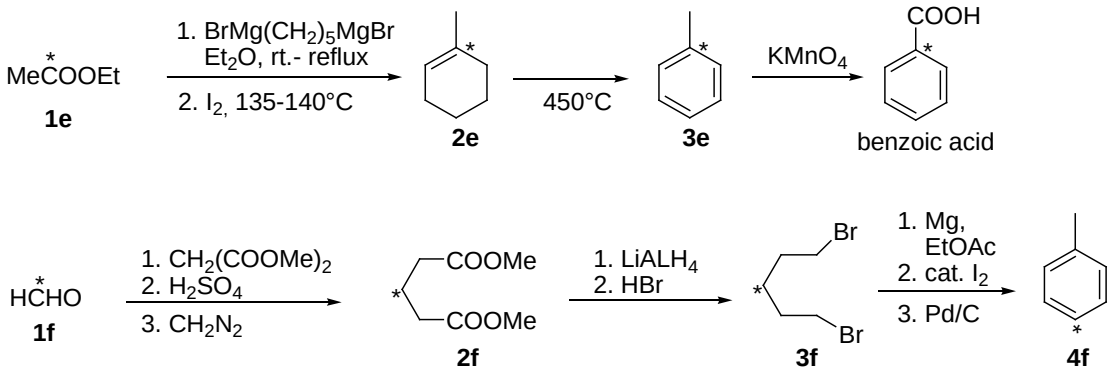

Figure 10: Synthesis of [1-^{14}C] and [4-^{13}C] toluene (50) (47) .* indicates the position of the heavy atom introduced.

The first reaction depicted above starts from [1-^{14}C] acetate **1e**, which reacts with the Grignard reagent prepared from pentamethylene dibromide. Further transformation yields the intermediate [1-^{14}C]-1-methylcyclohexene **2e**. The subsequent dehydrogenation, performed with Pt or Pd at high temperature, yields the [1-^{14}C] toluene **3e**, which is the desired aromatic precursor (48) (49). Further treatment with $KMnO_4$ makes the benzoic acid affordable.

In the second approach the 1,5-dibromopentane **3f** can be prepared in its [3-^{13}C]-labeled form, starting from [^{13}C] formaldehyde **1f**. Further steps make the [4-^{13}C] toluene **4f** accessible. This route gives the possibility to introduce the carbon isotope in different positions in the ring by varying the label position in the starting material (47).

Aromatization of cyclohexene derivatives to obtain the aromatic precursor does not give satisfying results, due to low yields and isotopic scrambling. Different labeled alkylbenzenes can be obtained by variation of the labeled precursors (47).

Table 2 shows different reaction pathways.

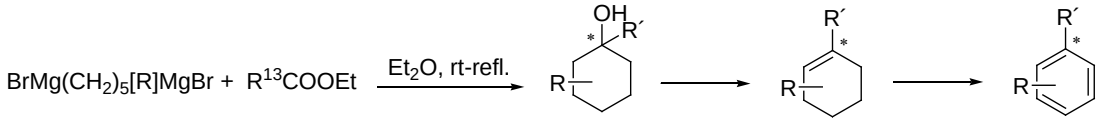

R	R´	Dehydration conditions	Dehydrogenation conditions
H	Me	---	Pt-Al_2O_3, 400°C
H	Me	cat. I_2, 140°C	Pd, maleic acid, 120°C
H	Et	---	Pt-Al_2O_3, 400°C – 450°C
H	Pr	---	Pt-Al_2O_3, 400°C – 450°C
H	Ph	cat. I_2, 140°C	DDQ, benzene, refl.
3-Me	Me	TsOH, Toluene, refl.	Pd, maleic acid, 130°C
2,4-Me_2	H	TsOH, Toluene, refl.	Pd, maleic acid, 130°C

Table 2: Different conditions for the direct formation of substituted ^{13}C-arenes (47).

The formation of labeled arenes can be approached differently by taking advantage of the self-condensation of labeled malonates and pyruvates. Figure 11 shows the synthesis of 1,3,5-trilabeled aromatic rings, obtained from 2- and 3-labeled sodium pyruvate via a cyclotrimerization, to yield the aromatic structure.

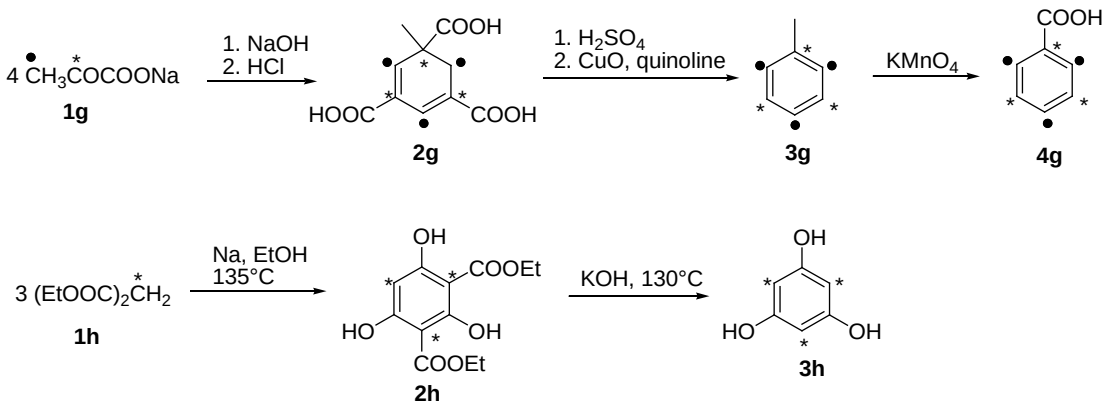

Figure 11: Synthesis of 1,3,5-trilabeled aromatic rings (47).

Sodium pyruvate can be obtained in its labeled form starting from the commercially available, labeled pyruvic acid. Treatment of ^{13}C sodium pyruvate **1g** with sodium hydroxide and hydrochloric acid, followed by a decarboxylation under acidic conditions, yields the labeled methyl-dihydro trimeric acid **2g**. Reaction with CuO and quinoline yields the desired labeled product **3g** in good yields. However, large quantities of ^{13}C-pyruvic acid are needed for the preparation of the starting material as oxalic acid is produced as a side product during the reaction (47) (50) (51). Starting from labeled diethyl malonate **1h**, a [1,3,5-^{13}C] triol derivative **3h** can be synthesized (52).

1.3.2. Ring Closing Metathesis as tool for construction of cyclic compounds

Ring Closing Metathesis (RCM) has become an important tool for the preparation of cyclic compounds. The olefin metathesis catalysts, also known as Grubbs catalysts, are one of the most interesting ruthenium complexes due to their simple handling and their high tolerance to a variety of functional groups. Although RCM is generally used for ring closing of alicyclic compounds, preparations of arenes have been reported as well (53). The synthesis of benzene derivatives has been described using ruthenium catalysts in dichloromethane (Figure 12). The catalysts are derivatives of the benzylidene complex of $RuCl_2[P(c\text{-}C_6H_{11})_3]_2$. Following the RCM, a dehydration reaction using p-TsOH yields the final aromatic ring (54).

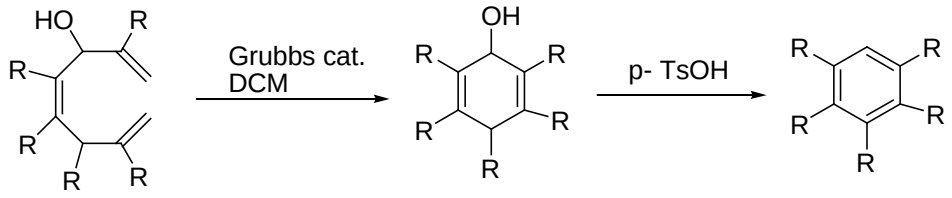

Figure 12: Synthesis of benzene derivatives by RCM (47).

While obtaining cyclohexane derivatives is comparatively simple, the achievement of the aromatic ring however often proves difficult. Preparing triene as starting material would

be ideal, as it could be subject to ring closing, in which case the double bonds would already be contained in the primary structure (47).

A different approach is shown in Figure 13, where a 4-methylene-1,7-octadien-3-ones **1i** has been used for RCM. The advantage of this compound is, that it contains an external C-C double bond which, after ring closure, can isomerize to yield the intermediate 6-methylenecyclohex-2-enone **2i**, which contains the endocyclic double bond (47) (55).

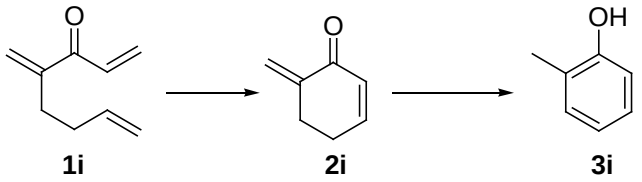

Figure 13: RCM from 4-methylene-1,7-octadien-3-ones (47).

The combination of different reaction types such as dehydration, oxidation or isoaromatization with the ring closing metathesis gives the possibility to yield a variety of aromatic structures. Promising starting materials for the preparation of labeled arenes are for example 1,3-diols, that can be prepared in their labeled form by an allylation reaction, starting from 3-hydroxycarbonyl derivatives using a labeled allylmetallic reagent (47).

2. Synthetical work

2.1. The approach

The designed route focuses on three building blocks, derivatives **A**, **B** and **C** (Figure 14). The γ,δ-unsaturated aldehyde synthon **A** (56) as well as the bromomethyl methacrylic acid derivative **B** (57) are both accessible starting from acetic acid, which is commercially available with different isotope patterns. Hydantoin **C** (58) is accessible from commercially available labelled glycine.

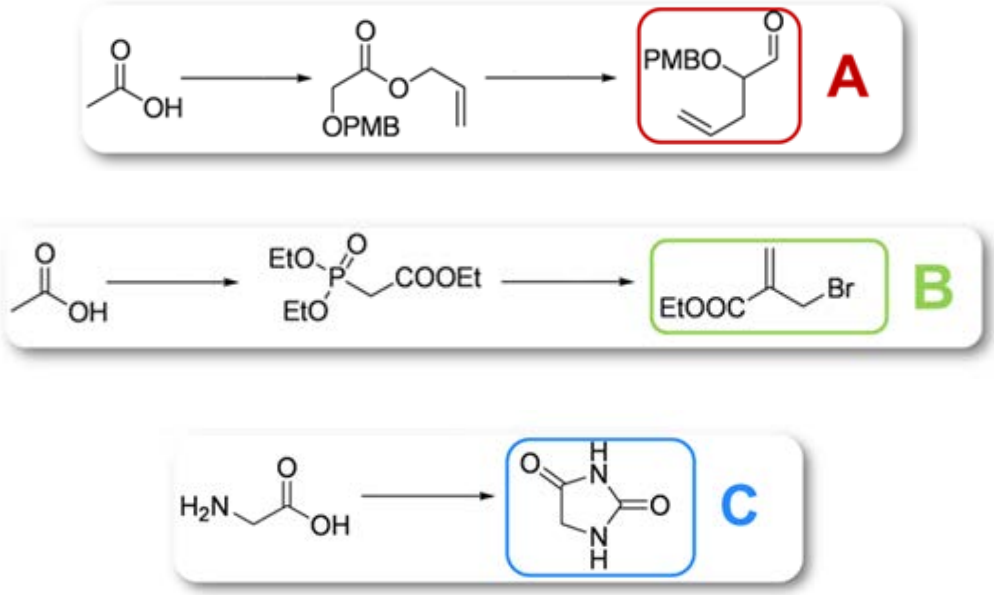

Figure 14: Building blocks derivatives.

First, a prototype reaction, used for testing the reaction sequence with special focus on the key-step reactions (RCM, In mediated elongation), was made, using D-glyceraldehyde as a starting material (Figure 15). Even though this precursor is not available in a labeled form, it is an inexpensive and solid starting point for the synthesis of the intermediates, which are themselves important in the approach for the synthesis of phenylalanine.

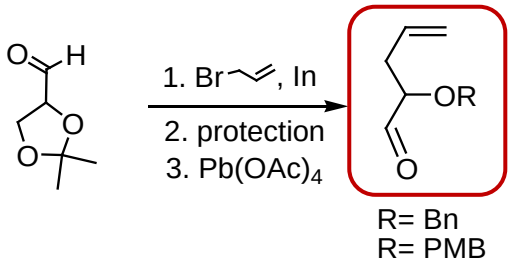

Figure 15: Building block accessible from D-glyceraldehyde.

Chain elongation with the bromomethyl methacrylic acid derivative (Figure 16) was achieved by applying the indium-mediated allylation method, generating a suitable synthon for applying a ring closing metathesis reaction using the Grubbs II catalyst (59). An elimination reaction, followed by aromatization, should make a benzoic acid derivative available, which, after reduction to benzaldehyde, is subject to the final condensation reaction with hydantoin to generate the target amino acid. The final transformation from benzoic to amino acid has been developed earlier (58).

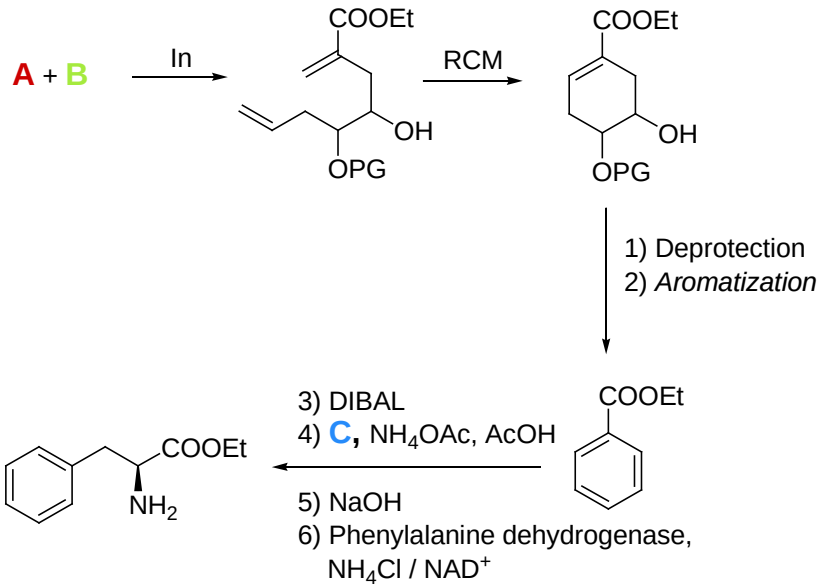

Figure 16: Reaction sequence starting from building blocks A and B.

It was assumed that a successfully carried out sequence, using a labeled source, would make the final amino acid available in a labeled form. The aim was to achieve a robust strategy, giving access to aromatic amino acids that contain ^{13}C-labels in defined positions. The synthesis of the above mentioned building blocks from simple labeled

substrates was planned to lead to a versatile route in order to generate a variety of Phe labeling patterns, tailor-made to meet the requirements of specific NMR experiments in order to study protein structure dynamics.

The further development of the synthesis allows to obtain the desired amino acid Phenylalanine, selectively labeled as shown in Figure 17, starting from different accessible labeled sources such as ethyl bromoacetate and bromoacetic acid, easily synthesizable from acetic acid.

Figure 17: ^{13}C labeling positions and corresponding sources of label.

2.2. The prototype reaction

As already mentioned in paragraph 2.1, the proof of concept reaction sequence towards phenylalanine starts with the easily accessible D-glyceraldehyde. This educt is not available in any labeled form, it may however be used as inexpensive source for the preparation of building block **A**. Once the first building block is achieved, this route, via an indium mediated elongation reaction, enables the next important step in the pathway, the introduction of building block **B**. Following this approach it is possible to investigate the reactivity of the substrates and to find the optimal reaction conditions.

The reaction sequence shown in Figure 18 has been carried out with two different protecting groups (indicated by RX), in order to investigate the stability and reactivity of the free hydroxyl group, simultaneously investigating the deprotection procedures. As protecting groups benzyl (Bn) and p-methoxybenzyl (PMB) were used.

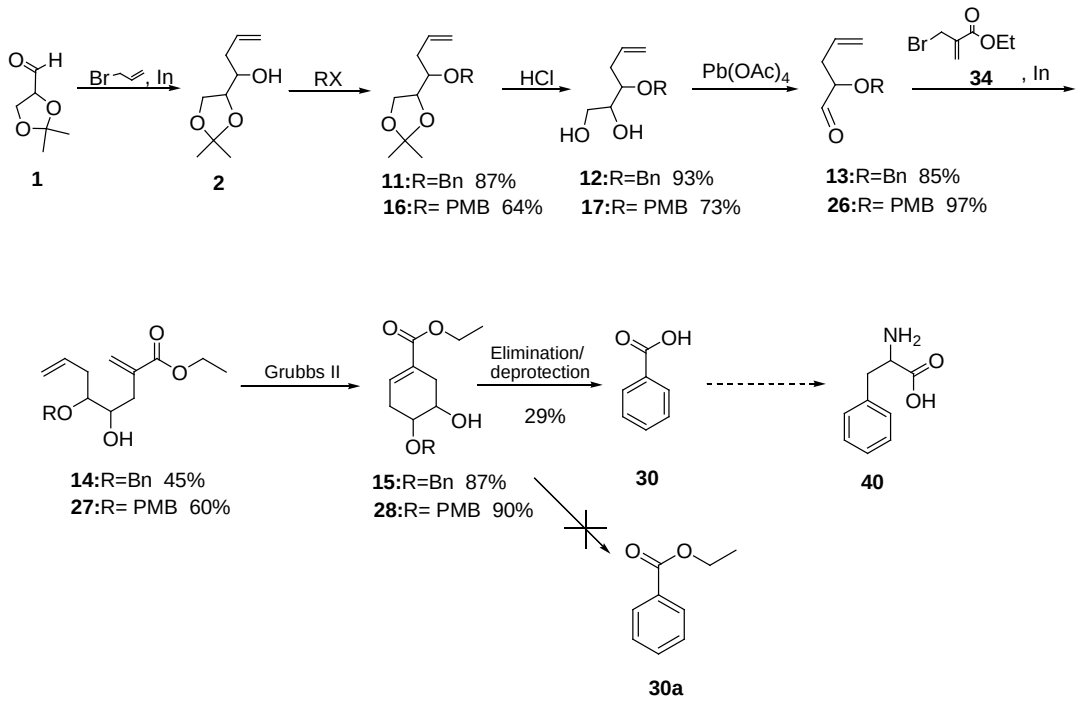

Figure 18: Sequence of the prototype reaction.

Intermediate **2** was obtained through an indium mediated allylation reaction, starting from D-glyceraldehyde **1**. The followed procedure is described in further detail in part B,

in chapters 2.1 and 3.1.1. Although a stereocenter is introduced at the C4 position in this reaction, the stereochemistry of the molecule is of no further interest, as it has no impact on the outcome of the procedure. Therefore no further investigations were made in regards to the separation of the obtained diastereomers.

Further protection reactions were performed, in order to obtain protected alcohol **11**/**16**, protected by either a benzyl or a *p*-methoxybenzyl group. Both protection procedures proof unproblematic and show satisfying yields.

An acidic deprotection under high temperature yields diol **12**/**17** (60) and a subsequent cleavage of the free diols will result in the first building block **A**.

Two different procedures were applied, depending on the protecting group present in the molecules. Starting from diol **12**, lead tetraacetate (1.5 eq, in diethyl ether) was used to cleave the carbon-carbon bond in the *vicinal* diol (glycol). This reaction is useful in the formation of ketones and aldehydes and involves a favorable five membered cyclic intermediate. It is therefore possible to obtain aldehyde **13** with sufficient yields. An alternative oxidative cleavage (61) was used for the diols cleavage of compound **17**, by treatment with sodium periodate (1.5 eq, in tetrahydrofuran), in order to yield aldehyde **26**.

Through an indium mediated allylation reaction, the aldehyde functionality was subsequently elongated with bromomethyl methacrylic acid derivative **34** (building block **B**). Through this elongation reaction compounds **14** and **27** were obtained, which represent the key intermediates for the ring closure reaction.

As reported in literature (62), indium mediated reactions are solvent dependent, as the solvent plays an important role for the formation of the active organometallic species. Table 3 shows the different attempts, that were carried out with the purpose to increase the yield of the reaction.

Keeping the indium and allylbromide equivalents constant allowed investigating the optimal solvent through alteration of both the used ratio and the applied temperature. It was possible to obtain a satisfactory yield of 55% from aldehyde **26**, by the use of H_2O / EtOH at a temperature of 45°C– 50°C.

solvent	ratio	eq. In	eq. allylbromide	temp. [°C]	yield [%]
H_2O / EtOH	3:2	1.8	1.5	rt	41
THF / H_2O	3:1	1.8	1.5	20	---
DMF	---	1.8	1.5	20	---
DMF / H_2O	3:1	1.8	1.5	20	---
EtOH / H_2O	2:1	1.8	1.5	20	4
H_2O / EtOH	3:1	1.8	1.5	20	31
H_2O / EtOH	3:1	1.8	1.5	45 - 50	55

Table 3: Indium mediated allylation conditions.

Ring closing metathesis (RCM) (63) yields educts **15**/**28**. The coupling of the two terminal alkenes, yielding the benzoic ester derivative, was performed by using the Grubbs´ catalyst second generation (64) in dichloromethane at reflux. The treatment of **14**/**27** with Grubbs´ catalyst first generation did not prove successful.

Compared with other generations, the Grubbs´ catalyst first generation suffers from a reduced activity. RCM and cross metathesis of sterically hindered or electronically deactivated olefin is difficult to perform with the mentioned catalyst (65). Although Grubbs´ catalysts tolerate diverse functional groups in alkenes, it is assumed that the electron-withdrawing properties of the ester functionality present in compound **14**/**27** decrease the catalytic properties of the first generation Grubbs catalyst. Second generation Grubbs catalyst however promotes the RCM.

Further deprotection and elimination of the free hydroxyl group yielded the aromatic ring **30** as benzoic acid. Optimization of the reaction towards the final benzoic ester **30a** proved unsuccessful, it was however possible to synthesize benzoic acid **30** instead.

The above mentioned deprotection steps are shown in further detail in the below Table 4. Cleavage of the benzyl protecting group proved unsuccessful, as standard deprotection procedures (Pd/H_2) (60) are not applicable, due to the olefinic double bond in the ring. Reaction sequences with a benzyl protecting group have therefore been abandoned.

Table 4 further shows the different approaches applied for deprotection of the *p*-methoxybenzyl group. As described below, the best yields were achieved using triflic acid (66).

reagent / solvent	temp. [°C]	yield [%]	reagent / solvent	temp. [°C]	yield [%]
HCl conc. / H_2O	reflux	---	DDQ (1.1 eq) in DCM / H_2O	5 – rt	---
p-TsOH in DCM	rt	---	DDQ (2 eq) in DCM / H_2O	5 – rt	---
p-TsOH in DCM	40	---	CAN Ac. / H_2O	rt	43
H_2SO_4 in DCM	rt	---	TfOH in DCM	45	41
H_2SO_4 in DCM	40	---	TfOH in DCM	rt	95

Table 4: Cleavage conditions of the protecting groups benzyl and *p*-methoxybenzyl.

Different procedures (67) (68) (69) for the dehydrogenation of the diols, present on the ring, were performed, including the treatment with dehydration agents, such as the Burgess reagent, but proved unsuccessful. In this case however it was possible to recover the starting material. Furthermore, different acidic conditions in combination with different temperatures and reaction times were investigated. Treatment of the diols with a 1M solution of H_2SO_4 in CH_3COOH under reflux enabled to yield benzoic acid **30** with 29% from compound **29**, as shown in Table 5.

reagents and conditions	solvent	Temp [°C]	yield [%]
TfOH, 0.5 eq	DCM	rt	---
TfOH, 0.8 eq + 0.8 eq, mol sieves 4Å	DCM	120	---
TfOH, 1.5 eq	DCM	reflux	---
TfOH, 1 eq + 2eq	DCM	rt	---
TfOH, 0.5 eq + 2 eq	DCM	reflux	---
Burgess, 2.8 eq	Toluol	rt	---
1. p-TsOH, Py 2. Burgess	1. THF 2. Toluol	rt	---
1. p-TsOH, Et_3N 2. t-BuOK	THF	rt	---
Ac_2O / TEA	DCM	rt	---
H_2SO_4 1M in CH_3COOH	---	120	29%

Table 5: Aromatization conditions.

The elongation with hydantoin (building block **C**) was performed and published previously (70) and is further described in chapter 2.5.

The prototype reaction rendered successful as it was possible to perform the main steps achieving satisfactory yields. The approach further proved that *p*-methoxybenzyl is the preferable protecting group, as its cleavage proved more effective. The previously described methods and conditions were applied equally in the following work.

2.3. Approaches to the synthesis and preparation of building block A

Figure 19 shows the three different approaches that were followed towards the aromatic amino acid. All three approaches share the same intermediate **26**. Approach **I** represents the synthetic strategy and prototype reaction described in chapter 2.2, starting from D-glyceraldehyde. As starting material approaches **II** and **III** use the commercially available ethyl bromoacetate and bromoacetic acid respectively. While route **I** starts from D-glyceraldehyde, an unlabeled compound, route **II** and **III** start from chemicals that can be purchased in both labeled and unlabeled form, both being inexpensive and easily synthesizable.

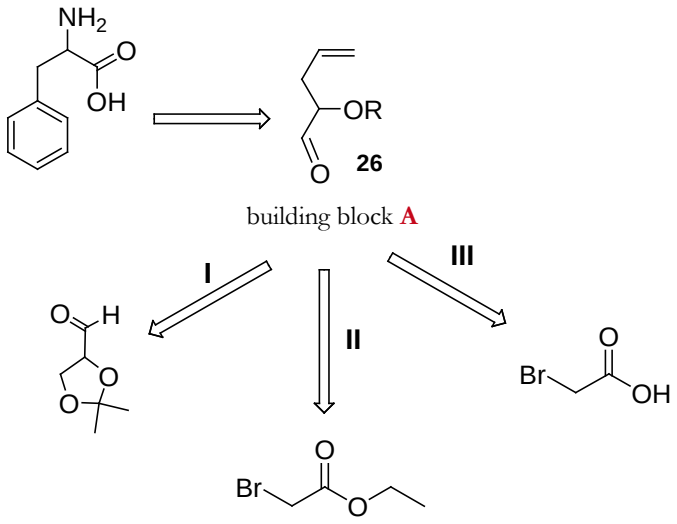

Figure 19: Three different approaches applied.

Both these acetic acid derivatives make it possible to start introducing labeled isotopes from the beginning of the synthesis on, as they are the first source of label. It is possible to achieve building block **A** independently of the synthesis' starting point.

2.3.1. Introduction to the reaction sequence towards labeled intermediates

The prototype reaction allowed to optimize all reaction steps and all reaction sequence parameters, starting from building block **A** until the final aromatic precursor. Using a labeled starting material will necessitate to investigate a synthetic approach, leading from this new starting material to building block **A**. Once this synthetic route towards building block **A** is developed, the prototype- reaction steps can be implemented accordingly.

The two chosen approaches to follow, in order to yield building block **A** in a labeled form, are both starting from non-aromatic precursors, commercially available or easily accessible from labeled acetic acid. Starting materials for these approaches are bromoacetic acid and ethyl bromoacetate.

Although the synthetic approaches to yield aldehyde **26** in a labeled form are different, once achieved, the prototype reaction was carried out unchanged thereafter.

2.3.1.1. Reaction sequence starting from ethyl bromoacetate

The starting material in the first attempt towards the synthesis of Phe, is ethyl bromoacetate **18**, the ethyl ester of bromoacetic acid. It is commercially available in its non-labeled as well as in its [1-^{13}C]/[2-^{13}C]-labeled form. It can however also be prepared in a simple two steps reaction, starting from acetic acid (71), which provides the most cost efficient solution.

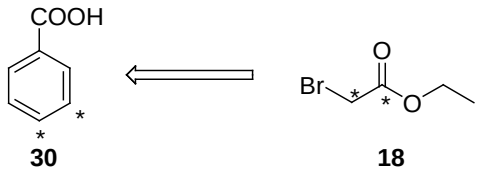

30 **18**

Figure 20: Retrosynthesis of benzoic acid from ethyl bromoacetate. * indicates the possible labeled positions deriving from acetic acid.

It was therefore chosen as stating material and first source of label. This approach is meant to be a straight forward synthesis towards building block **A** and it should make the aromatic intermediate achievable within eight steps.

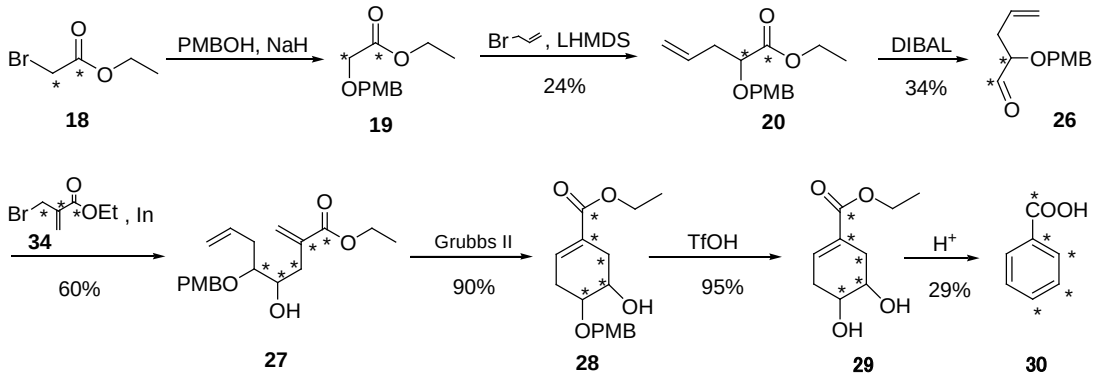

Figure 21: Reaction sequence starting from ethyl bromoacetate.

As shown in Figure 21, elimination of the Br moiety of compound **18** through substitution with *p*-methoxy benzyl alcohol in presence of sodium hydride yields molecule **19**. Subsequent elongation at the α-carbon with allyl bromide in presence of a strong non-nucleophile base yields the ester **20**, which can be reduced to the desired aldehyde **26**. This second reaction step results in a 24% yield of allyl derivative, therefore different procedures as well as different bases were tested. The preparation of fresh LHMDS was carried out as well but did not result in any improvement of the yield. In Table 6 different reaction conditions tested are shown with their corresponding yield.

eq. LDA	solvent	eq. allylbromide	Temp. [°C]	Yield [%]
1.5	THF	1.5	-78	---
0.9	THF	1.2	-78	---
eq. LHMDS	**solvent**	**eq. allylbromide**	**Temp. [°C]**	**Yield [%]**
1.2	THF	1.3	-78 / -50 / -78	---
0.9	THF	1.2	-78	---
1.2	THF	1.3	-78	22
1.8	THF	1.3	-78	---

Table 6: Reaction conditions for elongation at α-carbon.

Treatment with DIBALH at -78°C for the reduction to aldehyde **26** proved to be successful. Although the yield of the reaction was 34%, the reaction product was proven by NMR spectroscopy after purification on column chromatography, on silica gel. In order to improve the yield of this reaction, temperatures from -50°C to -78°C were tested, additionally requiring very slow addition of the reagent. Subsequent reaction steps of the prototype reaction, as already described in chapter 2.2, including ring closing metathesis and indium mediated elongation, yielded the intermediate **30**.

Allyl bromide as labeling source is not commercially available and highly difficult to be synthetically prepared, labeling positions are therefore limited. Figure 21 shows the possible positions that labeled ^{13}C atoms can be introduce into (indicated with *).

The possibilities of adapting this synthetic route for labeling strategies is limited, as it was not possible to increase the low yields of the sequence' first two steps.

2.3.1.2. Reaction sequence starting from bromoacetic acid

The first source of label for the second pathway was bromoacetic acid, which is commercially available in its [1-^{13}C]/[2-^{13}C]-labeled forms and it can be easily synthetically prepared from inexpensive acetic acid via a bromination reaction.

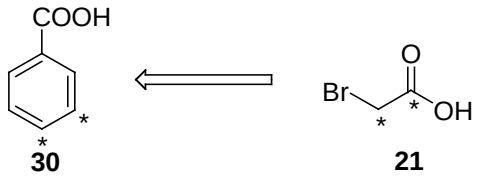

Figure 22: Retrosynthesis of benzoic acid from bromoacetic acid. * indicates the possible labeled positions deriving from acetic acid.

Reaction of acetic acid derivative **21** with *p*-methoxy benzyl alcohol in presence of sodium hydride allows the substitution of the Br moiety and to yield compound **22**, which is used for the subsequent step without previous purification. Elongation reaction with allyl alcohol in presence of DCC and DMAP yields intermediate **23**. Allyl alcohol is commercially available in its [1-^{13}C]- and [2-^{13}C]-labeled forms, therefore giving the possibility to introduce ^{13}C-patterns into two additional positions in the ring (72). Subsequent Ireland-Claisen Rearrangement, performed with LHMDS in presence of

TMSCl at -78°C, yields the carboxylic acid **24**. Direct DIBAL reduction of the acidic functionality of compound **24** to the aldehyde proved unsuccessful. Although different conditions, such as increasing the temperature from -78°C to -30°C and using different solvents, were applied, the reaction never yielded the desired product. The difficulties were overcome by first performing an esterification reaction with $TMSCHN_2$ in diethyl ether, in order to obtain compound **25**. Methyl ester **25** can subsequently be reduced with DIBAL to yield the aldehyde **26** with yields above 90%.

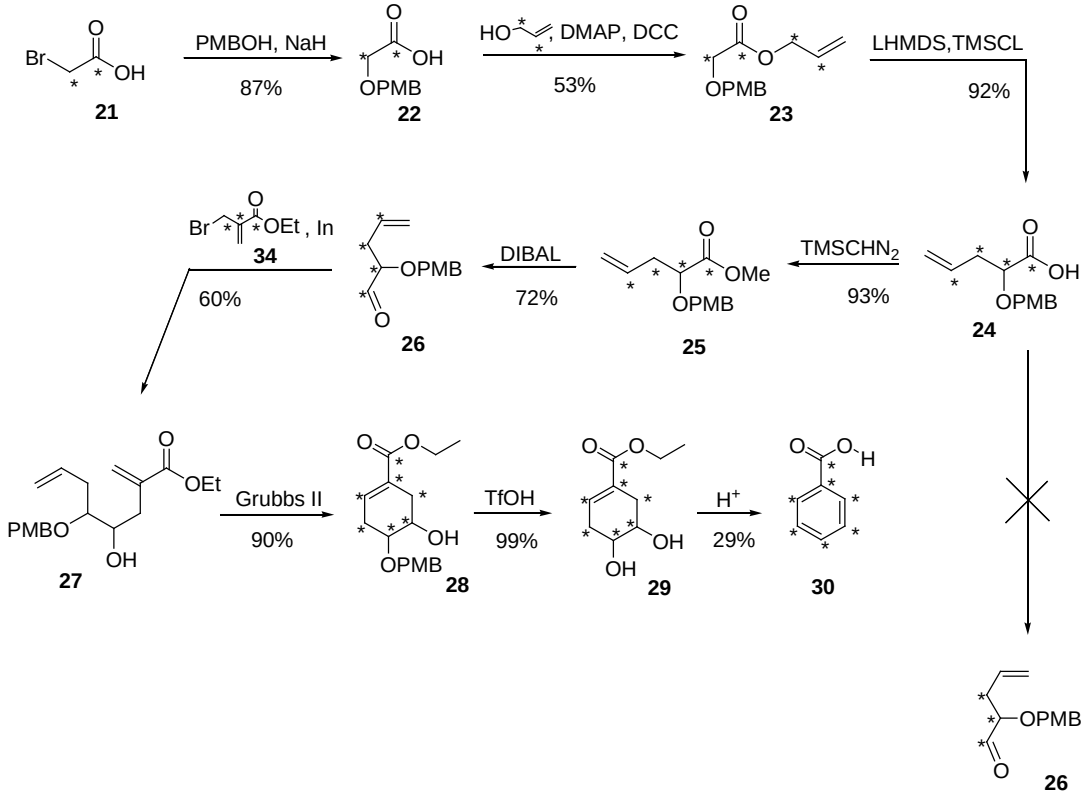

Figure 23: Reaction sequence starting from bromoacetic acid.

As shown in Table 7, attempts for the methylation reaction of compound **24** to **25** with MeCl in acetyl chloride did not result in any product. An alternatively applicable method follows the treatment of compound **24** with MeOH in DMP resulting the desired methyl ester with sufficient yields (83%).

reagents	solvent	temp. [°C]	yield [%]
MeCl (50ml), Acetyl Chloride (7ml)	---	reflux	---
MeOH (3 eq.), DMP (1.2 eq)	---	reflux	---
MeOH (3 eq.), DMP (1.2 eq)	---	rt	83
$TMSCHN_2$ in Hexane (2 eq.)	Toluol / MeOH	rt	24
$TMSCHN_2$ in Et_2O (2 eq.)	Toluol / MeOH	rt	93

Table 7: Esterification conditions

Two methods can therefore be used for the synthesis of compound **25**: esterification with $TMSCHN_2$ as well as methylation with MeOH in DMP. Although $TMSCHN_2$ represents a comparatively expensive reagent, the major advantage is the low reaction time (see chapter 4, Experimental work).

Although this sequence requires additional steps compared to the previous synthesis, adopting this method allows to yield the key building block **A** in high yields. The introduction of allyl alcohol in its labeled form makes this synthesis comparatively more effective in labeling regards.

2.4. Preparation of building block B

As mentioned earlier, building block **B** as bromomethyl methacrylic acid derivative **34**, represents a suitable source of label in the synthesis. Different preparatory methods of these compounds have been described in literature. Reactions such as dehydrobromination of β,β'-dibromoisobutyric esters or acid, or bromination of t-butyl or Ethyl α-(Hydroxymethyl)acrylate with Phosphorus(III) Bromide can be applied (73). The most suitable reaction in the case of this work, for the preparation of ethyl 2-(bromomethyl)acrylate, is a Wittig-Horner (HWE) reaction in combination with a subsequent bromination (74) (75).

The reaction performed for obtaining labeled ethyl 2-(bromomethyl)acrylate starts from acetic acid (Figure 24), as it is one of the most inexpensive and commercially available isotope-labeled compounds, with >99% ^{13}C at both carbon atoms.

At first a triethyl phosphonoacetate is obtained, which is then treated with formaldehyde and K_2CO_3 and is further subject to a HWE mechanism to yield the intermediate alkene. A final bromination reaction with PBr_3 yields the methyl acrylate derivative **34**.

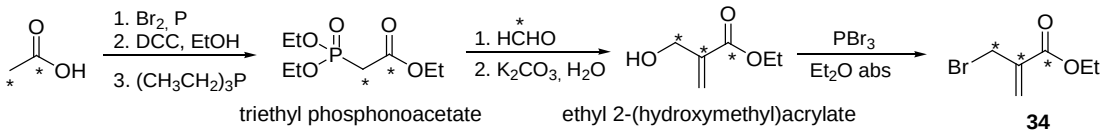

Figure 24: Preparation of building block B.

Formaldehyde is used as an additional source for the incorporation of stable isotopes into compound synthon **B**. It is commercially available as ^{13}C-formaldehyde.

Preparation of building block **B** in the above depicted way gives the possibility to obtain an intermediate, labeled in three different positions (*).

2.5. Preparation of building block C

Preparation of building block **C** was not performed in this work, however a short description based on published data is given.

Starting from the inexpensive labeling source ^{13}C-glycine, building block **C** is prepared via a two-steps reaction. Treatment of glycine with KOCN under acidic conditions yields the desired hydantoin, which can be subsequently coupled to the aromatic precursor previously prepared. Following an enzymatic amination of phenyl pyruvate with the usage of L-phenylalanine dehydrogenase, the desired L-phenylalanine can be obtained (70).

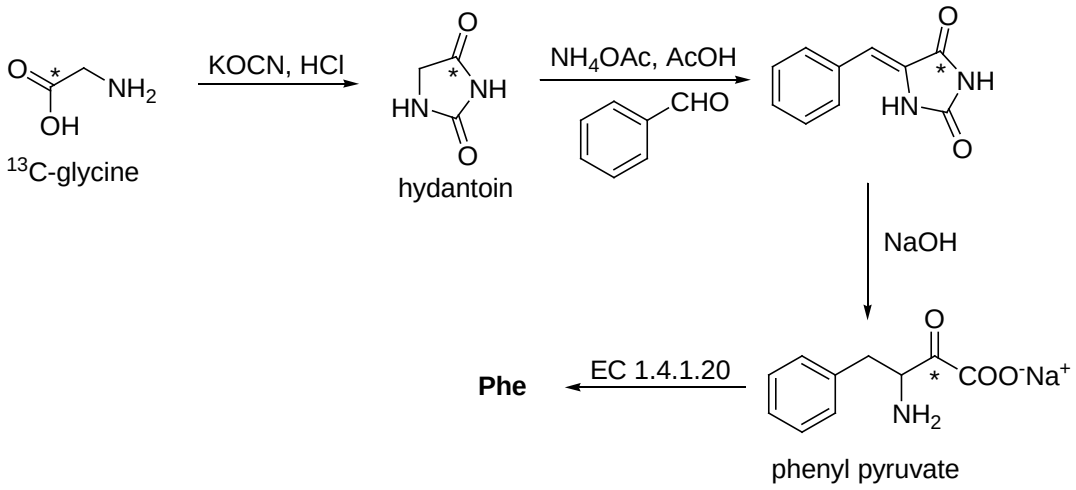

Figure 25: Preparation of building block C.

The presented pathway makes the aromatic amino acids as well as the keto acid phenyl pyruvate accessible. This allows to adopt the synthesis for different overexpression methods (previously described in chapter 1.2.2)

3. Discussion and conclusions

This work aimed to obtain a straight-forward and versatile synthetic route towards the preparation of aromatic amino acids and precursors which can subsequently be used for the incorporation into proteins for NMR studies.

Figure 26 shows the three performed routes with the common intermediate aldehyde **26** as well as the final pathway, leading from aldehyde **26** to the final aromatic amino acid precursor **30**.

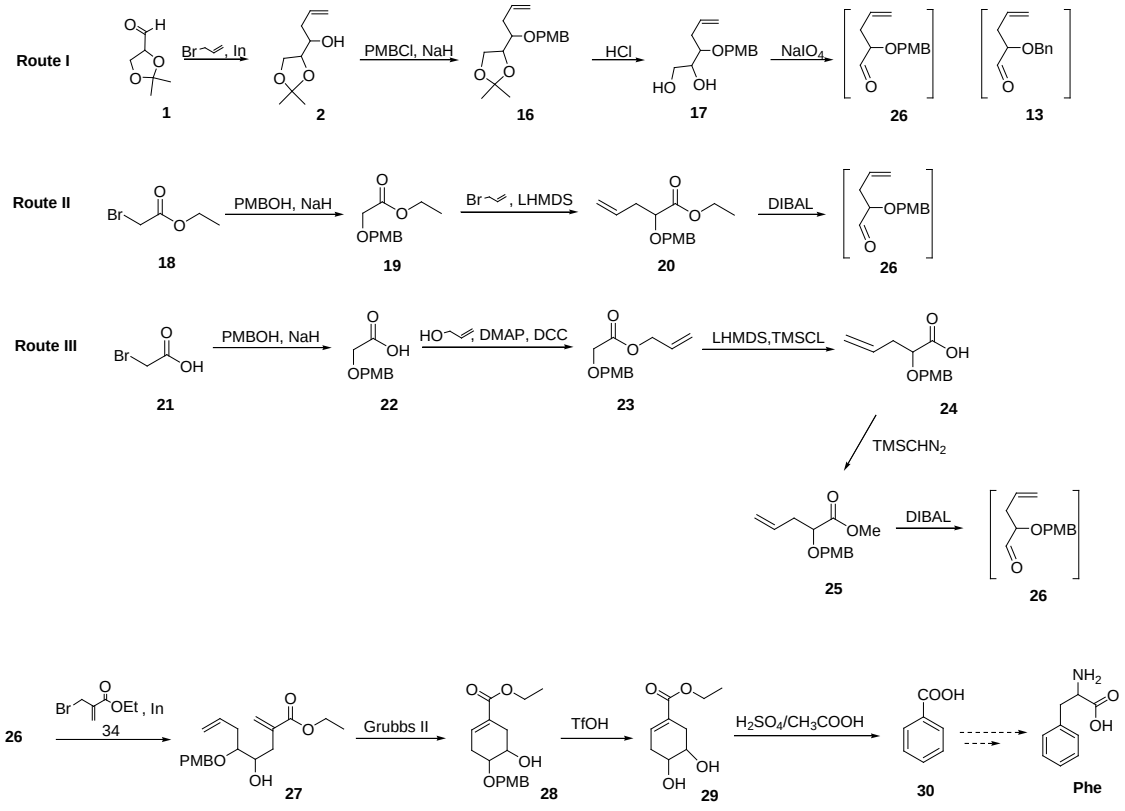

Figure 26: Overview of the three performed syntheses.

Route I, the "prototype reaction", aimed at the improvement and optimization of the key reaction steps in order to develop the prototype reaction. D-glyceraldehyde was used as an inexpensive starting material that can be prepared in a simple way. Although it is not available in a labeled form, this compound proved to be optimal to yield building block **A**, which the subsequent synthesis is based upon. All key steps, such as elongation reactions, the ring closing metathesis as well as the aromatization to the final phenyl derivative, were carried out successfully. The aromatization reaction required particular attention, as the dehydration of the diols proved to be elaborated. The desired aromatic ring could be obtained with a yield of 29%.

Route II allowed to achieve aldehyde **26**, starting from compound **18**, with a 34% yield. This pathway will allow to obtain aromatic amino acid as phenylalanine, having the aromatic ring being selectively labeled consecutively from the C1- to the C4-position. The side chain of Phe can as well be labeled via reaction with hydantoin, building block **C**. Figure 27 shows the five different label positions as well as each positions' source of label.

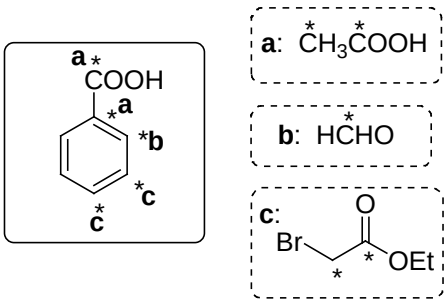

Figure 27: Labeled positions(*) and corresponding source of label of route II.

Route III, starting from compound **21** yielding the intermediate aldehyde **26**, represents the comparatively best synthetic route, allowing every position of the molecule to be labeled selectively. The side chain of Phe can be labeled as well through reaction with hydantoin, as previously described. The below Figure 28 shows the different labeling patterns as well as the corresponding labeled positions.

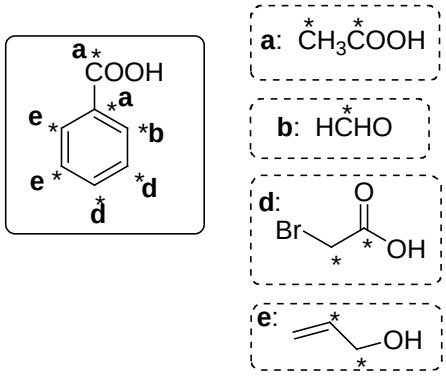

Figure 28: Labeled positions(*) and corresponding source of label of route III.

A comparison of all three carried out routes is shown in Table 8 below. The total number of steps, the percental yield of building block **A** as well as the number of labeled positions on the aromatic precursor is shown for each of the carried out routes.

Route	Total number of steps	Yield of building block A	No. of labeled positions (on aromatic precursor)
I	9	97%	3
II	8	34 %	5
III	10	72 %	7

Table 8: Comparison of three performed routes.

Although carried out with non-labeled starting materials, these syntheses represent a way of synthesizing fully labeled phenylalanine and its precursors. ^{13}C-labeling patterns can be introduced in a cost-effective way through the use of inexpensive labeling sources such as [^{13}C]-acetic acid, [^{13}C]-formaldehyde, [^{13}C]-allyl alcohol and [^{13}C]-glycine.

4. Experimental work

Solvents: anhydrous solvents were distilled from P_2O_5 (dichloromethane, chloroform) or sodium (diethylether, toluene) and stored over molecular sieves (4 Å). Anhydrous tetrahydrofurane was purchased from Sigma-Aldrich.

Evaporation of the solvents was accomplished using a Büchi rotavapor R-210 in combination with an Ilmvac LVS 310p ecoflex vacuum system.

Purification methods: column chromatography was performed using silica gel 60 (0.040-0.063 μm, 240-400 mesh) available from Merck. Thin layer chromatography (TLC) was performed on precoated silica gel glass plates (Merck 60 F254). TLC detection was carried out using a UVAC-60 neolab ultraviolet lamp (254 and 366 nm) and/or by treatment with one of the following detecting reagents: Mo-$Ce(SO_4)_2$ complex solution (48 g $(NH_4)_6Mo_7O_{24}$*4H2O and 2 g $Ce(SO_4)_2$ in 100 ml 10% H_2SO_4), $KMnO_4$ solution (0.5% in 1N NaOH).

NMR spectroscopy measuremets: spectra were recorded on a Bruker Avance DRX400 spectrometer, AV400 spectrometer or DRX600 spectrometer. Chemical shifts are given in ppm, coupling constants are given in Hz. Spectra are referenced to the residual solvent signal 7.26 ppm (^1H), 77.16 ppm (^{13}C) for $CDCl_3$.

(S)-2,2-dimethyl-1,3-dioxolane-4-carbaldehyde [1]

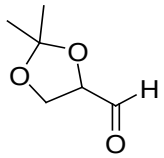

$C_6H_{10}O_3$
Mol. Wt.: 130,14

D-Mannitoldiacetonide (4.014g, 15.2mmol) was dissolved in dry CH_2Cl_2 (40ml) under argon atmosphere. After cooling to 5°C, $Pb(OAc)_4$ (1.2eq, 18.3mmol) was added in small portions over a period of 30 minutes. After the addition, the resulting suspension was stirred for 2.5h at room temperature. The completion of the reaction was controlled by TLC (1:1 PE:EE). The mixture was filtrated over celite and the solvent was removed to obtain a clear, highly viscous solution. The crude product was purified by vacuum distillation (33-41°C at 10.8mm Hg). The colorless product **1** (1.92g) was stored at -22°C.

Yield: 97%

^{1}H-NMR ($CDCl_3$, 400 MHz): δ 9.65 (d, 1H, -C**H**O), 4.33 (m, 1H, -C**H**CHO, J=2.15 Hz, J=7.27 Hz), 4.8 (m, 2 H, -C**H$_2$**CHCHO, J=7.27 Hz), 1.40 (s, 3H, -C**H$_3$**), 1.35 (s, 3H, -C**H$_3$**) ppm.

1-((S)-2,2-dimethyl-1,3-dioxolan-4-yl)but-3-en-1-ol [2]

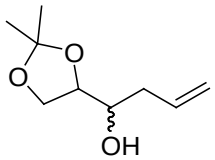

$C_9H_{16}O_3$
Mol. Wt.: 172,22

The protected D-glyceraldehyde **1** (0.140g, 1.08mmol) was transferred into an Erlenmayer flask and dissolved in a mixture of THF:H_2O 4:1 (1 mL). A fine powder of indium (1.5eq, 1.61mmol) and allyl bromide (4.0eq, 4.20mmol) was added. The change of the clear mixture to a milky suspension indicated the start of the reaction. After the initiation of the reaction, the sonication was carried out for 3 more hours. The completion of the reaction was controlled by TLC (PE:EE 3:1). The product was extracted with EtOAc (3x 20ml) and the combined organic layers were washed with a saturated solution of NH_4Cl and dried over anhydrous $MgSO_4$. The solvent was evaporated under reduced pressure to obtain the crude product. The product was purified by column chromatography on silica with PE:EE 3:1 to yield 0.155g of final product **2**.

Yield: 83%

^{1}**H-NMR** ($CDCl_3$, 400 MHz): δ 5.75 (m, 1H, -C**H**CH_2), 5.10(m, 2H, -CHC**H$_2$**), 4.01 (q, 2H, -C**H$_2$**CH-, Hz, J=6.02 Hz, J=9.17 Hz), 3.92 (m, 1H, -C**H**CH_2-, J=6.02 Hz, J=9.17 Hz), 3.73 (m, 1H, -C**H**OH) 2.22 (m, 2H, -C**H$_2$**$CHCH_2$), 1.9 (s, 1H, -C**H**OH), 1.35 (s, 3H, -C**H$_3$**), 1.30 (s, 3H, -C**H$_3$**) ppm.

^{13}**C-NMR** ($CDCl_3$, 400 MHz): 134.35 (-**C**HCH_2) 118.80 (-**C**$(CH_3)_2$) 78.49 (-**C**HCH_2) 70.18 (-**C**HOH) 65.59 (-**C**H_2CH-) 37.99 (-**C**H_2CHCH_2) 26.95 (-**C**H_3) 25.67 (-**C**H_3)

1,3-Dioxolane, 2,2-dimethyl-4-[1-(phenylmethoxy)-3-butenyl] [11]

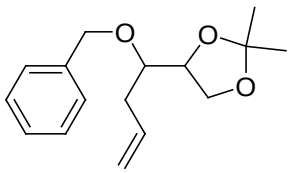

$C_{16}H_{22}O_3$
Mol. Wt.: 262,34

Compound **2**(3.160g, 18.3mmol) was diluted in DMSO (10mL) and cooled at 10°C. After potassium hydroxide (2.3eq, 42.8mmol) and benzyl bromide (1.5eq, 27.7mmol) were added, the suspension was stirred 17h at 25°C. In order to quench the reaction, ice-H_2O (20mL) was poured to the mixture. An extraction with Et_2O (3 x 20ml) followed. The organic phase was subsequently washed with $NaHCO_3$ sat., dried over $MgSO_4$ and finally concentrated under reduced pressure to yield 4.16g of final product **11**.

Yield: 87%

^{1}**H-NMR** ($CDCl_3$, 400 MHz): δ 7.34-7.27 (m, -**Ph**), 5.95-5.85 (m, CH_2=C**H**-), 5.17-5.07 (m, C**H$_2$**=CH-, J=1.99 Hz), 4.67-4.57 (q, Ph-C**H$_2$**-), 4.12-4.07 (q, -CH-C**H**-CH_2-, J=6.25 Hz), 4.05-4.01 (q, -CH-CH-C**H$_2$**-, J=6.25 Hz), 3.91-3.87 (q, -CH-CH-C**H$_2$**-„ J=6.25 Hz), 3.59-3.55 (m, -C**H**-CH-CH_2-, J=6.03 Hz), 2.47-2.30 (m, CH_2=CH-C**H$_2$**-, J=1.99 Hz, J=6.03 Hz), 1.41 (s, -C**H$_3$**), 1.35 (s, -C**H$_3$**) ppm.

5-Hexene-1,2-diol, 3-(phenylmethoxy) [12]

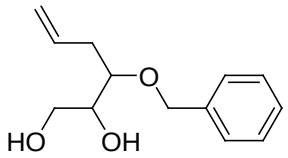

$C_{13}H_{18}O_3$
Mol. Wt.: 222,28

Compound **11** (4.905g, 18.7mmol) was dissolved in THF:H_2O 1:1 (70mL) and acidified with HCl conc. to pH 1-2. The reaction was stirred at 60°C overnight and it was followed by TLC (PE:EE 1:1). The extraction of the product was performed with Et_2O (2x15ml). The combined organic layers where washed with a saturated solution of $NaHCO_3$ and dried over anhydrous $MgSO_4$. The solvent was removed under reduced pressure in order to obtain 3.86g of the final product **12**.

Yield: 93%

^{1}**H-NMR** ($CDCl_3$, 400 MHz): δ 7.38-7.34 (m, -**Ph**), 5.92-5.80 (m, CH_2=C**H**-, J=10.11 Hz, J=7.06 Hz), 5.18-5.09 (m, C**H$_2$**=CH-, J=10.11 Hz), 4.56-4.45 (q, Ph-C**H$_2$**-), 3.8-3.6 (m, -CH-C**H**-C**H$_2$**-), 3.67-3.61(m, -C**H**-CH-CH_2-, J=6.19 Hz), 2.51-2.33 (m, CH_2=CH-C**H$_2$**-, J=1.30 Hz) ppm.

4-Pentenal, 2-(phenylmethoxy) [13]

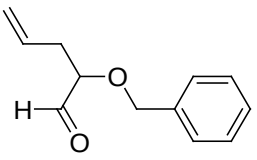

$C_{12}H_{14}O_2$
Mol. Wt.: 190,24

Compound **12** (4.236g, 19.1mmol) was dissolved in CH_2Cl_2 (200mL), cooled to 0°C and $Pb(OAc)_4$ (1.3eq, 26.6mmol) was added in portions. Then the mixture was stirred for 2.5h at rt. The reaction process was followed by TLC (PE:EE = 1:1). The suspension was subsequently filtrated. H_2O (10ml) was added to the filtrate and an extraction with EtOAc (3x20ml) was performed. The solution was concentrated under reduced pressure to yield 3.6g of final product **13**.

Yield: 85%

^{1}**H-NMR** ($CDCl_3$, 400 MHz): δ 9.65 (d, -C**H**=O, J=2.03 Hz), 7.36-7.35 (m, -**Ph**), 5.87-5.77 (m, CH_2=C**H**-, J=10.17 Hz, J=7.02 Hz), 5.18-5.11 (td, C**H$_2$**=CH-), 4.69-4.58 (q, Ph-C**H$_2$**-), 3.85-3.81 (dt, -C**H**-CH=O, J=2.03Hz), 3.51-3.46(m, CH_2=CH-C**H$_2$**-, J=7.02 Hz) ppm.

ethyl 5-(benzyloxy)-4-hydroxy-2-methyleneoct-7-enoate [14]

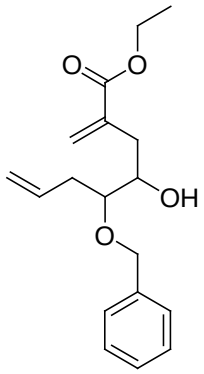

$C_{18}H_{24}O_4$
Mol. Wt.: 304,38

Aldehyde **13** (0.200g, 1.1mmol) was dissolved in H_2O (5ml) into an Erlenmeyer flask. Indium (1.5eq, 1.7mmol) and Ethyl-2-(bromomethyl)acrylate (1. eq, 1.4mmol) were subsequently added. Then the suspension was sonicated 15h at 25°C. White precipitate had formed due to the formation of indium salts. This precipitate can be destroyed by adding some drops of HCl 1M. The suspension was decanted to remove unreacted indium. Afterwards an extraction with ethyl acetate (3x25ml) followed. The combined organic layers were washed with NH_4Cl sat. (10ml), dried over $MgSO_4$ and concentrated under reduced pressure. In order to purify the crude product, a column chromatography (solvent: PE:EE= 3:1) was made. Fractions were collected and concentrated under reduced pressure to yield 0.151g of the final compound **14**.

Yield: 45%

^{1}**H-NMR** ($CDCl_3$, 400 MHz): δ 7.34(d, -**Ph**), 7.29 (m, -**Ph**), 6.23 (dd, C**H$_2$**=CH-CH_2-, J=1.40 Hz, J=7.18 Hz), 5.88 (m, CH_2=C**H**-CH_2-), 5.64 (dd, C**H$_2$**=CH-CH_2-), 5.11 (m, C**H$_2$**=C-), 4.60(m, C**H$_2$**-Ph), 4.20 (m, -C**H$_2$**-CH_3), 3.83 (m, -C**H**-OH), 3.44 (m, -C**H**-O-CH_2-), 2.51 (m, -C**H$_2$**-CH-CH-C**H$_2$**-, -OH), 1.29 (m, -C**H$_3$**) ppm.

ethyl 4-(benzyloxy)-5-hydroxycyclohex-1-enecarboxylate [15]

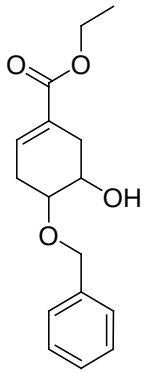

$C_{16}H_{20}O_4$
Mol. Wt.: 276,33

The educt **14** (0.087g, 0.3mmol) was dissolved in dry CH_2Cl_2 (25mL). The catalyst **8** ((1,3-Bis(2,4,6-trimethylphenyl)-2-imidazolidinylidene)dichloro(phenylmethylene)-(tricyclohexylphosphine)ruthenium), commonly known as Grubbs Catalyst 2nd generation (0.1eq, 0.03mmol), was added. The catalyst used for the reaction has been purchased by Sigma-Aldrich (CAS: 246047-72-3). It can eventually also be prepared in situ as described below. The mixture was stirred 3h at 40°C. The reaction process was monitored by TLC (toluene:acetone = 6:1). At reaction completion, the solution was concentrated under reduced pressure. Purification by column chromatography (solvent: toluene/acetone = 9/1) followed. Fractions were collected and finally concentrated under reduced pressure to yield 0.072 g of the final product **15**.

Yield: 87%

^{1}**H-NMR** ($CDCl_3$, 400 MHz): δ 7.32(m, -**Ph**), 6.83 (m, -CH_2=C**H**-), 4.61 (m, -C**H$_2$**-Ph), 4.64 (m, -C**H$_2$**-CH_3, J=7.06 Hz), 3.86, 3.68 (m, C**H-**OH), 3.53(m, -C**H**-O-CH_2-), 2.63, 2.25 (m, -C**H$_2$**-CH-CH-C**H$_2$**-, -O**H**), 1.27 (dt, -C**H$_3$,** J=7.06 Hz) ppm.

Preparation in situ of Grubbs Catalyst 2nd generation.

The preparation of the mentioned catalyst brakes down into four steps. The information for the synthetical procedures have been collected from the following literature sources:

- Abrams M. B., Scott B. L., Baker R. T., Organometallics, 2000, 19, 4944-4956.
- Blum A.P., Ritter T., Grubbs R.H., Organometallics 2007, 26, 2122-2124.

Step 1)

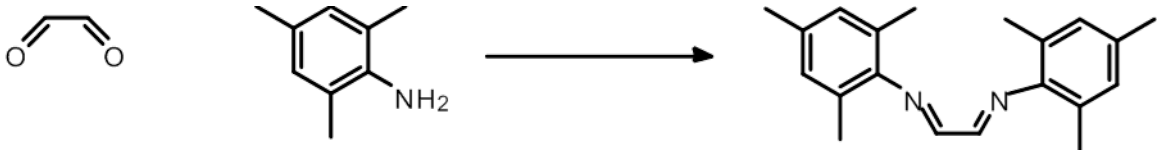

Mesityl amine (31,3ml, 222mmol) and Ethanol (222ml) were placed in a 500mL RBF. Glyoxal (40% sol. in water) (12,72ml, 111 mmol) was added *via* syringe over 15min and the contents were stirred at 25°C for 18h. The solution was filtered and the solid washed with 30mL toluene (0°C) and dried in vacuum. A second crop was obtained by concentrating the ethanol/water solution to a volume of 10mL, cooling and filtering. The solid was washed with 10mL ethanol at 0°C and 20mL toluene at 0°C yielding additional bisimine after drying in vacuum.

Step 2)

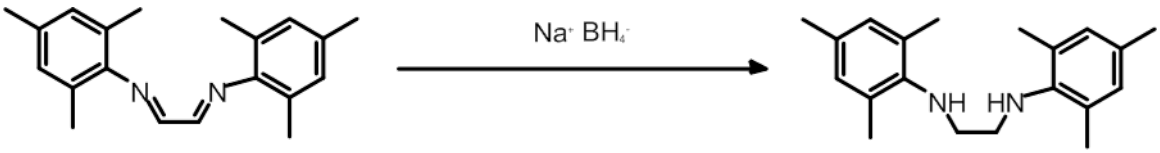

A round-bottom flask, equipped with a magnetic stir bar, a solid addition funnel and a water-cooled reflux condenser, was charged with previously prepared bisimine (9,87g, 33,8mmol). Ethanol (504ml) was added to the flask and the bright yellow solution cooled to 0°C. Sodium borohydride (12,77g, 338mmol) was added to the solution via the addition funnel over the course of 50min. The 0°C bath was removed and replaced with a heating mantle; the solution was refluxed for 45min, affording a colorless solution and a white precipitate. The solution was cooled to 25°C, and 80ml of an aqueous saturated NaCl solution were added slowly to the flask, acquiring and then maintaining a gentle

reflux. Upon cooling to room temperature, the solution was filtered using a medium porosity filter frit, and the white insoluble material was washed once with 200ml of H_2O. The combined ethanol and aqueous solutions were diluted with 160ml of additional water and extracted with 240ml of chloroform. The organic layer was separated, and volatiles were removed under reduced pressure, (without any drying over any drying agent before!), yielding a small amount of yellow oil which crystallized upon standing in air. The yellow solid was then dissolved in 40ml of THF and stirred over 4 Å sieves for 2 days. The solution was filtered and volatiles were removed in vacuum, leaving a clear yellow oil which crystallized upon standing under N_2, affording amine as a white crystalline mass.

Step 3)

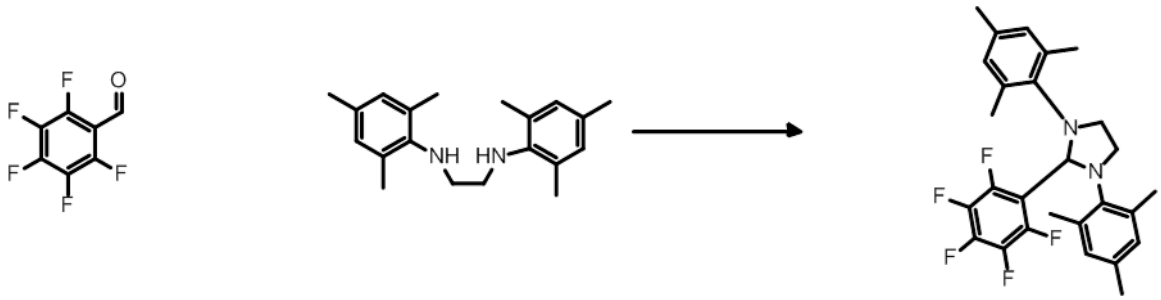

In a 100ml flask, equipped with a stir bar, the previously obtained crystalline mass (3800 mg, 12,82mmol) was dissolved in AcOH (7ml). Pentafluorobenzaldehyde (4260mg, 21,73mmol) was then added and the reaction stirred overnight. The yellow precipitate was placed in a glass frit and washed with cold methanol to afford 1,3-dimesityl-2-(pentafluorophenyl)imidazoline as a white powder.

Step 4)

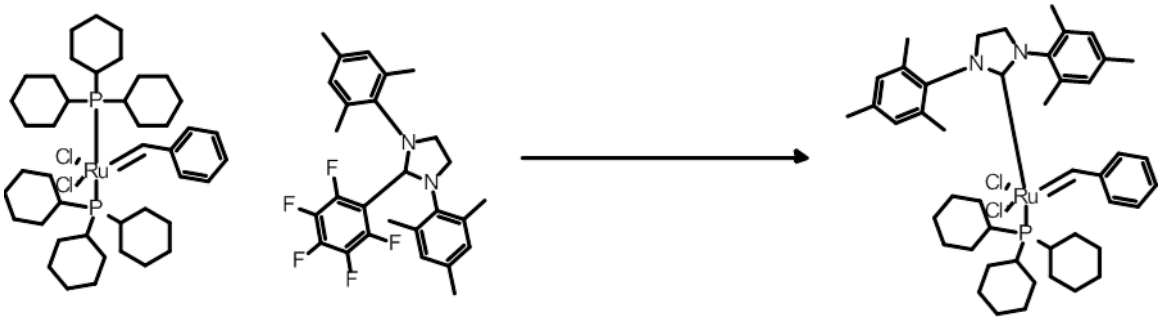

A Schlenk flask equipped with a stir bar was charged with 1,3-dimesityl-2-(pentafluorophenyl)imidazoline (0,865g, 1,823mmol) and Grubbs catalyst 1st generation (1g, 1,215mmol) purchased by Sigma-Aldrich (CAS: 172222-30-9). Toluene (36,8ml) was added. The flask was evacuated and purged with Argon for three times. It was then placed into an oil bath at 60 °C and stirred for four hours.

The reaction mixture was reduced in vacuum and purified by flash column chromatography (tlc or color of fractions) on silica gel (10% ether/pentane) to afford a reddish-brown solid. The spectrum showed the product and minor impurities. The solid was recrystallized three times from pentane at -78°C to yield the desired pure product Grubbs catalyst 2nd generation .

Although ^{1}H and ^{31}P NMR spectra matched the data reported in the literature, the desired catalyst was obtained in unsatisfying yields.

4-(1-(4-methoxybenzyloxy)but-3-enyl)-2,2-dimethyl-1,3-dioxolane [16]

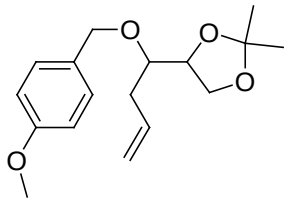

$C_{17}H_{24}O_4$
Mol. Wt.: 292,37

The educt **2** (1.13g, 6.6mmol) was solved in 3ml dry CH_2Cl_2 under argon and cooled to 0°C. To the solution, PMBCl (1.2eq, 7.92mmol) was added drop wise, and TBACl (0.05eq, 0.33mmol) was added. In a separate flask, a solution of NaH in dry CH_2Cl_2 (2.5eq, 16.5mmol) was prepared, cooled to 0°C, and added drop wise to the previous solution. The reaction mixture was stirred overnight at 60°C under Argon and was monitored via TLC (PE/EE 1:1). When the starting material was consumed, the reaction was quenched by addition of 10ml ethanol. The solvent was removed under reduced pressure, followed by an extraction with Et_2O (3x15ml). The organic layers were combined, washed with saturated $NaHCO_3$ (1x20ml) solution, dried over $MgSO_4$ and concentrated under reduced pressure to yield 1.23g of the final product **16**.

Yield: 64%

^{1}H-NMR ($CDCl_3$, 400 MHz): δ 7.25(m, -**Ph**), 6.86(m, -**Ph**), 5.88 (m, CH_2=C**H**-), 5.11 (m, C**H$_2$**=CH-), 4.55 (m, -C**H$_2$**-Ph-), 4.07 (m, -C**H**-C**H$_2$**-O-), 3.86 (m, -CH-C**H$_2$**-O-), 3.81 (s, C**H$_3$**-O-Ph-), 3.54 (m, -C**H**-O-CH_2**-),** 2.35(m, -C**H$_2$**-), 1.41 (s -C**H$_3$**), 1.34 (s -C**H$_3$**), ppm.

3-(4-methoxybenzyloxy)hex-5-ene-1,2-diol [17]

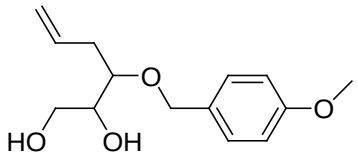

$C_{14}H_{20}O_4$
Mol. Wt.: 252,31

The educt **16** (0.987g, 3.37mmol) was dissolved in THF (20ml). A pH value of 2 was formulated by addition of concentrated HCl. Then the solution was stirred at 60° C for 18 hours. The reaction was followed by TLC (PE:EE 1:1). At reaction completion, an extraction with diethyl ether (3x10ml) was performed. The organic layers were combined and washed with sat. $NaHCO_3$ solution (2x10ml), dried over $MgSO_4$ and concentrated under reduced pressure. Purification of the crude product by column chromatography (PE/EE 1:1) yields 0.627g of diol **17**.

Yield: 73%

^{1}H-NMR ($CDCl_3$, 400 MHz): δ 7.25(m, -**Ph**), 6.86(m, -**Ph**), 5.88 (m, CH_2=C**H**-), 5.13 (m, C**H$_2$**=CH-), 4.53 (m, -C**H$_2$**-Ph-), 3.81 (s, C**H$_3$-**O-Ph-), 3.7 (m, -C**H-CH$_2$-**OH-), 3.62 (m, -CH-C**H$_2$-**OH-), 2.42 (m, -C**H-**O-CH_2**-, -CH$_2$ -),** 2.09(m, -C**H$_2$**-), ppm.

Ethyl 2-(4-methoxybenzyloxy)acetate [19]

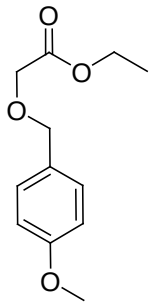

$C_{12}H_{16}O_4$
Mol. Wt.: 224,25

Ethyl bromoacetate **18** (0.500g, 2.9mmol) was added dropwise to a suspension of NaH (2.5eq, 7.48mmol) in dry THF (10ml) at 0°C. The mixture was stirred at rt. until the evolution of gas had ceased. A solution of *p*-methoxybenzyl alcohol (1.1eq, 3.0mmol) in dry THF (7ml) was added to the reaction at 0°C via a canula and the resulting mixture was stirred at rt. until the evolution of gas had stopped. Tetrabutylammonium chloride (0.05eq, 0.37mmol) was added and the resulting mixture was heated for 4 hours at reflux. After the mixture was cooled at 0°C and hydrolization with EtOH, the solvent was removed under reduced pressure yielding 0.652g. The product **19** was used for the next step without further purification.

^{1}H-NMR ($CDCl_3$, 400 MHz): δ 7.23 (d, -Ar-), 6.81 (d, -Ar-), 4.49(s, -Ar-C**H$_2$**-O-), 4.15 (q, -C**H$_2$**-CO, J=7.22 Hz), 3.74 (s, C**H$_3$**-O-), 1.21 (t, -CH$_2$-**CH$_3$**, J=7.15 Hz) ppm.

ethyl 2-(4-methoxybenzyloxy)pent-4-enoate [20]

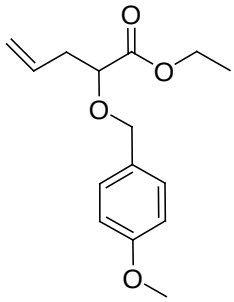

$C_{15}H_{20}O_4$
Mol. Wt.: 264,32

Ester **19** (0.652g, 2.90mmol) was dissolved in dry THF and cooled at -78°C. A solution of LHMDS 1M in THF (1.2eq, 3.48mmol) was added dropwise to the previous solution. After stirring for 15-20min, the addition of allyl bromide (1.3eq, 3.77mmol) followed. The reaction was stirred at -78°C for one additional hour and was then warmed up to room temperature over 10 hours. After quenching the reaction with some drops of HCl 1N, the solvent was evaporated under reduced pressure and an extraction with EtOAc (3x15ml) was performed. The organic phases were combined, dried over $MgSO_4$ and concentrated. In order to purify the crude product a column chromatography (solvent: PE:EE= 3:1) was made. Fractions were collected and concentrated to yield 0.187g of the final compound **20**.

Yield: 24%

^{1}H-NMR ($CDCl_3$, 400 MHz): δ 7.27 (d, -Ph-), 6.89 (d, -Ar-), 5.81 (m, -C**H**=CH_2), 5.07 (m, C**H$_2$**=CH-), 4.64 (d, - Ph-C**H$_2$**-O-, J=11.40 Hz), 4.38 (d, -Ph-C**H$_2$-**O-, J=11.40 Hz), 4.20 (m, -C**H$_2$**-CH_3), 3.96 (t, -C**H-**), 3.80 (s, C**H$_3$**-O-), 2.50 (t, -C**H$_2$**-CH-), 1.28 (t, -CH_2-C**H$_3$)** ppm.

2-(4-methoxybenzyloxy)acetic acid [22]

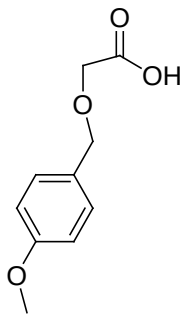

$C_{10}H_{12}O_4$
Mol. Wt.: 196,2

Bromoacetic acid **21** (8g, 57.57mmol) was added portion wise to a suspension of NaH (3.2eq, 184.23mmol) in dry THF (160ml). The mixture was stirred at room temperature until the complete evolution of gas had stopped. The reaction mixture was than cooled at 0°C and a solution of *p*-methoxybenzyl alcohol (2eq, 11.14mmol) in dry THF (120ml) was added dropwise. The final mixture was stirred at room temperature until the evolution of gas decreased. Afterwards the reaction was refluxed for four hours. The mixture was then cooled at 0°C; the excess of NaH was hydrolyzed with EtOH (20ml) and was concentrated. The resulting yellow oil was diluted in Et_2O and the organic layer was extracted with a saturated solution of $NaHCO_3$. The aqueous layer was acidified to pH 1 with HCl 1N, extracted with Et_2O, dried over $MgSO_4$ and concentrated under reduced pressure to yield 9.87g of compound **22**. The resulting compound **22** was used without further purification for the next step.

^{1}H-NMR ($CDCl_3$, 400 MHz): δ 7.28 (d, -Ph-), 6.89 (d, -Ph-), 4.58 (s, - Ph-C**H**$_2$-O-), 4.10 (s, -C**H**$_2$-O-), 3.80 (s, C**H**$_3$-O-) ppm

^{13}C-NMR ($CDCl_3$, 400 MHz): 174.14 (-**C**=O) 159.73 (-Ph) 129.60 (-Ph) 129.99 (Ph-) 113.19 (-Ph) 73.19 (Ph-**C**H$_2$-O-) 66.28 (-O-**C**H$_2$-) 55.48 (-O-**C**H$_3$) ppm.

allyl 2-(4-methoxybenzyloxy)acetate [23]

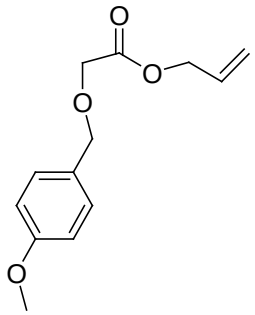

$C_{13}H_{16}O_4$
Mol. Wt.: 236,26

Acid **22** (9.87g, 50.31mmol) was dissolved in dry DCM (83ml) and cooled to 0°C. Afterwards DCC (1.1eq, 55.34mmol) and DMAP (0.5eq, 25.15mmol) were added portion wise. The reaction was stirred overnight at room temperature. After filtration, the mixture was concentrated under reduced pressure. The crude product was than purified by column chromatography (PE:EE 9:1) to yield 2.90g of compound **23**.

Yield: 24%

^{1}H-NMR ($CDCl_3$, 400 MHz): δ 7.29 (d, -Ph-), 6.88 (d, -Ar-), 5.92 (m, -C**H**=CH_2), 5.29 (m, C**H$_2$**=CH-), 4.61 (dd, -CH-C**H$_2$**-O-), 4.57 (s, -Ph-C**H$_2$**-O-), 4.09 (s, -C**H$_2$**-O-), 3.08 (s, C**H$_3$**-O-) ppm.

^{13}C-NMR ($CDCl_3$, 400 MHz): 170.12 (-**C**=O) 159.54 (-Ph) 131.75 (CH_2=**C**H-) 129.78 (-Ph) 129.15 (Ph-) 118.81 (**C**H_2=CH-) 113.91 (-Ph) 73.00 (Ph-**C**H_2-O-) 66.83 (-O-**C**H_2-) 65.42 (-CH-**C**H_2-O-), 55.29 (-O-**C**H_3) ppm.

2-(4-methoxybenzyloxy)pent-4-enoic acid [24]

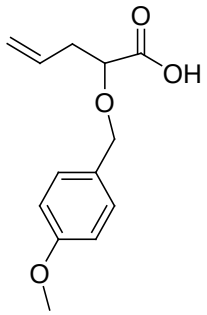

$C_{13}H_{16}O_4$
Mol. Wt.: 236,26

A Solution of LHMDS 1M in THF (2.0eq, 37.16mmol) was cooled at -78°C, then allyl ester **23** was added dropwise via a canula. The mixture was stirred one hour at -78°C and TMSCl (5eq, 92.9mmol) was added portion wise. The reaction mixture was stirred an extra hour at the mentioned temperature and gradually was let reach room temperature over 12 hours. Th reaction was quenched by adding HCl 1M at 0°C. The amount of acid necessary to quench the reaction is indicated by the reaction itself, as its colour varied from cloudy to clear yellow. The mixture was than concentrated and the aqueous phase was extracted with DCM (3x25ml). The organic phases were combined, dried over $MgSO_4$ and concentrated to yield 4.746g of compound **24**. The crude product was used for the next step without further purification.

^{1}H-NMR ($CDCl_3$, 400 MHz): δ 7.27 (d, -Ph-), 6.89 (d, -Ar-), 5.81 (m, -C**H**=CH_2), 5.12 (m, C**H$_2$**=CH-), 4.56 (dd, -Ph-C**H$_2$**-O-), 4.09 (m, -C**H**-CH_2-), 3.81 (s, C**H$_3$**-O-), 2.57 (m, -CH-C**H$_2$**-) ppm.

MS: (ESI, 4 kV) m/z (rel. Int.): 259.09 (100.0%).

methyl 2-(4-methoxybenzyloxy)pent-4-enoate [25]

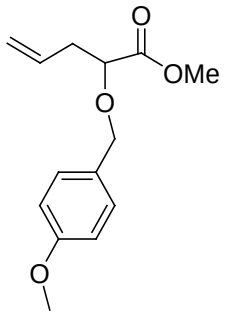

$C_{14}H_{18}O_4$
Mol. Wt.: 250,29

Procedure **a)**

Acid **24** (0.447g, 1.89mmol) was dissolved in a mixture of toluol:MeOH 1:1 (10ml). $TMSCHN_2$ 2M in Et_2O (2eq, 3.78mmol) was added drop wise to the resulting solution. The reaction was stirred not longer than 10 min and immediate evaporation under reduced pressure was performed. The crude product was purified by column chromatography (PE:EE 3:1) to yield 0.445g of ester **25**.

Yield: 93%

Procedure **b)**

Acid **24** (4.746g, 20.10mmol) was dissolved in dry MeOH (60.3ml), followed by the addition of a catalytically amount of *p*-TsOH (0.080g). DMP (1.2eq, 24.12mmol) was added drop wise to the reaction mixture. The reaction was stirred overnight at room temperature. After additional two hours of stirring, after addition of molecular sieves 4 Å to eliminate the water produced during the process, the reaction was filtrated, concentrated under reduced pressure, washed one time with $NaHCO_3$ solution (5ml) and extracted with DCM (3x 20ml). The organic phases were combined, dried over $MgSO_4$ and concentrated. The crude product was than purified by column chromatography (PE:EE 3:1) to yield 4.191g of compound **25**.

Yield: 83%

^{1}H-NMR ($CDCl_3$, 400 MHz): δ 7.27 (d, -Ph-), 6.87 (d, -Ar-), 5.81 (m, -C**H**=CH_2), 5.08 (m, C**H$_2$**=CH-), 4.53 (dd, -Ph-C**H$_2$-**O-), 3.98 (t, -C**H**-CH_2-, J=6.43 Hz), 3.82 (s, C**H$_3$**-O-), 3.73 (s, C**H$_3$**-O-), 2.51 (m, -CH-C**H$_2$**-, J=6.43 Hz) ppm.

^{13}C-NMR ($CDCl_3$, 400 MHz): 172.68 (-**C**=O), 159.42 (-Ph), 133.08 (CH_2=**C**H-), 129.50 (-Ph), 129.35 (Ph-), 117.88 (**C**H_2=CH-), 114.02 (-Ph), 77.46 (-CH_2-**C**H-), 73.00 (Ph-**C**H_2-O-), 57.79 (-O-**C**H_3-), 51.79 (-O-**C**H_3), 37.32 (-CH-**C**H_2-), ppm.

MS: (ESI, 4 kV) m/z (rel. Int.): 273.11 (100.0%).

2-(4-methoxybenzyloxy)pent-4-enal [26]

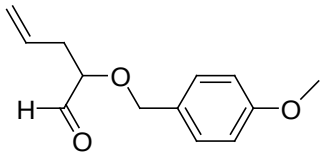

$C_{13}H_{16}O_3$
Mol. Wt.: 220,26

Procedure **a)**

The educt **17** (0.114g, 0.47mmol) was solved in 10ml THF and 15ml water and cooled at 0°C. To the solution, $NaIO_4$ was added (1.2eq, 0.56mmol), the reaction mixture was stirred for some minutes at 0°C, then for 2h at room temperature. The process was followed by TLC (PE/EE 1:1). Afterwards the mixture was extracted with Et_2O (3x10ml), the combined organic layers were washed with brine (2x10ml), dried over $MgSO_4$ and concentrated under reduce pressure. Column chromatography (PE:EE 2:1) was performed to yield 0.101g of aldehyde **26**.

Yield: 97%

Procedure **b)**

The educt **20** (0.164g, 0.62mmol) was solved in dry CH_2Cl_2 under argon and cooled at -78°C. DIBAL 1.0M in heptane (1.0eq, 0.620mmol) was added drop wise to the solution over 30min. After the addition, the reaction was stirred for 1 hour at -78°C. The excess of DIBAL was quenched with MeOH (5ml) and a saturated solution of hydrogen sulphate (3ml). The reaction was let reach room temperature and an extraction with Et_2O (4x10ml) was performed. The combined organic layers were washed with brine (1x5ml), dried over $MgSO_4$ and concentrated under reduce pressure. Column chromatography (PE:EE 3:1) was performed to yield 0.012g of aldehyde **26**.

Yield: 25%

Procedure **c)**

The educt **25** (0.150g, 0.59mmol) was dissolved in dry CH_2Cl_2 under argon and cooled at -78°C. DIBAL 1.0M in toluol (1.2eq, 0.72mmol) was added drop wise to the solution. After the addition, the reaction was followed by TLC (PE/EE 3:1) and stirred at -78°C until the starting material was consumed. At reaction completion, the excess of DIBAL was quenched with MeOH (10ml).The reaction was let reach room temperature and an extraction with Et_2O (4x10ml) was performed. The combined organic layers were washed with brine (1x5ml), dried over $MgSO_4$ and concentrated under reduce pressure. Column chromatography (PE:EE 3:1) was performed to yield 0.096g of aldehyde **26**.

Yield: 72%

^{1}H-NMR ($CDCl_3$, 400 MHz): δ 9.62 (d, -C**H**O, J=2.04 Hz), 7.25(m, -**Ph**), 6.88(m, -**Ph**), 5.80 (m, CH_2=C**H**-), 5.12 (m, C**H$_2$**=CH-), 4.57 (m, -C**H$_2$**-Ph-), 3.81 (s, C**H$_3$-**O-Ph-), 3.78 (m, -C**H-,** J=2.04 Hz), 2.46 (m, **-CH$_2$ -)**, ppm.

ethyl 5-(4-methoxybenzyloxy)-4-hydroxy-2-methyleneoct-7-enoate [27]

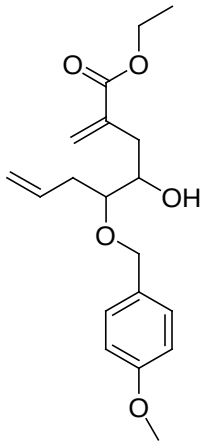

$C_{19}H_{26}O_5$
Mol. Wt.: 334,41

Aldehyde **26** (2.131g, 9.67mmol) was portioned in three Erlenmeyer flasks and each portion was dissolved into a mixture of H_2O:EtOH 3:1 (20ml/flask). For each portion, Indium (1.8eq), Ethyl-2-(bromomethyl)acrylate 7 (1.5eq) and LiCl (0.07eq) were subsequently added. Then the suspension was sonicated at 50°C until complete consumption of the starting material (TLC PE:EE= 3:1). White precipitate had formed due to the formation of indium salts. This precipitate can be destroyed by adding some drops of HCl 1M. The suspension was decanted to remove unreacted indium. After combining the content of each flask, an extraction with ethyl acetate (4x30ml) followed. The combined organic layers were washed with NH_4Cl sat. (20ml), dried over $MgSO_4$ and concentrated under reduced pressure. In order to purify the crude product a column chromatography (solvent: PE:EE= 3:1) was made. Fractions were collected and concentrated under reduced pressure to yield 1.957g of the final compound **27**.

Yield: 60%

^{1}H-NMR ($CDCl_3$, 400 MHz): δ 7.26(dd, -**Ph**), 6.88 (dd, -**Ph**), 6.23 (dd, C**H$_2$**=C-, J=1.40 Hz, J=7.18 Hz), 5.81 (m, CH_2=C**H**-), 5.64 (dd, C**H$_2$**=C-), 5.11 (m, C**H$_2$**=CH-), 4.53(m, C**H$_2$**- CH_3), 4.21 (m, -C**H$_2$**-Ph-), 3.81 (m/s, -C**H**-OH, -O-C**H$_3$**), 3.42 (m, -C**H**-OH), 2.50 (m, -C**H$_2$**-CH-CH-C**H$_2$**-, -OH), 1.29 (m, -C**H$_3$**) ppm.

^{13}C-NMR ($CDCl_3$, 400 MHz): 167.83 (-**C**=O) 159.34 (-**C**-O-) 137.80 (-**C**=CH_2) 134.93(-**C**H=CH_2) 130.58 (-**C**-CH_2-) 129.50 (-**Ph**) 127.43 (**C**H_2=C-) 117.51 (**C**H_2-CH-) 113.87 (-**Ph**) 81.31(-**C**H-O-) 71.86(-**C**H_2-O-) 71.75 (-**C**H-OH) 60.97 (-**C**H_2-CH_3) 55.29 (-O-**C**H_3) 36.46 (-CH-**C**H_2-CH-) 34.81(-C-**C**H_2-CH-) 14.18 (-CH_2-**C**H_3) ppm.

ethyl 4-(4-methoxybenzyloxy)-5-hydroxycyclohex-1-enecarboxylate [28]

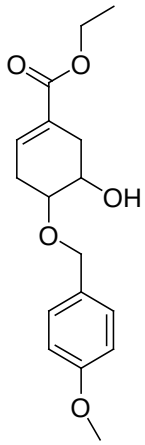

$C_{17}H_{22}O_5$
Mol. Wt.: 306,35

The educt **27** (1.957g, 8.86mmol) was dissolved in dry CH_2Cl_2 (500mL). The catalyst **8** ((1,3-Bis(2,4,6-trimethylphenyl)-2-imidazolidinylidene)dichloro(phenylmethylene)-(tricyclohexylphosphine)ruthenium), common known as Grubbs Catalyst 2nd Generation (0.12eq, 0.7mmol), was added. The catalyst used for the reaction was purchased from Sigma-Aldrich (CAS: 246047-72-3). It can eventually also be prepared in situ (as described for compound **15**). The mixture was stirred 12h at 45 C. The reaction process was monitored by TLC (PE:EE= 2:1). At reaction completion, the solution was concentrated under reduced pressure. Purification by column chromatography (solvent: PE:EE= 1:1) followed. Fractions were collected and finally concentrated under reduced pressure to yield 1.626g of the final product **28**.

Yield: 90%

^{1}**H-NMR** ($CDCl_3$, 400 MHz): δ 7.27(dd, -**Ph**), 6.88 (dd, -**Ph**), 6.47 (m, C**H**=C-), 4.56 (m, C**H**$_2$-CH_3, J=7.16 Hz), 4.18 (m, C**H**$_2$=C-), 4.13 (m, C**H**-O-), 3.81 (s, -C**H**$_3$**-O-**), 3.60-3.50 (m, -C**H**-OH), 2.91-2.13 (m, -C**H**$_2$-CH-CH-C**H**$_2$-, -OH), 1.27 (dd, -C**H**$_3$**,** J=7.16 Hz) ppm.

^{13}**C-NMR** ($CDCl_3$, 400 MHz): 166.67 (-**C**=O) 159.45 (-**C**-O-) 135.65 (-C=**C**H-) 130.14 (-**C**-CH_2) 129.47 (-**Ph**) 129.47 (-**Ph**) 128.43 (-CH-**C**-) 113.99 (-**Ph**) 77.85 (-**C**H-O-) 71.28 (-

CH_2-O-) 69.53 (-**C**H-OH) 60.56 (-**C**H_2-CH_3) 55.30 (-O-**C**H_3) 31.25 (-C-**C**H_2-CH-) 27.80 (-CH-**C**H_2-CH-) 14.25 (-CH_2-**C**H_3) ppm.

ethyl 4,5-dihydroxycyclohex-1-enecarboxylate [29]

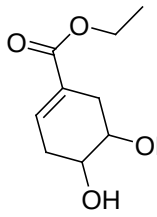

$C_9H_{14}O_4$
Mol. Wt.: 186,21

Procedure **a)**

The educt **28** (0.467g, 1.52mmol) was dissolved in dry CH_2Cl_2 (5mL). Triflic acid (0.5eq, 0.76mmol) was added drop wise under a light flow of Argon. The mixture was stirred 10 to 20min at room temperature. The reaction process was monitored by TLC (PE:EE= 1:1). At reaction completion, the solution was concentrated under reduced pressure. Purification by column chromatography (solvent: PE:EE= 1:1) followed. Fractions were collected and finally concentrated under reduced pressure to yield 0.312g of the final product **29**.

Yield: complete conversion.

Procedure **b)**

Compound **28** (0.840g, 2.74mmol) was dissolved in acetone/water mixture (20.7ml : 3ml). A first portion of solid CAN (0.5eq, 1.37mmol) was added and the reaction was stirred for 15min at room temperature. In the meanwhile a CAN solution, in the previously mentioned solvent mixture, was prepared (0.750g in 1.5ml acetone : water). The CAN solution was added drop wise and a change in color from yellow to green was observed. The reaction was monitored by TLC (PE:EE 1:1). At reaction completion, the solution was concentrated under reduced pressure. An extraction with EtOAc (2x20 ml)

was performed. The organic phases were collected and dried over $MgSO_4$. After evaporation of the solvent the crude product was obtained. Purification by column chromatography (PE:EE 1:1) yielded 0.220g of compound **29**.

Yield: 43%

^{1}H-NMR ($CDCl_3$, 400 MHz): δ 6.83 (dd, -C**H**=C-), 4.18 (q, C**H$_2$**-CH$_3$, J=7.15 Hz), 3.97 (m, C**H-**OH), 3.72 (m, -C**H**-OH), 2.88-2.22 (m, -C**H$_2$**-CH-CH-C**H$_2$**-, 2x -OH), 1.27 (dd, -C**H$_3$,** J=7.15 Hz) ppm.

^{13}C-NMR ($CDCl_3$, 400 MHz): 166.26 (-**C**=O) 136.03 (-C=**C**H-) 128.34 (-**C**-CH-) 71.54 (-**C**H-OH) 68.63 (-**C**H-OH) 60.68 (-**C**H$_2$-CH$_3$) 33.06 (-CH-**C**H$_2$-CH-) 31.12 (-CH-**C**H$_2$-CH-) 14.24 (-**C**H$_3$) ppm.

benzoic acid [30]

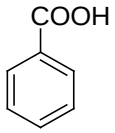

$C_7H_6O_2$
Mol. Wt.: 122,12

Ester **28** (0.580g, 3.114mmol) was dissolved in a solution of H_2SO_4 1M in acetic acid. The reaction mixture was stirred overnight at 120°C. At reaction completion an extraction with EtOAc (2x5ml) was performed. The organic phases were combined, dried over $MgSO_4$ and evaporated under reduced pressure. The crude product was purified by column chromatography (PE:EE 1:1) to yield 0.109g of compound **30** as white precipitate.

Yield: 29%

^{1}H-NMR ($CDCl_3$, 400 MHz): δ 8.12 (d, 2x-C**H**-, J=7.15 Hz), 7.61 (t, -C**H**-), 7.48 (t, 2x-C**H**-, J=7.15 Hz), ppm.

^{13}C-NMR ($CDCl_3$, 400 MHz): 171.68 (-**C**=O), 134.16 (-**C**H-), 130.61 (2x-**C**H-), 129.63 (-**C**-), 127.85 (2x-**C**H-) ppm.

IR: C=O, 1682cm^{-1}

Part B

Towards the synthesis of potentially bioactive 3-Deoxy-sugars

1. Introduction and aim of the project

1.1. Aim of the project

This project aimed to investigate new strategies for the synthesis of deoxy-carbohydrates. One of the goals was to develop a versatile and flexible synthetic route for the preparation of 3-Deoxy-sugars on a preparative scale.

This approach was set up as a reaction sequence, which is shown in the retro synthetic scheme below (Figure 29).

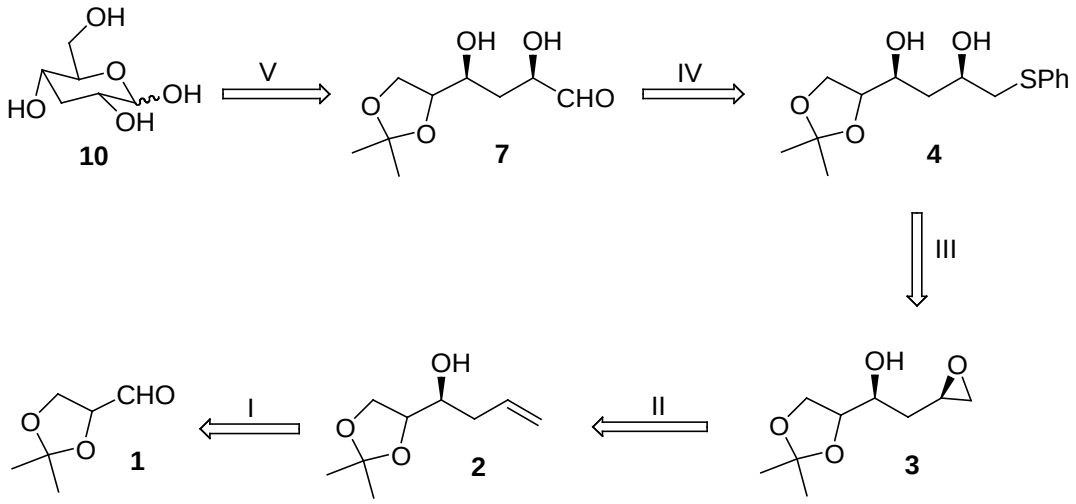

Figure 29: Synthetic strategy for the synthesis of 3-Deoxy-sugars.

The sequence starts with easily accessible D-glyceraldehyde, obtained from commercially available D-mannitol. The strategy towards the target deoxy sugar breaks down into the following five steps

I. the indium-mediated allylation reaction of the aldehyde,

II. the selective epoxidation,

III. the regioselective epoxide opening,

IV. the Pummerer rearrangement and

V. the cyclization to the final sugar.

Based on this approach it was assumed that synthesising iminosugars by changing the starting material from D-glyceraldehyde to (*S*)-(-)-3-Boc-2,2-dimethyloxazolidine-4-carboxaldehyde, commonly known as Garner´s aldehyde, would be possible as well. The planned approach was based on the following retrosynthetic scheme (Figure 30):

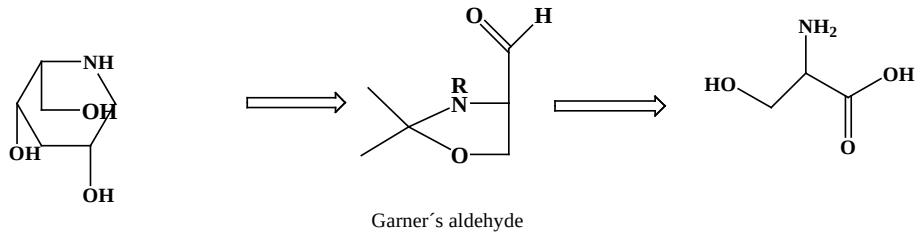

Garner´s aldehyde

Figure 30: Retrosynthetic strategy starting from Garner´s aldehyde.

Although this work focuses solemnly on the synthesis of 3-deoxy sugars, the possibility to cover both, the synthesis of iminosugars as well as of 3-deoxy sugars, with only one route, suggests to be a powerful tool for future works. From a theoretical perspective the adaption of this pathway for both compounds seemed achievable.

1.2. The biological role of carbohydrates

Carbohydrates have several biological functions, including the ability to store and transport energy (e.g.: starch, glycogen) and are also known as structural components of the cellulose in plants and cartilage in animals (76).

In the last decade, important progresses in the field of glycomics have been made. Glycomics studies the role of carbohydrates in biological processes, with the purpose to understand and clarify the different interactions between carbohydrate–carbohydrate, carbohydrate–protein, and carbohydrate–nucleic acid interactions (as shown in Figure 31) (77).

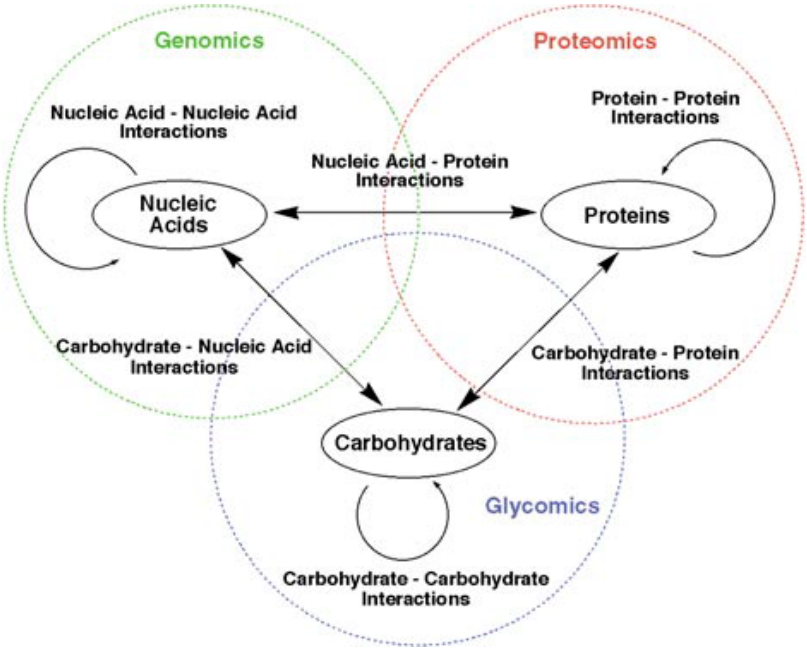

Figure 31: Interactions of biopolymers (78).

Different forms of carbohydrates are studied, as in each form (glycopeptides, glycolipids, glycosaminoglycans, proteoglycans or other glycoconjugates) entirely different biological processes may be involved. Carbohydrates present on the cell surface are used as linkage sites for other cells, bacterials, viruses, toxins, hormones and other different substances as an example. Other examples of important processes are signal transduction and inflammation (77) (78).

1.3. Deoxy sugars

Deoxy sugars are defined as monosaccharides having one or more hydroxyl groups substituted by a hydrogen atom. The mentioned carbohydrate family may be found in different plants, bacterial and fungi and in addition they show interesting biological activities (79). They are used as structural component of antibiotics (79) (80) and are components of many natural products of which three examples are shown in Table 9.

No.	name	structure
1	L-fucose, 6-deoxy-L-*galacto*-hexose	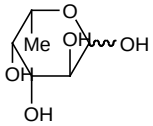
2	L-Rhamnose, 6-deoxy-L-mannose	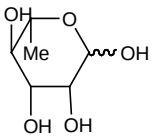
3	Cordycepose, 3-deoxy-D-*erythro*-pentose	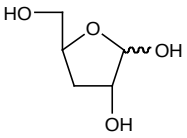

Table 9: Example of different deoxy sugars and theirs structures.

Structural differences can be observed, inheriting different properties to the respective component. L-Fucose (**1**) is a characteristic component of glycan structures. It is found on mammalians, insects and plant cell surfaces (81). L-Rhamnose (**2**) is a common glycone component of glycosides from many plants. This sugar can also be found as component of outer cell membrane bacteria such as Mycobacterium genus, the organism that causes tuberculosis (82). The only example of naturally present 3-deoxy sugars is cordycepose (**3**), the carbohydrate component of cordycepin, a derivative of the nucleoside adenosine (83).

The substitution of the hydroxyl group(s) by a hydrogen atom is as well of major importance as it may vary the biological function of the molecule, therefore also influencing the metabolism of the sugar molecule. It was however shown that the surface-properties of an organism can be altered by including a deoxy sugar as a structural component, therefore altering the compounds or organisms way of interfacing with its surrounding. Examples include the use of sialic acid as time-passage marker for the control of the glycoprotein circulation or the linkage of deoxy sugars to a glycine which can regulate the water-lipid solubility and simultaneously regulate the cardiac glycosides (84).

1.4. Biosynthesis of Deoxy sugars

Ribonucleotide reductase is the most prominent enzyme involved in the biosynthesis of deoxy sugars, as it is involved in the formation of deoxyribonucleotide (84) (Figure 32), the monomer units of the DNA.

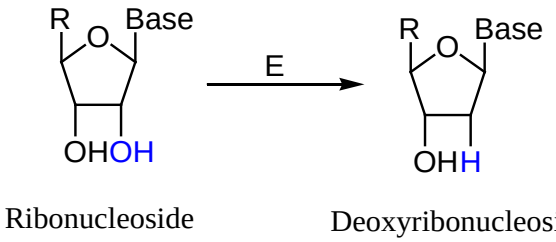

Figure 32: Conversion from ribonucleoside to deoxyribonucleoside.

Ribonucleotides are easily synthesized using simple components such as amino acids, tetrahydrofolate derivatives, NH_4^+ and CO_2. The biological synthesis of deoxyribonucleotides on the other hand is an enzymatic reaction, catalyzed by ribonucleotide reductase (RNR) which' major purpose is the synthesis of DNA.

RNR was furthermore subject for investigations in anti-bacterial, anti-viral and anti-cancer drug development as well as cancer therapy. Recently a human RNR, being regulated by the p53 protein, was discovered which actively suppresses the formation of a tumor. This is specifically interesting as p53 protein forms various forms of cancer when mutated, which was found to be the case in more than 80% of human tumors (85) (86).

Studies of the mechanics of ribonucleotide reductase were made for 2-deoxy sugars and independently from the cofactor and structure, being different each time, a common radical mechanism has been understood (87). RNR is built by two components, a reductase and a radical generator, which produces and stores a radical used in the first step of the reaction sequence (86).

The same type of mechanism was elucidated also for the biosynthesis of 3-deoxy sugars via radioisotopes labeling studies. The main step in the biosynthesis of cordycepin is given by a radical mechanism which goes from adenosine to the final sugar (88).

1.4.1. Structure and function of Ribonucleotide reductase

Three classes of ribonucleotide reductase have been defined. Each class is characterized by different compositions and different co-factors (89). The structure of Class I has been obtained from *E.Coli* in the 1950s, containing a hydroxy urea sensitive tyrosyl radical and a diiron-oxo metal site, which are the characteristics of the enzyme (90). Isolation of the enzyme from *Lactobacillus Leichnannii* gives the structure belonging to Class II in which the enzyme has an adenosylcabalamin co-factor (91). Lastly, Class III includes an oxygen-sensitive enzyme.

Class	Occurrence	Cofactor	Active radicals	Reduction system
I	Mammals	Fe^{3+} -O^{2} -Fe^{3+}	Tyrosyl –cysteinyl	Thioredoxin/ glutaredoxin
	Plants, Yeast, DNA-viruses, *E. coli*			
	Prokaryotes	Fe^{3+} -O^{2} -Fe^{3+}	Tyrosyl -cysteinyl	Redoxin
II	Prokaryotes	Adenosyl cobalamin	Adenylyl -cysteinyl	
III	Prokaryotes (anaerobs)	[Fe-S] S-adenosin-methionine	Glyeyl -cysteinyl	Formate

Table 10: Classes of ribonucleotide reductase.

Independent of the class, and therefore the differently applied mechanisms, the common feature to all enzymes is the generation of a radical specie during their reaction (92).

The *E. Coli* ribonucleotide reductase (RDPR) is used as a prototype for the explanation of the radical mechanism. As described in literature (93) (94), the structure has been elucidated by Stubbe et al. (95):

> "*The RNRs from E. coli and mammals, as well as those encoded by several medically important viruses (e.g. herpes simplex, and rabies), share a common quaternary structural motif and metallocofactor requirement. Each is composed of two homodimeric subunits, which are both required for catalytic activity. The larger subunit, designated*

R1, contains the following in each of its protomers: binding sites for the nucleoside diphosphate substrates and the nucleoside and deoxynucleoside triphosphate allosteric effectors and multiple cysteine residues which cycle between sulfhydryl and disulfide forms to deliver reducing equivalents to the substrate. The smaller subunit, R2, contains the enzyme's catalytically essential, complex metallocofactor, a oxo-bridged diiron (III) cluster in close proximity to a stable tyrosyl free radical […]" (95)

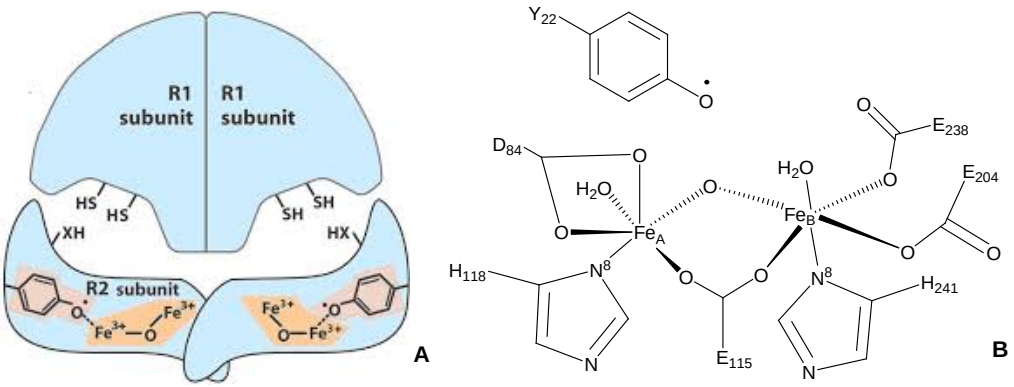

Figure 33: RDPR **A**: Schematic diagram of the interaction (94),

B: Proposed structure of the iron center (95).

As described in literature (96), the enzyme's active site is understood to be at the interface between the two subunits. A radical-mediated reduction reaction is responsible for the formation of the tyrosyl radical species.

1.4.2. Reaction radical mechanism

The reduction of the ribose moiety, present on a nucleoside di- or triphosphate, leads to 2´-deoxyribonucleoside. This reduction represents the core of the reaction sequence, performed from the enzyme ribonucleotide reductase. The proposed mechanism (Figure 34) for the formation of the radical intermediate involves, as initiation step, a one-electron oxidation of the substrate to form a cysteinyl radical (97). A hydrogen atom is taken from position 3 of the ribonucleotide in order to create the ribonucleotide radical. One of the redox-active thiols acts as a catalyst for the protonation of 2-hydroxyl and, as a consequence of this step, water is eliminated. Further steps involve a reduction of this radical intermediate, performed by dithiol oxidation via two one-electron transfers and a

protonation to create the 3-deoxynucleotide radical. The tyrosyl radical can then be regenerated through reduction to the dNDP product via oxidation of the tyrosine (98).

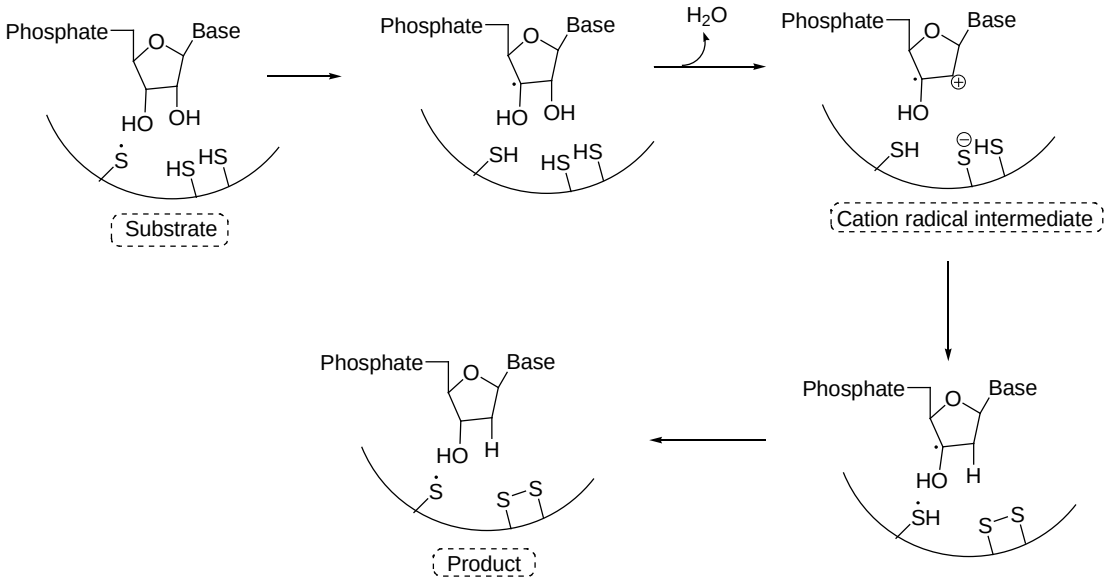

Figure 34: Proposed reaction mechanism (97).

1.4.3. From bio- to synthetic synthesis: the case of 3-deoxyadenosine

3-deoxy sugars are commonly prepared by nucleophile opening of the anhydro ring. The nucleophile specie used for this purpose must be subsequently reduced by hydride or hydrogenolysis to yield the desired deoxy function (99).

This chapter especially focuses on the synthesis of cordecypin (or 3-deoxyadenosin) which is the first reported nucleoside antibiotic, well-known in the traditional Chinese medicine (100).

The structure of this antibiotic (Figure 35) contains the one isolated 3-deoxy sugar from natural source, cordycepose, which appears in the structure as branched-chain sugar (101). Raphael and Roxburgh (102) describe the synthesis of this carbohydrate starting from diethyl-2-(dideoxyethyl)malonate.

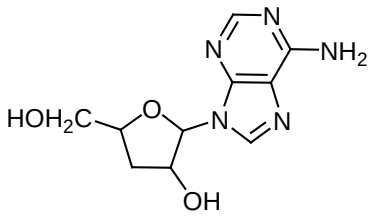

Figure 35: Structure of cordecypin.

Cordycepin is a purine nucleoside antimetabolite and antibiotic with potential antineoplastic activity. It is isolated from the fungus *Cordyceps militaris*. The capability of the structure to be phosphorylated gives important properties to the molecule. As an example, cordycepin triphosphate can be incorporated into RNA, the absence of a hydroxyl group at the position 3' makes the inhibition of the transcription elongation and RNA synthesis possible (103).

The synthesis of cordycepin was described in 1964 by Walton. The strategy towards the formation of a 2,5-di-*O*-benzoy-3-deoxy-D-ribofuranoyl intermediate, starts with the stereospecific reduction of methyl 2,3-anhydro-β-D-ribofuranoside **1m** over Raney nickel catalyst, which produces 3-deoxyribose derivative **2m**. Subsequent benzoylation with benzoyl chloride in presence of pyridine yields the furanoside derivative **3m**. Further reaction with hydrogen dromide in acetic acid allows the conversion from compound **3m**

to structure **4m** which, in two further steps, is coupled with a purine derivative to obtain the desired compound **5m** (104).

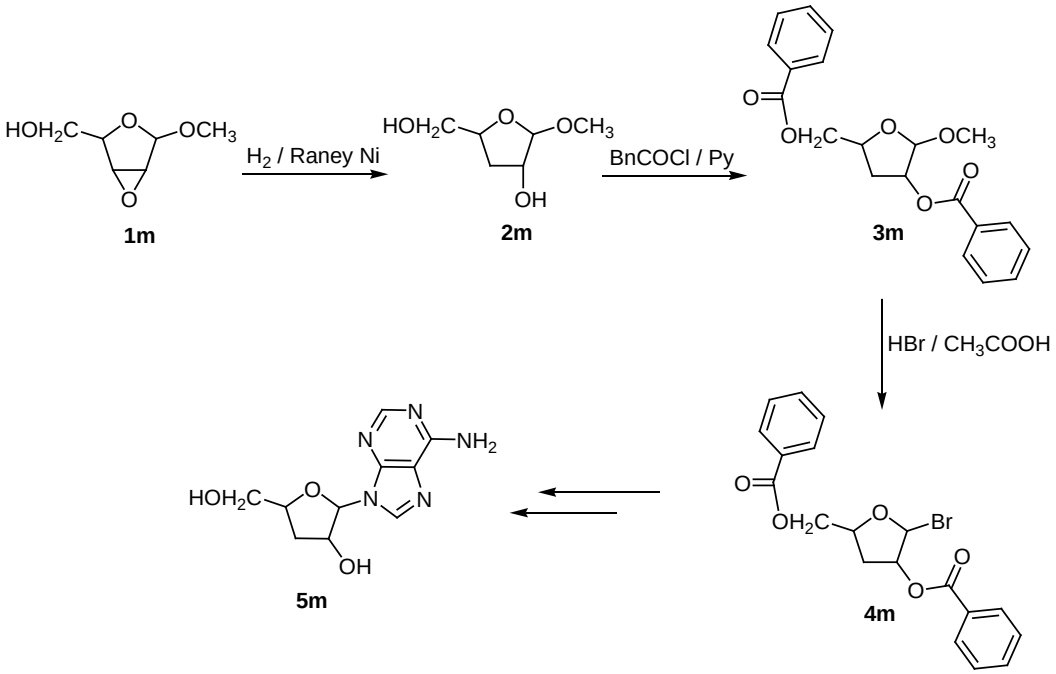

Figure 36: Synthesis of cordycepin described by Walton (104).

Recently, many other strategies were performed starting from sugar and non-sugar precursors as reported in the work from Chu et.al. (105), with the intent of improving the molecules reactivity. Azide derivatives of cordycepin are used in drugs as they perform more efficiently and increase the drugs half-life (105).

1.5. Synthetic strategies for the preparation of deoxy sugars: an overview

Several methods for the preparation of deoxy sugars as well as procedures for the total synthesis of deoxy sugars, starting from non-carbohydrate precursors, are published (106). A description of applicable methods for the synthesis of different deoxy sugars is given in this chapter, focusing specifically on monosaccharides.

Mono deoxy sugars can be prepared by applying reductive methods, starting from different compounds such as epoxides, thio sugars, carboxylate esters or, if possible, by direct reduction of hydroxyl groups. Other methods based on the reduction of carbonyl groups may be as well applied (107).

Preparation of deoxy sugars through reduction of deoxy-halo sugars: Several reducing agents may be used for the preparation. Raney nickel represents a specifically good reducing agent for chloro derivates (Figure 37). A secondary chloride may be selectively reduced if the reaction is performed in presence of triethylamine. (108)

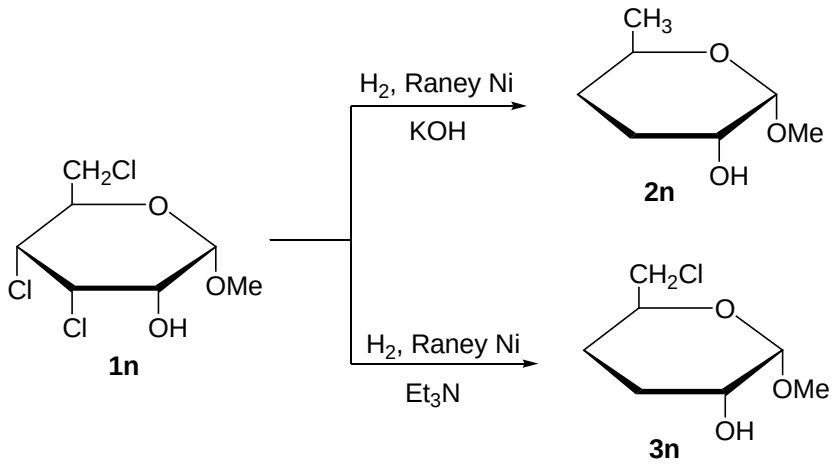

Figure 37: Reaction from chloro derivatives (107).

Preparation of deoxy sugars from sulfonates: Reduction of mesylates or tosylates can be achieved either directly or by creating an intermediate epoxide or halide. Reduction agents in this case may be lithium aluminium hydride or lithium triethyl borohydride. In the example given in Figure 38, tosylate **1p** is treated with lithium triethyl borohydride. The mechanism produces an epoxide intermediate to yield the final sugar 3-deoxy glycoside **2p**. The 2-deoxy sugar **5p** can instead be obtained starting from ditosylate **3p** via reduction of isomeric epoxide of compound **4p** (109).

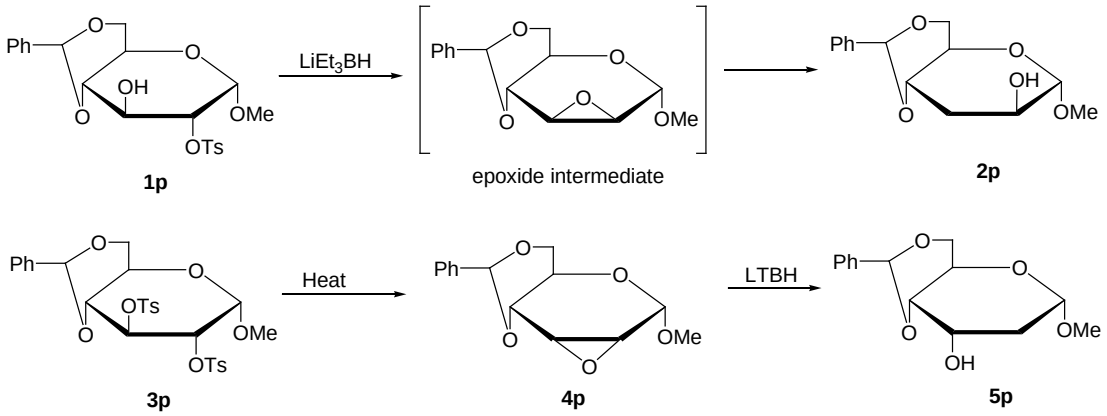

Figure 38: Reaction starting from sulfonates (107).

Preparation of deoxy sugars through radical-mediated deoxygenation: This type of mechanism can be performed by conversion of a hydroxyl group into a thiocarbonyl derivative and a subsequent reduction using tributyltin hydride. An example (Figure 39) were, starting from the 1,2:5,6-di-*O*-isopropylidene-α-D-glucofuranose **1q**, the 3-deoxy derivative **3q** can be yielded, is described in literature (110). The desired product is synthesized through a two-step reaction: conversion of compound **1q** into methyl xanthane **2q** and subsequent reduction with tributyltin hydride.

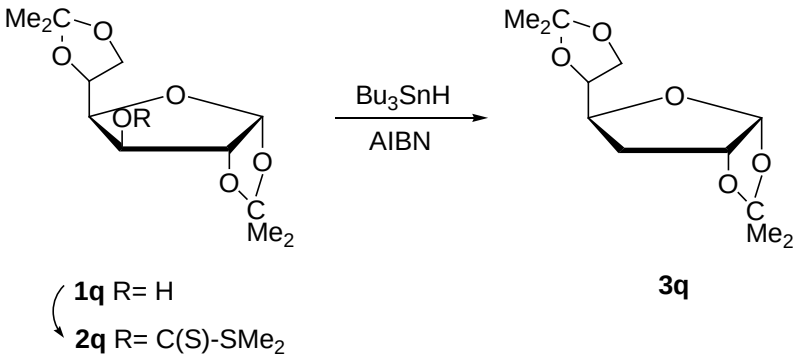

Figure 39: Conversion of 1,2:5,6-di-*O*-isopropylidene-α-D-glucofuranose to 3-deoxy derivative (107).

Starting from L-arabinose, this strategy can be applied also for the synthesis of compound **5r** (Figure 40) (111).

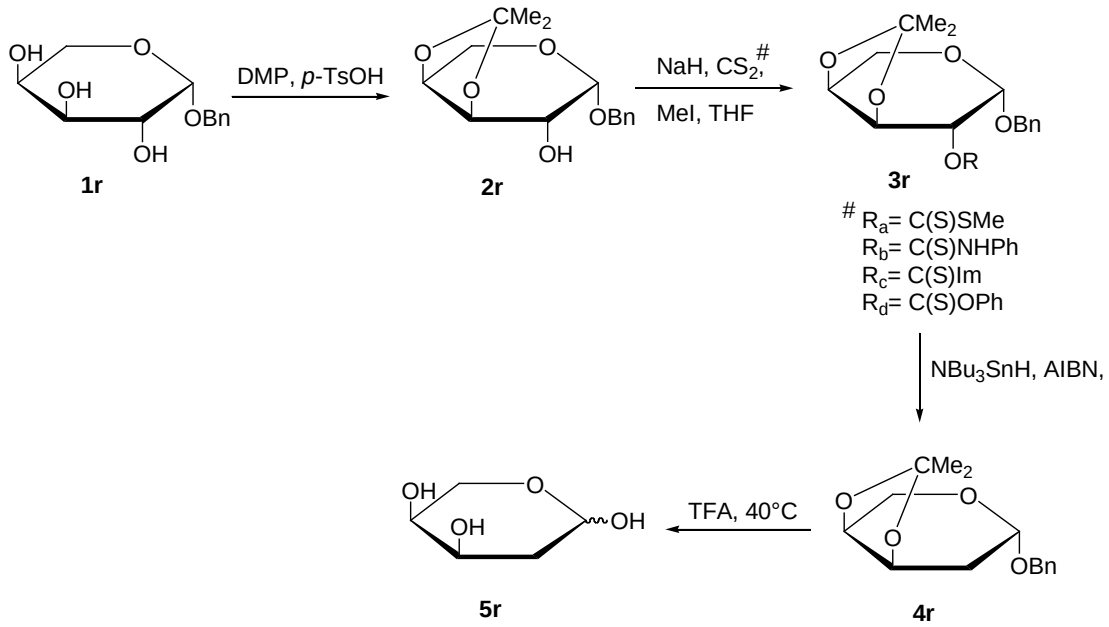

Figure 40: Synthesis of 2-deoxy-L-*erythro*-pentose (107).

By adopting the same strategy, 3-deoxy and 4-deoxy-β-D-hexopyranosides can be synthesized. The starting material is a galactoside derivative in this case (112) .

Due to the toxicity of the reagent used for this synthesis and the difficulty observed during the work up of the reactions, tributyltin as well as triphenyltin hydrides were replaced by silan derivatives such as [tris(trimethylsilyl)silane] (113) or the more expensive di- and triphenylsilane (114).

1.6. Brief introduction to iminosugars

Iminosugars are glycomics, characterized by the exchange of the endocyclic oxygen by a nitrogen atom. A lot of efforts were made towards a proper synthetic pathway for the formation of these sugars and of their non-synthetic analogs, in order to be able to perform structural studies and investigate the activity.

A variety of iminosugars have been isolated as natural products from both plants and microorganisms (e.g. fungi and bacteria) and they can generally be classified into five structural groups (115):

- polyhydroxylated pyrrolidines,
- piperidines,
- indolizidines,
- pyrrolizidines and
- nortropanes.

Polyhydroxylated piperidines represent the main class of glycosidase inhibitors.

Different challenges can be addressed for characterizing the structure of an iminosugar such as that

1. at least four contiguous stereogenic centres must be obtained with high stereochemical control,
2. the piperidine-ring must be generated efficiently and
3. due to the large number of functional groups, protecting groups must be selected carefully (115).

Iminosugars typically show excellent inhibitory properties against a number of enzymes of medicinal interest including glycosidases (116), glycosyltransferases, metalloproteinases or nucleoside-processing enzymes (117).

As a consequence of their inhibitory activity, iminosugars are vastly supporting developments of new therapeutic agents to a wide range of diseases. Various different structures are currently involved in clinical tests for the treatment of diabetes, the treatment of viral infections and a range of genetic diseases (e.g. cystic fibrosis and lysosomal storage disorders) (118).

The general approach for iminosugar-preparation involves carbohydrates as starting materials and through various transformations a nitrogen atom is introduced into the molecule (119).

2. Theoretical background for the key-reaction steps

2.1. Indium mediated allylation reaction

The metal-mediated addition of allyl-, aryl- and vinyl-halides to carbonyl groups, represents a versatile tool for chain elongation at the carbonyl functionality and is a powerful tool used in carbohydrate chemistry. Principally the process is comparable with the Grignard reactions, with the exception that the organometallic species will not be formed previously, but created in situ. The main benefit of this method is the possibility to be carried out in aqueous media (120).

Literature states, that many metals such as Al, Zn, Pb, Sn or Mg can be applied for these types of reactions but due to economic and environmental concerns, the mild reaction conditions and the simplicity of handling the metals, In and Zn have found the widest application (121) (122).

Indium is a metal of the 3rd group in the periodic table, which is characterized by soft plastic properties. The melting point is 157°C, which is comparably low. Indium is stable to air oxidation, water and bases, and its major advantage is its comparatively low toxicity.

The reactivity of metal catalyzed reactions is based on the capability to transfer electrons from the metal surface to an organic substrate. Therefore, the choice of the metal specie is based on the ionization potential, which the electron-transfer abilities of the catalyst are directly linked to.

Table 11 shows the ionization potential of different metals. As indicated by the table, compared with all other metals, In has the lowest first ionization potential, suitable for this transformation (zinc, tin or magnesium) (121).

metal	**Zn**	**Mg**	**Sn**	**In**	**Li**	**Na**
first ionization potential (eV)	9.39	7.56	7.43	5.79	5.39	5.12

Table 11: Ionization potential of different metals.

The use of indium for Barbier type reactions was first reported in 1991 by Li and Chan (121). In this work the focus was placed on a new synthesis performed in aqueous media (Figure 41).

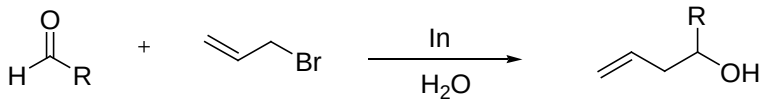

Figure 41: Indium Barbier type reaction.

The most significant aspect of the synthesis, as reported by Li and Chan (121), is its simplicity, only requiring to stir the mixture of the three compounds at room temperature. The ratio of the chemicals involved is 1:1.5:1, no protection of hydroxyl groups, if present in the substrate, is required as well as no promoter was needed (121).

2.1.1. Mechanism of the indium mediated reaction

As mentioned already in the previous paragraph, indium has become a popular metal due to its ability of tolerating diverse functional groups as well as diverse reaction conditions.

Many efforts in this area have been made in order to understand the mechanism of the formation of the active species. In this paragraph three different mechanisms are presented in chronological order.

Luche (123) first postulated the concept for the explanation of the mechanism of allylation reactions as a radical mechanism (Figure 42).

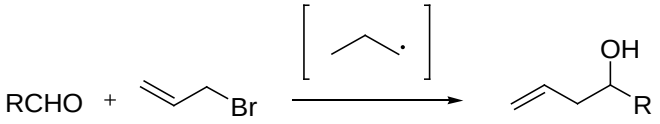

Figure 42: First proposed radical reaction mechanism.

A second proposed mechanism is based on the idea that a relatively low first ionization potential is favouring a single electron transfer (SET) process (Figure 43), taking place on the metal surface, on which the radical species is generated. It is proposed that during this process an allylindium intermediate is formed, which subsequently reacts with the initial substrate (124).

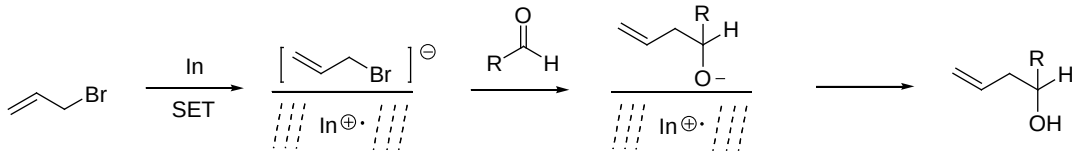

Figure 43: Single electron transfer reaction mechanism (SET).

Further studies revealed that, depending on the solvents used, two different indium intermediates can be formed. These are either sesquihalide intermediate $R_3In_2X_3$, when performed in organic solvents, or an allylindium(I) species, when performed in water. However, recent contributions, employing a variety of new strategies, including NMR, ESI-MS, kinetic studies, conductivity as well as X-ray crystal structures, demonstrate that the structures are more accurately described as diallylindium bromide and monoallylindium dibromide (125) (126).

Reactions between indium and aldehydes can produce several organoindium complexes such as allylindium(I), allylindium(III) dihalide, diallylindium(III) halide, triallylindium(III) and allylindium sesquialide (127). As all mentioned reactions are solvent-dependent, so are their intermediate complexes as well as their outcomes.

Araki et.al. proposed different allylindium compounds as intermediates, shown below in Figure 44 (128).

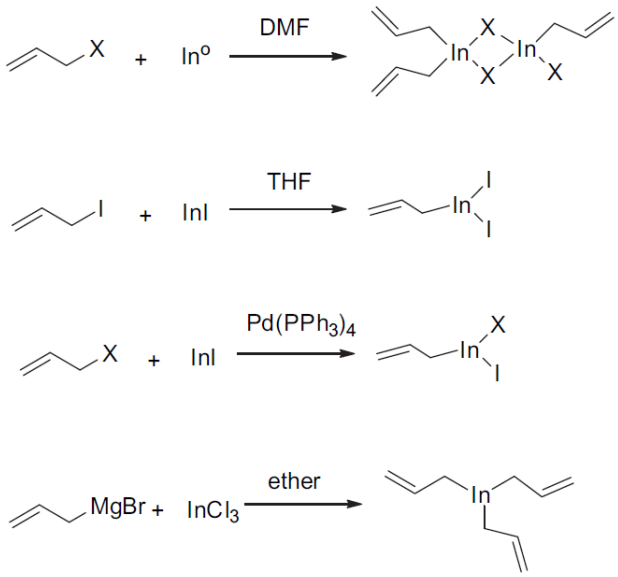

Figure 44: Allylindium compounds proposed as intermediates (128).

The conclusion Araki et.al. could draw during their studies were, that the solvent plays a major role in the formation of organoindium intermediates (62). By measurement of ^{1}H-NMR it was proposed, that aqueous solvents promote the formation of a more hydrolytically stable organoindium species. Polar aprotic solvents however produce a organoindium species with two different oxidation states (129) (130) (131).

2.1.2. Stereochemistry: theoretical explanation

The stereochemical result of the indium-mediated allylation of carbohydrates differs significantly between protected and unprotected sugar derivatives. The mechanism follows the Chelat-Cram model in case of an unprotected sugar. Through complexation of the indium with the carbonyl oxygen and the neighbouring hydroxy group, the nucleophile attack of the alkyl group is controlled in such a way, that a **syn**-configuration is formed between the newly generated hydroxy group at C1-position and the OH-group at the existing C2-atom of the aldehyde (Figure 45). This favorization can reach high diastereoselectivity towards the **syn(threo)**-product.

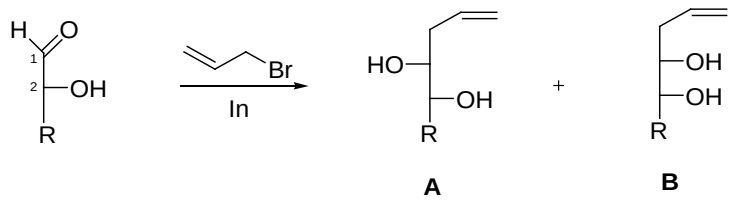

Figure 45: Stereochemical outcoming starting from an unprotected carbohydrate: A, threo product, B, erithro product.

The stereochemical situation changes when protected sugar derivatives are used as starting material. Through substitution of the hydroxy group at the C1-position with a respective protection group, the chelating effect of the indium is suppressed and the reaction will follow the Felkin-Anh model. Here the protection group acts as a "bulky group" at the C2-position, the molecule “re-structures” and the addition is conducted at the sterically least interfered side. The reaction builds an **anti(erythro)**-configuration (Figure 46) (61).

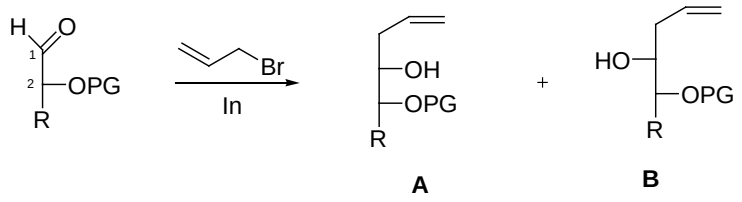

Figure 46: Stereochemical outcome starting from a protected carbohydrate: A, erythro product; B, threo product.

In this model, the three substituents at the stereogenic center are classified according to their size: S = small, M = medium and L = large. Through this model, the conformations of the transition state are analyzed and the steric effects, capable of destabilizing this transition state, can as well be evaluated.

When the substituent L is placed at 90° to the carbonyl oxygen and the substituent M is close to the carbonyl oxygen as well, the nucleophile will approach along the Bürgi-Dunitz trajectory from the opposite side of the substituent L. This is due to the minimized steric effects. The transition state in which a substituent is exactly 90° in respect to the carbonyl carbon is preferred, due to the stabilization of the LUMO of the carbonyl. The LUMO-orbitals are stabilized by the σ* orbital of the substituent, oriented

perpendicularly. The more stable the LUMO is, the stronger the interaction with the HOMO of the approaching nucleophile will be. Therefore, the observed stereo selectivity is a combination of a stereo-electronic and a steric-hindrance effect. While the first one favors a perpendicular substituent, the latter favors the approach of the nucleophile from the direction of the position held by the small substituent (61) (132).

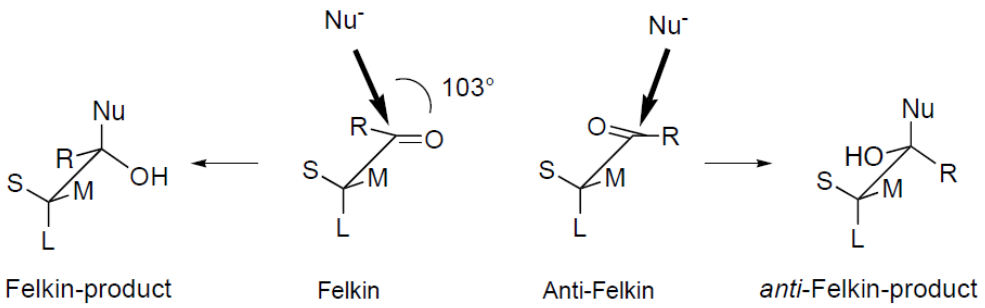

Figure 47: Felkin-Anh model

A different case occurs if the carbonyl compound has an electron withdrawing group on the stereocenter such as NR_2, OH or OR. In this case, the conformation assumed by the carbonyl compound is different. A rigid chelate conformation is formed, and the attack of the nucleophile occurs from the opposite side of the remaining L substituent.

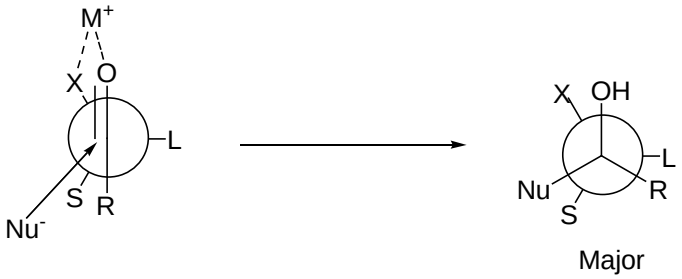

Figure 48: Felkin-Anh model of compound with electron withdrawing groups

When applied to the protected D-glyceraldehyde, as shown in Figure 49, **A** represents the Felkin-Anh product, which is favoured due to the lesser sterical effect of the isopropyliden protecting group, while **B** represents the Anti-Felkin-Ahn product.

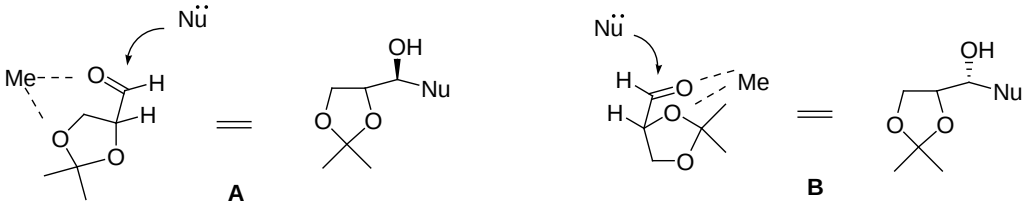

Figure 49: A, represents the Felkin-Anh product which is favoured, **B**, represents the Anti-Felkin-Ahn product.

2.2. Epoxidation

2.2.1. Fructose derivative as catalyst: Shi epoxidation

The commonly known Shi catalyst, developed in 1996, can be prepared from the very inexpensive and commercially available D-fructose via a 2 steps reaction (Figure 50). It is a highly effective epoxidation catalyst (133).

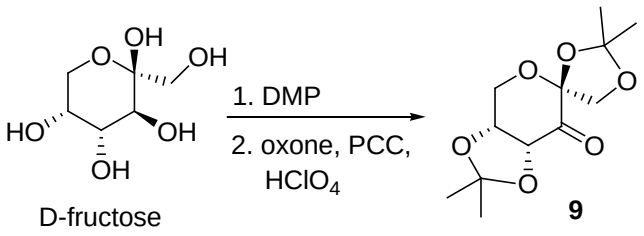

Figure 50: Shi catalyst preparation sequence.

Ketone **9** is the simplest of the Shi catalysts, almost seen as a "precursor" for the more complex structures. A variety of ketones were prepared to better understand the reactivity between the catalysts and the substrates. Shi reports (134) (135) that variation of the functional groups confers important diversity to the structure in the catalytic properties. It is reported, that structural variations showed increase in the reactivity as well as the replacement of the pyranoside oxygen by a carbon atom showed electronic effects on the catalyst (136). Figure 51 shows some of the different catalysts prepared.

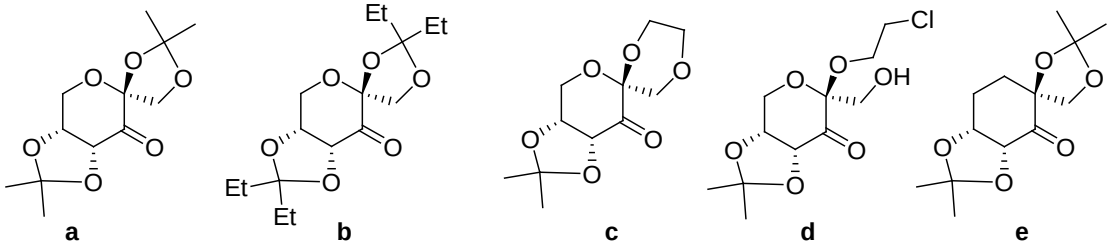

Figure 51: Different structures of catalyst (136).

Formation of a dioxirane specie, being usually generated from Oxone, represents the active side of the catalyst through which the desired epoxide is generated (137). The epoxidation can be performed using isolated dioxiranes or dioxiranes formed in situ. Figure 52 shows the catalytic cycle of the epoxidation, with special focus on the formation of the dioxiran specie and the regeneration of the catalyst (135).

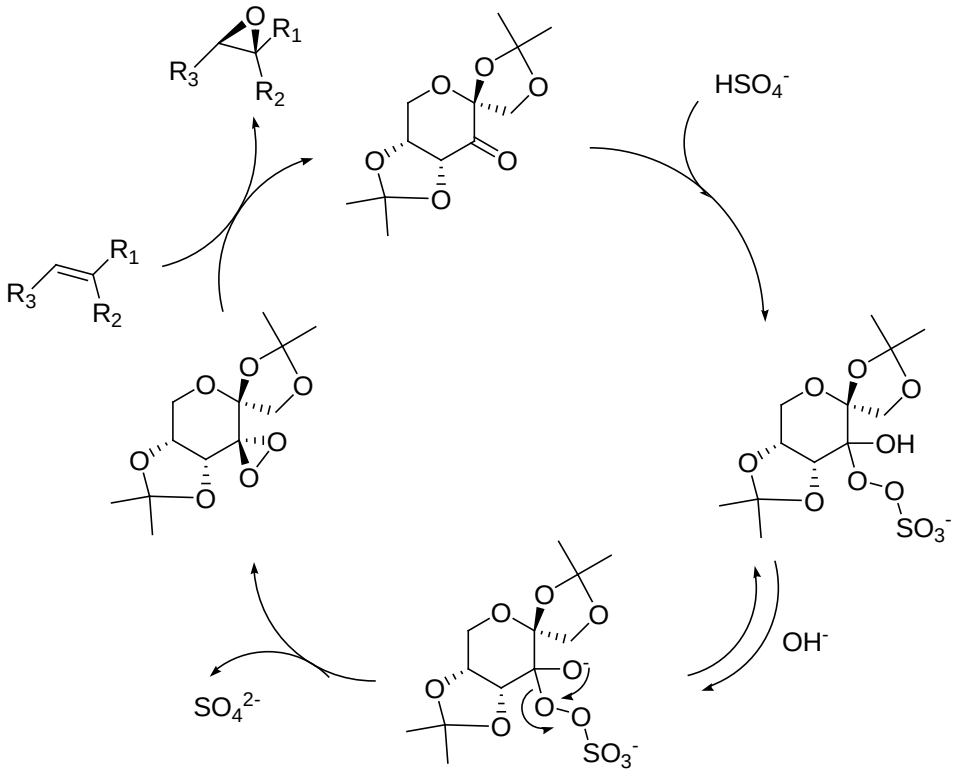

Figure 52: Catalytic cycle of the dioxirane shi epoxidation (135).

The stereochemical communication between substrate and catalyst is generally efficient in this catalyst, as the stereocenters are close to the reacting center. The optimal pH for the dioxirane epoxidation is 7-10. At higher pH, Oxone tends to decompose. However, at pH 7–8 the Shi catalyst decomposes due to a competing Baeyer-Villiger reaction. By increasing the pH to 10.5 (by addition of K_2CO_3), the amount of ketone can be reduced to a catalytic amount (30 mol%) and the amount of Oxone can be reduced to a stoichiometric amount, suggesting that at this pH the ketone is sufficiently reactive to compete with the decomposition of Oxone (138).

2.2.2. Stereochemistry of the epoxidation

As already explained in chapter 2.2.1, it is proposed that the Shi epoxidation proceeds through a dioxirane intermediate which limits possible competing approaches. Figure 53 shows two possible ways of how the double bond of the olefin can attack the oxirane ring.

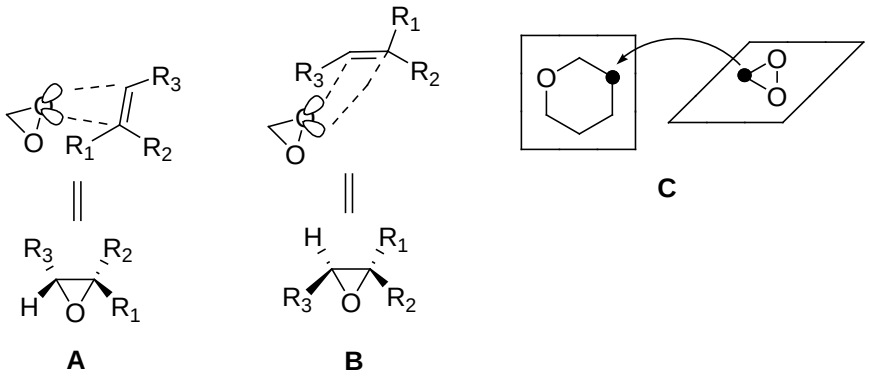

Figure 53: Possible ways of how the double bond of the olefin can attack the oxirane ring: **A**, *spiro* transition state and **B**, planar transition state. **C**, *spiro* compost.

In **A**, the *spiro* transition state is shown, whereas **B** is the main competing pathway, called *planar* transition state. The *spiro* transition state is believed to be electronically favored, as a result of a stabilizing interaction between an oxygen lone pair of the dioxirane and the π* orbitals of the olefin (138).

Although the effect of the *planar* transition state depends on the olefin substituents, it is the less favored. Not less important is to mention that a *spiro* compost is formed. Generally, a *spiro* compound is a bicyclic compound, characterized by two different rings which are placed on two different planes connected via a single carbon atom (Figure 53, C). In this specific case the dioxirane ring is connected to the six membered ring of the catalyst by a so called *spiro carbon*. Although this structure does not present any stereogenic centers, spiroatoms may be centers of chirality. The chirality derives from an axis of chirality in which the substituents are held in a spatial arrangement which is not superimposable onto its mirror image.

The transition state analysis performed by Shi and co-workers (139) (140) (141) proved that the *spiro* transition state is favored if the reaction takes place with alkene containing conjugated groups. The conjugated system can diminish its σ^* orbital energy and thus improve the stabilization of the interaction of secondary orbitals.

Other observations suggested that by decreasing the size of the olefin or by changing its substituent, the enantiomeric excess can be changed. The *spiro* transition state can be favored by decreasing the size of R_1, whereas an increase in size of R_3 disfavors the *planar* transition state. Another important factor to determine the formation of a *spiro* compound is the interaction of the olefin with the oxygen atoms of the catalyst. Figure 54 shows this interaction for the planar transition state proving its disfavor.

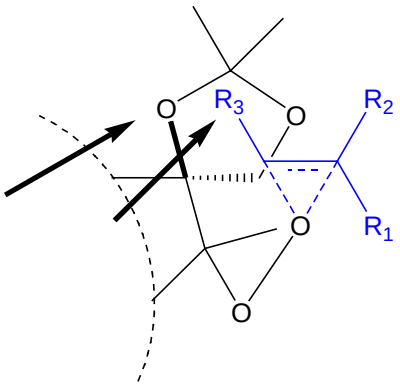

Figure 54: Interaction of the olefin with the oxygen atoms of the catalyst for the *planar* transition state.

2.2.3. Opening of the epoxide

Epoxides, as the one shown in Figure 55, have two potential sides for nucleophilic attack. As it is the least hindered, it is evident that C-1 is the most reactive electrophilic site for a range of nucleophiles including thiolates and hydroxyl ions.

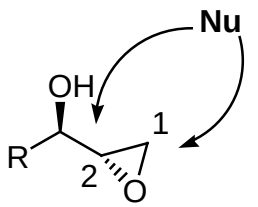

Figure 55: Potential sides for the attack of the nucleophile.

As described by Payne (142) in his early studies, opening of an epoxide at the C1-position can be carried out with a hydroxide ion to form a triol (Figure 56). The drawback of this reaction is that the obtained substrate is difficult to handle due to its three free hydroxyl groups.

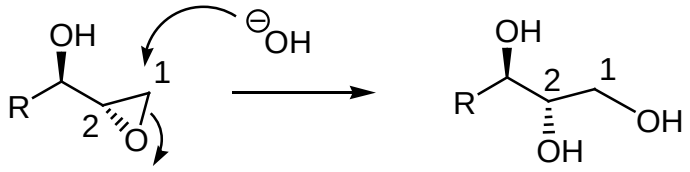

Figure 56: OH-mediated opening of the epoxide.

Ring opening of epoxides with thiols (Figure 57) is one of the most used procedures for the synthesis of β-hydroxy sulfides. As reported in literature (143), thiolysis of epoxides can be carried out in the presence of a base, a Lewis acid or in the presence of a heterogeneous catalysts. This method has been discovered by Sharpless and Masasume (144) (145) and represents a good alternative to Payne´s epoxydation.

.

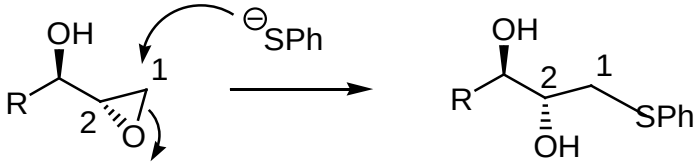

Figure 57: PhS-mediated opening of the epoxide.

The regioselectivity of the epoxide in the examples reported here (Figure 56 and Figure 57) favors the *erythro* configuration (2,3-*anti)* in both cases (146) .

In base-catalyzed reactions, the ring opening occurs usually at the less-substituted carbon, as this is the easily accessible position for the nucleophilic attack. In this case a steric factor dominates the process. In the case of acid-catalyzed reactions (Figure 58), the final orientation is determined by the ability of the carbon with the most substituents to stabilize the positive charge, formed by the bonding of a proton to the oxygen of the epoxide ring. The formation of this new bond makes the C-O bond weak. Depending on

the stage at which the nucleophile attacks, the orientation of the final molecule can adopt different configurations. For acid-catalyzed opening, an electronic factor is the dominating one. Steric control leads to an anti-Markovnikov regioselectivity, whereas electronic control results in a Markovnikov regioselectivity (147).

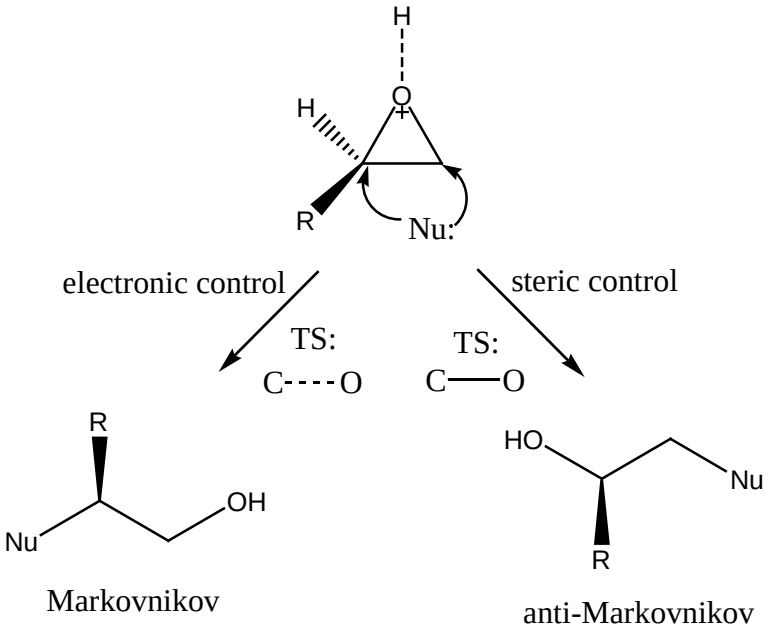

Figure 58: Stereochemistry of an acid-catalyzed epoxide opening (147).

3. Synthetical work

3.1. Planned synthesis of 3-deoxy sugars: graphical abstract

The approach followed in this work, as already presented in chapter 1.1, starts from the easily accessible and protected form of D-glyceraldehyde, known to be the simplest of all known aldoses.

An overview of the synthetic pathway is given in Figure 59. Each individual reaction step will be discussed in detail in further chapters.

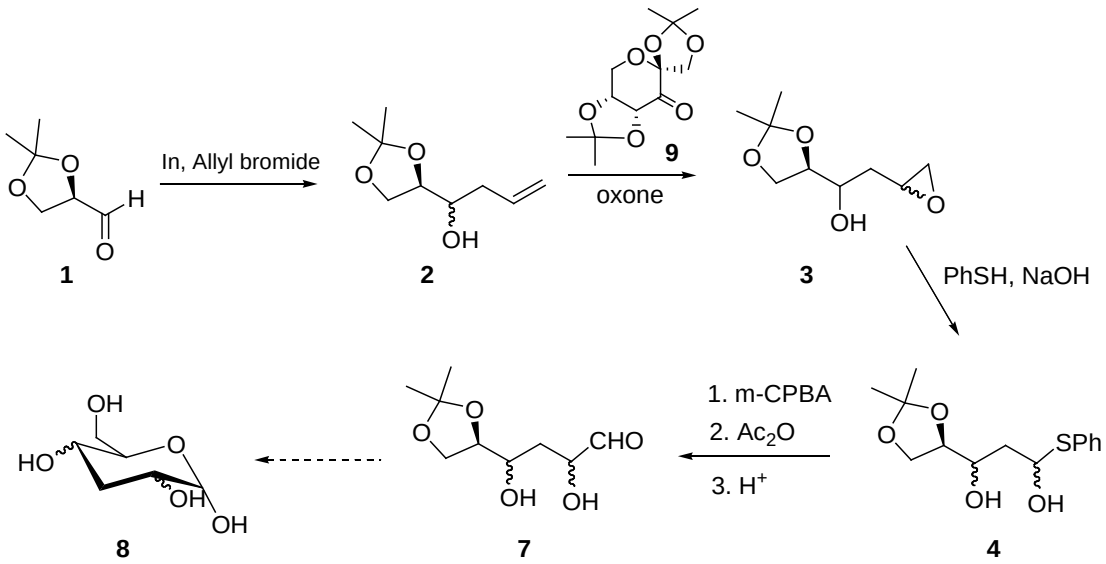

Figure 59: Synthetic strategy for the preparation of 3-Deoxy-sugars.

3.1.1. Stereochemical outcome of the reaction from O-Isopropyliden-D-glycerhaldehyde (1st step)

When *O*-Isopropyliden-D-glyceraldehyde **1** is treated with indium (1.4 eq) and allyl bromide (1.2 eq) compound **2** is obtained in a diastereomeric ratio of 4:1 (**2a-b**) erythro:threo configuration (Figure 60). According to the theory of the Felkin-Anh model, previously described in chapter 2.1.2, the stereochemistry of the reaction can be predicted. Through NMR studies, the diastereomeric ratio can be determined.

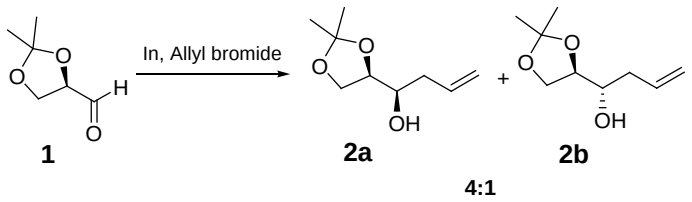

Figure 60: Indium-mediated allylation reaction.

During the experimental work it was experienced, as reported in literature, that by changing the solvent, the stereoselectivity of the reaction can be improved (as described in chapter 2.1.1). Table 12 shows, that a diastereomeric ratio of 5:1 can be achieved if the reaction takes place in pure ethanol, which however decreases the yield. A good compromise between yield and diastereomeric ratio has been found using a THF/H_2O mixture in a ratio of 4:1.

solvent	ratio	eq. In	eq. allyl bromide	yield [%]	dr
THF/H_2O	4:1	1.4	1.2	90	4:1
THF/H_2O	1:1	1.4	1.2	12	3:1
H_2O	-	1.4	1.2	0	-
DMF/H_2O	6:4	1.4	1.2	4	4:1
EtOH	-	1.4	1.2	48	5:1

Table 12: Reaction conditions and stereo chemical outcome.

After ^{1}H-NMR studies of the diastereomeric mixture, quantitative analysis were performed. The separation of the two diastereomers (Figure 60) could not be achieved by standard procedures on silica gel column chromatography. As reported by Schmid et.al. (148), the separation of this mixture is known not to be possible via common separation methods.

Due to the difficulties in obtaining a diastereomeric pure compound, the mixture was used "as is" in order to postpone separation of the mixture to a later step in the reaction sequence.

3.1.2. Selective epoxidation (2nd Step)

The strategy adopted to perform the epoxidation was to treat compound **2** with 0.3 eq of Shi catalyst **9** (2,2-dimethyl-10-oxo-1,3,6-trioxaspiro[4.5]decane-8,9-diyl diacetate) in the presence of a phase transfer catalyst (TBAHS) and the commercially available Oxone (potassium peroxomonosulfate) as stochiometric oxidant.

The reaction has been carried out in different solvents and reaction parameters, altering temperature and pH. Table 13 shows some examples of the different conditions applied. It was understood that Dioxan and CH_3CN as solvent generally provide higher yields.

solvent	T [°C]	pH	yield [%]
MeCN	0	6	---
Dioxan	rt	10	89
DMF	rt	10	24
MeCN	rt	10	90

Table 13: Example of different reaction conditions applied for the epoxidation step.

On the ^{1}H-NMR (Figure 61), that was carried out in order to study the obtained reaction product, a mixture of diastereomers can be observed. Substrate **3** was yielded from product **2**, which was not diastereomerically pure (dr. 4:1, see paragraph 3.1.1).

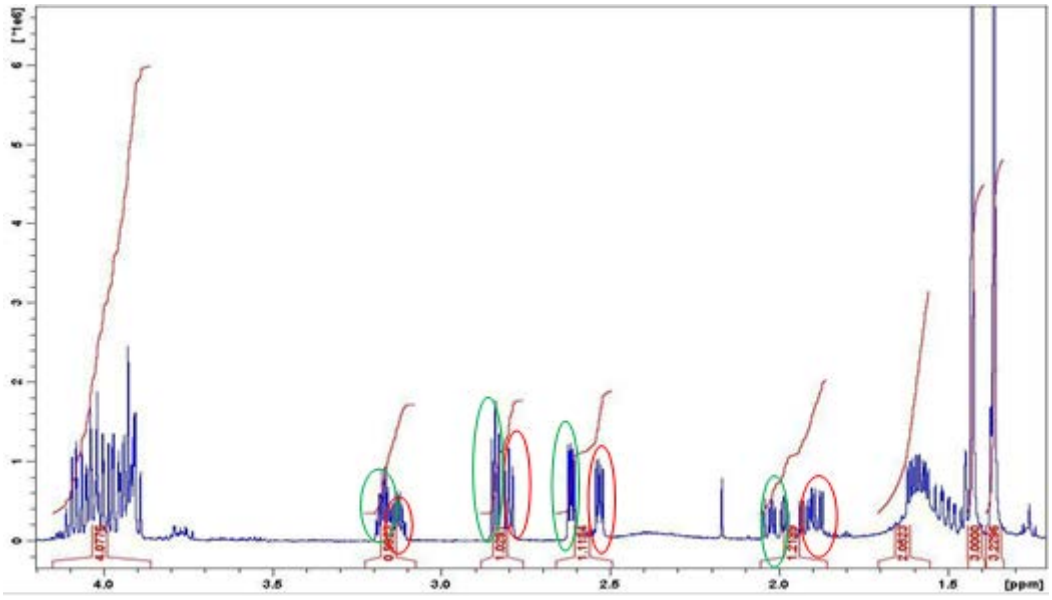

Figure 61: ^{1}H-NMR of the epoxyde specie which shows a mixture of diastereomers.

Both red and green circled peaks in the image above, might suggest two different structures each, **3a-d** (Figure 62).

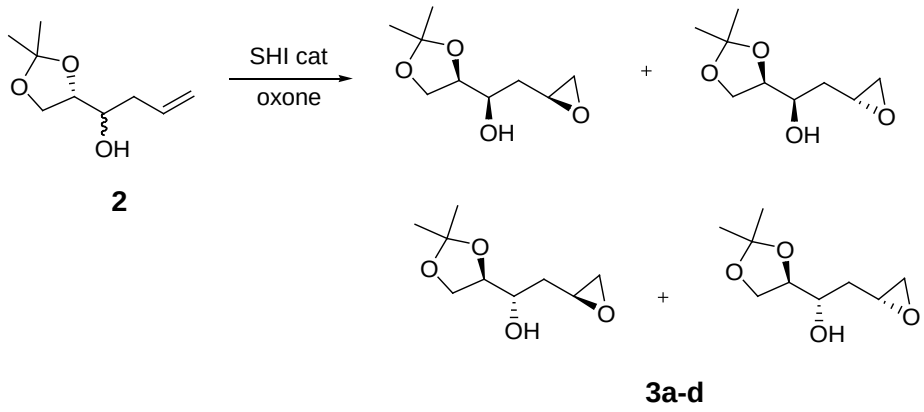

Figure 62: Structure of the four diastereomers of the epoxide.

Purification of the obtained mixture was performed by column chromatography on silica gel, applying different eluent mixtures. However, due to the almost equivalent Rf values of the different diastereomers (regarding the TLC performed on precoated silica gel glass plates), separation of the diastereomers was not possible.

The disadvantage of this approach is not only that the separation of the diastereomeric mixture was not achieved, but also that the definition of the ratio of the diastereomeric mixture obtained is challenging. The spectra in the above image suggests that the ratio between the two investigated mixtures is 1:1. Via NMR studies it was possible to prove the structure of the epoxide, which was then further treated with thio compounds to perform an opening of the terminal epoxide.

3.1.3. Regio-selective opening of the epoxide (3rd step)

Opening of the epoxide **3** was performed following a sulfide method (149). It was assumed that the great steric bulk of the *tert*-butyl and the phenyl group might improve - or at least not diminish - the regioselectivity exhibited for ring opening at the C1-position.

Referring to the previous step, in Figure 62 four different diastereomers (**3a-d**) are present as a mixture; treatment of epoxide **3** with base in the presence of thiophenol leads to an 83% yield of sulfide **4** as a diastereomeric mixture (Figure 63).

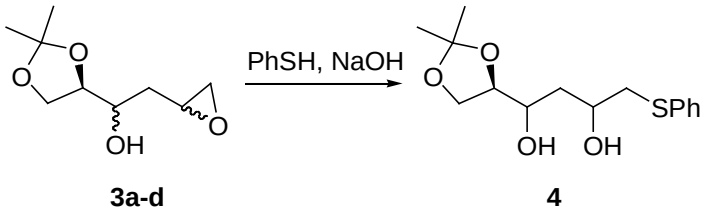

3a-d **4**

Figure 63: Opening of the epoxide.

An additional reaction was performed with *tert*-butylthiolate, which is described to be more selective than phenylthiolate (150). However, as reported in Table 14, a lower yield was obtained in this case.

eq. PhSH	eq. NaOH	Solvent	ratio	temp. [°C]	yield [%]
2.0	2.0	Dioxan/ H_2O	10:1	rt	0
2.0	2.0	Dioxan/ H_2O	10:1	65	27
1.2	2.5	THF	---	70	83
eq. *t*-BuSH	**eq. NaOH**	**Solvent**	**ratio**	**temp. [°C]**	**yield [%]**
1.2	2.5	THF	---	70	17

Table 14: Epoxydation conditions.

Although 2D- and ^{1}H-NMR studies were performed, the stereochemical outcome of the reaction could not be clarified due to the overlapping of the many signals of the mixture from the previous epoxidation step. Even though the stereochemical outcome of the last three steps was not understood and the results are NMR spectra of difficult interpretation, it was possible to understand the correct structure of the compound, which was confirmed also by MS spectroscopy. The compound was therefore used for the next step of the synthesis.

3.1.4. Pummerer rearrangment (5th step)

The Pummerer rearrangement can be used to introduce an aldehyde-functionality on the carbon next to the sulfur. The product of the Pummerer rearrangement is in the same oxidation state as an aldehyde and by hydrolysis of the product, the aldehyde can be obtained. The substrate of the classical Pummerer reaction is an alkyl sulfoxide which, upon O-activation, undergoes elimination to give a thionium ion, which is consequently attacked by a nucleophile (Figure 64). Generally, the sulfoxide can be activated using

acetic anhydride, trifluoroacetic anhydride (TFAA), trifluoromethanesulfonic anhydride (Tf_2O) or a silyl chloride (151).

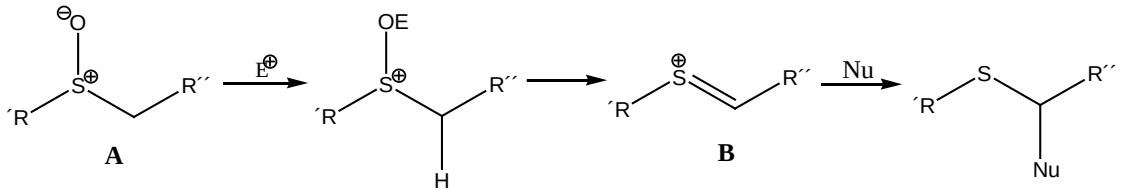

Figure 64: Classical Pummerer reaction: alkyl sulfoxide **A** and thionium ion **B.**

The previously introduced thiophenol group **4** is oxidized via treatment with m-CPBA at -78°C to yield the intermediate species **5** (Figure 65).

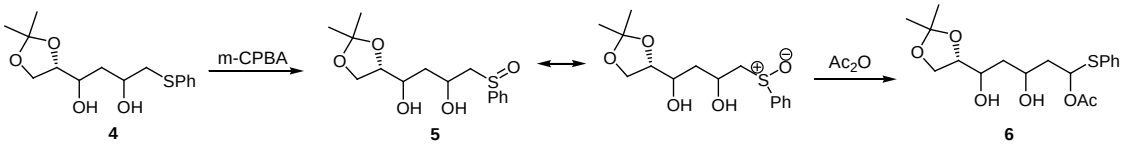

Figure 65: Oxidation and Pummerer rearrangement steps**.**

By proceeding with a Pummerer rearrangement of compound **5,** the hemithioacetal **6** is obtained with a 28% yield from compound **5**. Table 15 shows different reaction conditions for both steps.

reaction	**solvent**	**eq. m-CPBA**	**yield [%]**
Oxidation	DCM	1.1	40
Oxidation	DCM	1.3	78
Oxidation	EtOAc	1.3	14
reaction	**solvent**	**Eq. Ac_2O**	**yield [%]**
Rearrangement	---	2	28

Table 15: Reaction conditions for oxidaion and Pummerer rearrangement.

4. Conclusions

Although high-resolution ^{1}H NMR spectroscopy, ^{13}C- and 2D-NMR spectroscopy were performed in order to study the stereochemistry of the expected intermediate diastereomeric mixtures, only little information about the stereochemistry was gathered.

However, four different structures for the final sugar can be predicted (Figure 66):

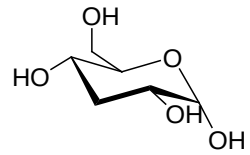

3-deoxy-α-D-ribo-hexopyranose

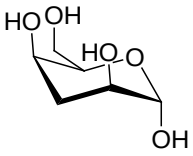

3-deoxy-α-D-lyxo-hexopyranose

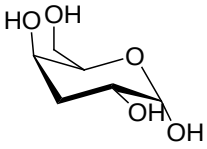

3-deoxy-α-D-xylo-hexopyranose

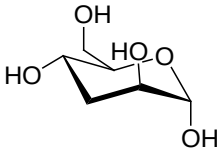

3-deoxy-α-D-arabino-hexopyranose

Figure 66: predicted structure for the final 3-deoxy sugar**.**

All the reactions were carried out in different solvents or solvent-mixtures, in different concentrations and different conditions in order to be able to improve the yield and the efficiency of each step.

The generation of the stereocenters is a crucial part of the synthesis. The metal-mediated allylation is one of the two key steps from which the stereochemical problems originate. It is not possible to improve the reaction any further as it is solvent dependent. Different solvent mixtures were applied. The only way of how to bypass the problem would be either to alternate the used metal or to develop an alternative separation method.

The second crucial point is the epoxidation step. Different types of catalysts or different reagents (m-CPBA) could be applied for the epoxidation.

Having optimized two key reactions (chain elongation and epoxidation), the first three steps have been carried out successfully.

Unfortunately, due to the stereochemical problem, the project was discontinued in order to develop a solution for the separation of the diastereomeric mixture which have been of a difficult point for the interpretation /clarification of NMRs data, that is needed to prove the structures.

5. Experimental work

Solvents: anhydrous solvents were distilled from P_2O_5 (dichloromethane, chloroform) or sodium (diethylether, toluene) and stored over molecular sieves (4 Å). Anhydrous tetrahydrofurane was purchased from Sigma-Aldrich.

Evaporation of the solvents was accomplished using a Büchi rotavapor R-210 in combination with an Ilmvac LVS 310p ecoflex vacuum system.

Purification methods: column chromatography was performed using silica gel 60 (0.040-0.063 μm, 240-400 mesh) available from Merck. Thin layer chromatography (TLC) was performed on precoated silica gel glass plates (Merck 60 F254). TLC detection was carried out using a UVAC-60 neolab ultraviolet lamp (254 and 366 nm) and/or by treatment with one of the following detecting reagents: Mo-$Ce(SO_4)_2$ complex solution (48 g $(NH_4)_6Mo_7O_{24}*4H_2O$ and 2 g $Ce(SO_4)_2$ in 100 ml 10% H_2SO_4), $KMnO_4$ solution (0.5% in 1N NaOH).

NMR spectroscopy measuremets: spectra were recorded on a Bruker Avance DRX400 spectrometer, AV400 spectrometer or DRX600 spectrometer. Chemical shifts are given in ppm, coupling constants are given in Hz. Spectra are referenced to the residual solvent signal 7.26 ppm (^1H), 77.16 ppm (^{13}C) for $CDCl_3$; 2.5 ppm (^1H), 39.52 ppm (^{13}C) for d6-DMSO.

(S)-2,2-dimethyl-1,3-dioxolane-4-carbaldehyde [1]

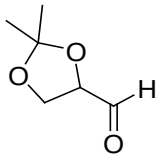

$C_6H_{10}O_3$
Mol. Wt.: 130,14

This procedure is described in the experimental part of part A of this work, in chapter 4.

1-((S)-2,2-dimethyl-1,3-dioxolan-4-yl)but-3-en-1-ol [2]

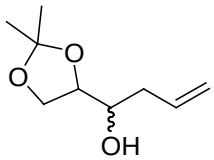

$C_9H_{16}O_3$
Mol. Wt.: 172,22

This procedure is described in the experimental part of part A of this work, in chapter 4.

1-((S)-2,2-dimethyl-1,3-dioxolan-4-yl)-2-(oxiran-2-yl)ethanol [3]

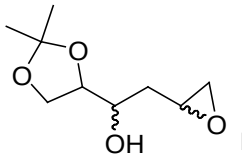

$C_9H_{16}O_4$
Mol. Wt.: 188,22

Tetrabutylammonium hydrogensulfate (0.04eq, 0.02mmol), Shi catalyst 1,2:4,5-Di-*O*-isopropylidene-β-D-*erythro*-2,3-hexodiulo-2,6-pyranose (0.3eq, 0.17mmol) and compound **2** (0.1g, 0.85mmol) were dissolve in dioxan (8.7ml) and 5.8ml of buffer solution (0.05M $Na_2B_2O_7 \cdot 10\ H_2O$ in $4 \cdot 10^{-4}$ M Na_2(EDTA)) was added. Oxone (1.38eq, 0.80mmol) was dissolved in 3.7ml of $4 \cdot 10^{-4}$ M Na_2(EDTA) and K_2CO_3 (5.8eq, 3.36mmol) was dissolved in 3.7ml H_2O_2. Within 1.5 hours both solutions, Oxone and K_2CO_3, were added through separate addition funnels. After the addition the pH of the mixture was 10. The reaction mixture was stirred for 2 hours at room temperature. TLC (EE:PE 3:1) was performed in order to control the reaction. The mixture was quenched by addition of DCM. The aq. phase was extracted with DCM (3x10ml) and the combined organic phases were washed with saturated NH_4Cl solution. The organic phase was dried over $MgSO_4$ and the solvent removed by rotary evaporation. The crude product was purified by column chromatography (PE:EE 18:1-1:1) to yield 0.95g of final product **3**.

Yield: 89%

^{1}**H-NMR** ($CDCl_3$, 400 MHz): δ 4.0 (m, 3H, -CHC**H**C**H$_2$**), 3.09 (m, 1H, -C**H**OH), 5.30 (td, 1H, -CH_2CHC**H$_2$**, J= 4.67 Hz, J= 16.27 Hz, J= 4.14 Hz), 2.33 (qd, 1H, -CH_2C**H**CH_2, J= 2.78 Hz, J= 30.35 Hz), 2.46 (s, 1H, -OH), 1.96 (m, 1H, -C**H$_2$**$CHCH_2$, J= 3.75 Hz), 1.54 (m, 1H, -CHC**H$_2$**CH-), 1.41 (s, 3H, -C**H$_3$**), 1.35 (s, 3H, -C**H$_3$**) ppm

^{13}**C-NMR** ($CDCl_3$, 400 MHz): 109.61 (-**C**$(CH_3)_2$) 79.25 (-CH**C**HCH_2) 69.54 (-**C**HOH) 66.55 ((-CHCH**C**H_2) 50.29 (-CH_2**C**HCH_2) 47.35 (-CH_2CH**C**H_2) 35.53 (-CH**C**H_2CH-) 26.97 (-**C**H_3) 25.59 (-**C**H_3)

1-((S)-2,2-dimethyl-1,3-dioxolan-4-yl)-4-(phenylthio)butane-1,3-diol [4]

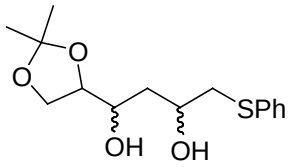

$C_{15}H_{22}O_4S$
Mol. Wt.: 298,4

NaOH (2.5eq, 1.3mmol) was added to a solution of compound **3** (0.100g, 0.53mmol) in THF (10ml). A slow addition of PhSH (1.2eq, 0.64mmol) followed and the reaction was heated at 70°C for 3 hours (TLC PE:EE 1:1). After completion of the reaction, the mixture was cooled to rt. and was extracted with DCM (3x10ml). The organic phases were combined, washed with NH_4Cl (10ml) and dried over $MgSO_4$. The solvent was removed and the crude product was purified by column chromatography (PE:EE 1:1) to yield 0.192g of the final product **4**.

Yield: 83%

^{1}**H-NMR** ($CDCl_3$, 400 MHz): δ 7.39 (dd, 2H, -Ph. J= 7.04 Hz, J= 30.25 Hz), 7.29 (dt, 2H, -Ph, J= 7.16 Hz, J= 30.25 Hz), 7.23 (tt, 1H, -Ph, J= 7.41 Hz, J= 30.25 Hz), 4.05 (m, 1H, -CHCHC**H**$_2$, J= 1.90 Hz), 3.92 (m, 3H, -C**H**C**H**C**H**$_2$), 3.84 (m, 1H, -CH_2C**H**CH_2-, J= 2.25 Hz), 3.10 (dd, 1H, -C**H**SPh), 2.92 (q, 1H, -C**H**SPh), 2.58 (s, 2H, -OH), 1.92 (td, 1H, -CHC**H**$_2$CH), 1.49 (m, 1H, -CHC**H**$_2$CH), 1.39 (d, 3H, -C**H**$_3$), 1.34 (s, 3H, -C**H**$_3$) ppm

1-((S)-2,2-dimethyl-1,3-dioxolan-4-yl)-4-(phenylsulfinyl)butane-1,3-diol [5]

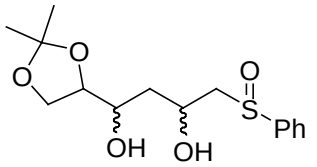

$C_{15}H_{22}O_5S$
Mol. Wt.: 314,4

Compound **4** (0.192g, 0.6mmol) was dissolved in dry DCM (10ml) and a powder of K_2CO_3 (3.0eq, 1.9mmol) was added to the solution. The reaction was cooled at -78°C and m-CPBA (1,3eq, 0.8mmol) was slowly added. The mixture was stirred for 2 hours at rt (TLC DCM: EE 1:3). At completion of the reaction, the mixture was quenched by addition of a sat. solution of sodiumcarbonate and was extracted with DCM (3x15ml). The combined organic phases were washed with saturated ammoniumcloride (10ml), dried over $MgSO_4$ and the solvent was removed under reduced pressure. The crude product was purified by column chromatography (DCM: EE 1:3) to yield 0.164g of product **5**.

Yield: 78 %

^{1}**H-NMR** ($CDCl_3$, 400 MHz): δ 7.93 (2H, -Ph), 7.58 (m, 3H, -Ph), 4.41 (m, 1H, C**H**$_2$CH-), 4.0 (m, 1H, C**H**$_2$CH-), 3.76 (m, 1H, -C**H**OH), 3.62 (m, 1H, -C**H**OH), 3.32 (m, 2H, -C**H**$_2$SOPh), 1.91 (m, 1H, -CHC**H**$_2$CH-), 1.74 (m, 1H, -CHC**H**$_2$CH-), 1.37 (dt, 6H, -C**H**$_3$), ppm

MS : (ESI, 4 kV) m/z (rel. Int.): 337.2 (100.0%).

2,4-dihydroxy-4-((S)-2,2-dimethyl-1,3-dioxolan-4-yl)-1-(phenylthio)butyl acetate [6]

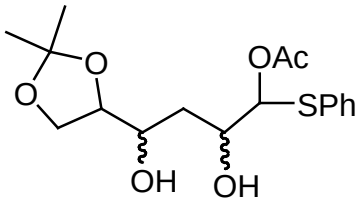

$C_{17}H_{24}O_6S$
Mol. Wt.: 356,43

Compound **5** (0,25g, 0.079mmol) was dissolved in Ac_2O (2eq, 1.52mmol). The reaction was stirred at 70°C overnight and for an additional 30min at reflux. After reaction completion the product was extracted with DCM (2x10ml) The combined organic phases were dried over $MgSO_4$ and the solvent was removed under reduced pressure. The crude product was purified by column chromatography (DCM: EE 1:3) to yield 0.08g of product **6**. Starting material of 0,16g, could be recovered as well.

Yield: 28 %

MS : (ESI, 4 kV) m/z (rel. Int.): 379.1 (100.0%).

Bibliography

1. **Wang L.** Computational Systems Bioinformatics Conference. 2005, p. 189-202.

2. **Vuister G. V.** J. Am. Chem. Soc. 1999, Vol. 116, p. 9206-9210.

3. **Jacobsen N.E.** NMR Spectroscopy Explained. 2007.

4. **Graham L.P.** An Introduction to Medicinal Chemistry, 3rd edition. 2005.

5. **Howard M.J.** Current Biology. 1998, Vol. 8, p. 403-408.

6. **James T.L, .** Foundamentals of NMR. 1998.

7. **Bertini I., McGreevy K.S., Parigini G.** NMR of Biomolecules, 3rd edition. 2012.

8. **Clore G.M., Gronenborn A.M.** Method in Enzymology. Vol. 239, p. 349-363.

9. **Verardi R., Traaseth N.J., Masterson L.R.** Isotope labelling in biomolecular NMR. Ateya, 2012.

10. **Wand A.J., Englandert S.W.** Protein Complexes Studied by NMR Spectroscopy. 1996, Vol. 7, p. 403-408.

11. **Muhanidram D.R., Kay L.E.** J.Magn. Res. B. 1994, Vol. 103, p. 203-216.

12. **Bertini I., McGreevy K.S., Parigini G.** NMR of Biomolecules, 3rd edition. 2012.

13. **Clore M.G., Gronenborn A.M.** TIBITECH. 1998, Vol. 16, p. 22-33.

14. **Bertini I., McGreevy K.S., Parigini G.** NMR of Biomolecules, 3rd edition. 2012.

15. **Clore G.M., Gronenborn A.M.** Prog. Biophys. molec. Biol. 1994, Vol. 62, p. 153-184.

16. **Schedlbauer A., Auer R., Ledelter K., Tollinger M., Kloiber K., Lichtenecker R., Ruedisser S., Hommelv U., Schmid W., Konrat R., Kontaxix G.** J. Biomol. NMR. 2008, Vol. 42, p. 111-127.

17. **Howard M.J.** Current Biology. 1998, Vol. 8.

18. **Harris R.K., Becker E.D.** J. Magn. Res. 2002, Vol. 156, p. 323-326.

19. **Lichtenecker R.** PhD Thesis. 2008, p. 4-5.

20. **Clore M.G., Gronenborn A.M.** Protein Eng. 1987, Vol. 1, p. 275-288.

21. **Garrett D.S., Seok Y-J., Peterkofsky A., Gronenborn A.M., Clore G.M.** Biochemistry. 1997, Vol. 36, p. 2517-2530.

22. **Yu H.** Proc. Nat. Acad. Sci., USA. 1992, Vol. 96, p. 332-334.

23. **Lichtenecker R., Weinhäupl K., Reuther L., Schörghuber J., Schmid W., Kontat R.** J. Biomol. NMR. 2013.

24. **Muchmore D.C., McIntosh L.P., Russel C.B.** Methods Enzy-mol. 1989, Vol. 177, p. 44-73.

25. **Becker W.G.** Briefings in Functional Genomics and Proteonoomics. 2008, Vol. 7, p. 371-382.

26. **Spirin A.S., Baranov V.I., Ryabova L.A.** Science. 1933, Vol. 242, p. 1162-1163.

27. **Bennett T., Farmer I.I., Venters R.A.** NMR of predeuterated Large Proteines. 2002, Vol. 16, p. 75-120.

28. **Patzelt H., Goto N., Iwai H., Lundstrom K., Fernholz E.** BioNMR in Drug Research. 2002, Vol. 1, p. 1-34.

29. **Lian L-Y., Middleton D.A.** Prog. Nucl. Magn. Res. Spec. 2001, Vol. 39, p. 171-190.

30. **Jordan J.B., Kriwacki R.W.** Cambrige Isotope Laboratories. *application note 16*.

31. **Tugarinov V., Kay L.E.** Chembiochem. 2005, Vol. 6, p. 1567-1577.

32. **Kainosho M., Torizawa T., Iwashita Y., Terauchi T., Ono A.M., Güntert P.** Nature. 2006, Vol. 440, p. 52-57.

33. **Tugarinov V., Kay L.E.** J. Am. Chem. Soc. 2003, Vol. 125, p. 13868-13878.

34. —. J. Am. Chem. Soc. 2003, Vol. 327, p. 5701-5706.

35. **Dewick P.M.** Medicinal Natural Products. 202, p. 121-165.

36. **Maeda H., Dudareva N.** Annu. Rev. Plant. Biol. 2012, Vol. 63, p. 73-105.

37. **Alves R., Chaleil R.A.G., Sternberg M.J.E.** J. Mol. Biol. 2002, Vol. 320, p. 751-770.

38. **Panwa E.M., Vitreschak A.G., Mironov A.A., Gelfand M.S.** Microbiology Letters. 2003, Vol. 222, p. 211-220.

39. **Euverink G.J.W.** Aromatic Amino acid biosynthesis in Actinomycetes. *PhD Thesis, Univ. Groningen.* 1995, p. 11-28.

40. **Herrmann K.M., Weaver L.M.** Annu. Rev. Plant Physiol. Plant Mol. Biol. 1999, Vol. 50, p. 473-503.

41. **Perez J.A., Ferguson S.J., Campbell I.D.** Febs Letters. 1990, Vol. 272, p. 34-36.

42. **Birtalan S., Fisher R.D., Sidhu S.S.** Mol BioSyst. 2010, Vol. 6, p. 1186.

43. **Kathleen V. K., Valentine K.G., Wand J.** J. Am. Chem. Soc. 2013, Vol. 135, p. 9560-9563.

44. **Raap J., Nieuwenhuis S., Creemers A., Hexspoor S., Kragl U., Lugtenburg J.** Eur. J. Org. Chem. 1999, p. 2609-2621.

45. **Hummel W., Schütte H.,Schmidt E., Wandrey C., Kula M.R.** Appl. Microbiol. Biotechnol. 1987, Vol. 26, p. 409.

46. **Takatori K., Nishihara M., Nishiyama Y., Kajiwara M.** Tetrahedron. 1998, Vol. 54, p. 15861-15869.

47. **Gregson T.J., Herbert J.H., Row E.C.** J. Label Compd. Radiopharm. 2011, Vol. 54, p. 1-32.

48. **Fields M., Leaffer M.A., Rothchild S., Rohan J.** J. Am. Chem. Soc. 1952, Vol. 74, p. 7498.

49. **Fields M., Leaffer M.A., Rohan J.** Science. 1949, Vol. 109, p. 35.

50. **Horman I., Yeo A.N.H., Williams D.H.** J. Am. Chem. Soc. 1970, Vol. 92, p. 2132.

51. **Akira K., Baba J.** J. Labe.l Compd. Radiopharm. 1992, Vol. 31, p. 109.

52. **Patschke L., Barz W., Grisebach H.** Zeitschr. Naturfosch. 1964, Vol. 19b, p. 1110.

53. **Yoshida K., Iamamoto T.** J. Am. Chem. Soc. 2005, Vol. 127, p. 10470.

54. **Yoshida K., Kawagoe F., Iwadate N., Takahashi H., Imamoto T.** Chem. Asian J. 2006, Vol. 1, p. 611.

55. **Yoshida K., Narui R., Imamoto T.** Chem. Eur. J. 2008, Vol. 14, p. 9706.

56. **Probst N. P.** J. Org. Chem. 2008, Vol. 73, p. 4338-4341.

57. **Reichwein F. J.** J. Am. Chem. Soc. 2003, Vol. 125, p. 1821-1824.

58. **Lichthenecker R. J.** PhD Thesis. 2008.

59. **Xu S.** Org. Lett. 2005, Vol. 7, p. 4605-4608.

60. **Green T.W., Wuts P.G.M.** Protective Groups in Organic Synthesis, 3rd edition. 1999.

61. **Carey F.A., Sundberg R.J.** Advanced Organic Chemistry, Part B 5th edition. 2007.

62. **Hayashi Y., Hirashita T., Mitsui K., Araki S.** Tetrahedron Lett. 2004, Vol. 45, p. 3225-3228.

63. **Van de Weghe P., Bisseret P., Blanchard N., Eustache J.** J. Organomet. Chem. 2006, Vol. 691, p. 5078-5108.

64. **Sanford M.S., Ulman M., Grubbs R.H.** J. Am. Chem. Soc. 2001, Vol. 123, p. 749.

65. **Schrodi Y., Pederson R.L.** AldrichimicaACTA. 2007, Vol. 40, p. 45-52.

66. **Jung M.E., Koch P.** Tetrahedron Lett. 2011, Vol. 52, p. 6051-6054.

67. **Ikeda H., Minegishi T., Miyash T.i, Lakkaraju P.S.** J. Phys. Chem. B. 2005, Vol. 109, p. 2504-2511.

68. **Gibson J.M., Thomas P.S., Thomas J.D.,Barker J.L., Chandran S.S., Frost J.W.** Angew. Chem. 2001, Vol. 113, p. 1999-2002.

69. **Rao S.N., O'Ferrall R.A.M., Kelly J.S.C., Boyd D.R., Agarwal R.** J. Am. Chem. SOC. 1993, Vol. 115, p. 5458-5465.

70. **Lichtenecker, R. J.** PhD Thesis. 2008.

71. **Natelson S., Gottfried S.** Org. Synth. 1955, Vol. 3, p. 381.

72. **Probst P.N., Haudrechy A., Ple K.** J. Org. Chem. 2008, Vol. 73, p. 4338–4341.

73. **Villieras J., Villieras M., Kloetzing R.J., Knochel P.** e-EROS, Encyclopedia of Reagents for Organic Synthesis. 2005.

74. **Boutagy J., Thomas R.** Chem. Rev. 1974, Vol. 74, p. 87-99.

75. **Wadsworth W., Emmons W.D.** Org. Synth. 1973, Vol. 5, p. 547.

76. **Kennedy J. F., White C. A.** Bioactive Carbohydrates. 1st ed, 1983.

77. **Ratner D.M., Adams E.W., Disney M.D., Seeberger P.H.** ChemBioChem. 2004, Vol. 5, p. 1375-1383.

78. **Seeberger P. H.** Chem. Commun. 2003, Vol. 10, p. 1115.

79. **Hanessian S.** Adv. Carbohydr. Chem. Biochem. 1996, Vol. 21, p. 143-207.

80. **Grisebach H.** Adv. Carbohydr. Chem. Biochem. 1978, Vol. 35, p. 81-126.

81. **Beckre D.J., Lowe B.J.** Glycobiology. 2003, Vol. 13, p. 41-53.

82. **Golan D.E., Tashjian A.H., Armstrong E.J., Armstrong A.W.** Principles of Pharmacology. 2nd ed., 2005.

83. **De Lederkreker R. M., Marino C.** Adv. Carbohydr. Chem. Biochem. 2008, Vol. 61, p. 143-215.

84. **Liu H., Thorson J. S.** Annu. Rev. Microbiol. 1994, Vol. 48, p. 223-256.

85. **Lonzano G., Elledge S.J.** Nature. 2000, Vol. 404, p. 24-25.

86. **Eklunda H., Uhlina U., Färnegardh M., Loganb D.T., Nordlund P.** Progress in Biophysics & Molecular Biology. 2001, Vol. 77, p. 177–268.

87. **Eliasson R., Fontecave M., Jörnvall H., Krook M., Pontis E.** Proc. Natl. Acad. Sci. 1990, Vol. 87, p. 3314-3318.

88. **Lennon M. B., Suhadolik R. J.** Biochem. Biophys. Acta. 1976, Vol. 425, p. 532-536.

89. **Reichard P., Ehrenberg A.** Science. 1983, Vol. 221, p. 514-519.

90. **Reichard P.** Biochem. Biophys. Acta. 1989, Vol. 1000, p. 49-50.

91. **Blakey R.L., Orme-Johnson W.H., Bozdech J.M.** Biochemistry. 1979, Vol. 18, p. 2335-2339.

92. **Stubbe J. A.** Annu. Rev. Biochem. 1989, Vol. 58, p. 259.

93. **Petersson L., Gräslund A., Ehrenberg A., Sjöberg B.M., Reichard P.** J. Biol. Chem. 1980, Vol. 255, p. 6706-6712.

94. **Natarajan S., Mathews R.** J. Biophys. Struct. Biol. 2011, Vol. 3, p. 38-48.

95. **Ravi N., Bollinger J.M., Huynh B.H., Edmonson D.E., Stubbe J.A.** J. Am. Chem. Soc. 1994, Vol. 116, p. 8007-8014.

96. **Carlson J., Fuchs J.A., Messing J.** Proc. Natl. Acad. Sci. 1984, Vol. 81, p. 4294-4297.

97. **Sjöberg B. M.** Structure and Bonding. 1997, Vol. 88, p. 141-173.

98. **Stubbe J. A.** Annu. Rev. Biochem. 1989, Vol. 58, p. 257-285.

99. **Wolfrom M. L.** Advances in Carbohydrate Chemistry. 1967, Vol. 21, p. 154-165.

100. **Nie S., Cui S.W., Xie M., Phillips A.O., Phillips G.O.** Bioactive Carbohydrate and Dietary Fibre. 2013, Vol. 1, p. 38-52.

101. **Bentley H.R., Cunningham K.G., Spring F.G.** J. Chem. Soc. 1951, p. 2301.

102. **Raphael R.A., Roxburgh C.M.** J. Chem. Soc. 1955, p. 3405.

103. **Siev M., Neinberg R., Penman S.** Journal of Cell Biology. 1969, Vol. 41, p. 510-520.

104. **Walton E., Nutt R.F., Jenkis S.R., Holly F.W.** J. Am. Chem. Soc. 1964, Vol. 86, p. 2952.

105. **Chu C.K., Kotra L.P., Manouliov K., Du J., Schinazi R.** Terapeutic Azide Compounds. 2001.

106. **Kirsching A., Jesberger M., Schonong K.U.** Concept for the total synthesis of doexy sugars. 2001, p. 507-540.

107. **Lederkremer R.M., Marino C.** Adv. Carbohydr. Chem. Biochem. 2008, Vol. 61, p. 143-216.

108. **Szarek W.A., Kong X.** Preparative Charbohydrate Chemistry. 1997, p. 105-126.

109. **Baer H.H., Hanna H.R.** Carbohydr. Res. 1982, Vol. 110, p. 19-41.

110. **Barton D.H.R., McCombie S.W.** J.Chem. Soc. Perkin I. 1974, p. 1574-1585.

111. **Chong Y., Chu C.K.** Carbohydr. Res. 2002, Vol. 337, p. 397-402.

112. **Lee T., Lee Y.C.** Carbohydr. Res. 1994, Vol. 251, p. 69-79.

113. **Chatgilialoglu C.** J. Org. Chem. 1988, Vol. 53, p. 3641-3642.

114. **Barton D.H.R, Jang D.O., Jaszberenyi J.C.** Synlett. 1991, p. 435-438.

115. **Compain P., Chagnault V., Martin O. R.** Tetrahedron Lett. . 2009, Vol. 20, p. 672-711.

116. **Stütz A.E.** Iminosugars as Glycosidase Inhybitors: Nojirimicin and Beyond. 1999.

117. **Greimel P., Spreitz J., Stütz A.E., Wrodnigg T.M.** Curr. Top. Med. Chem. 2003, Vol. 3, p. 513-523.

118. **Mathews, Van Holde, Ahern.** Biochemistry, 3rd. edition.

119. **McDonne J.L., Cronin L., O´Brien J.L., Murphy P.V.** J. Org. Chem. 2004, Vol. 69, p. 3565-3568.

120. **Ivkovi A., Matovi R.** J. Serb. Chem. Soc. 2002, Vol. 63, p. 141-148.

121. **Chan T.H., Li C.J.** Tetrahedron Lett. 1991, Vol. 48, p. 7017-7020.

122. **Li C.J., Chan T.H.** Tetrahedron Lett. 1991, Vol. 32, p. 70-77.

123. **Moyano A., Pericas M.A., Riera A., Luche J.L.** Tetrahedron Lett. 1990, Vol. 31, p. 7619-7622.

124. **Wei Z.Y., Chan T.H., Li C.J.** Can. J. Chem. 1994, Vol. 72, p. 1181-1192.

125. **Arif A.M., Bradley D.C., Frigo D.M., Hursthouse M.B., Hussian B.** J. Chem. Soc., Chem. Commun. 1985, p. 783-784.

126. **Yan Y., Chan T.H.** J. Am. Chem. Soc. 1991, Vol. 121, p. 3228-3229.

127. **Haddad T.D., HirayamaL.C., Singaram B.** J. Org. Chem. 2010, Vol. 75, p. 642–649.

128. **Bowyer, W. J.** Tetrahedron. 2011, Vol. 67, p. 7449-7460.

129. **Araki S., Ito H., Katsumura N., Butsugan Y.** J. Organomet. Chem. 1989, Vol. 369, p. 291-296.

130. **Araki S., Kamei T., Hirashita T., Yamamura H., Kawai M.** Org. Lett. 2000, Vol. 28, p. 47-84.

131. **Araki S., Horie T., Kato M., Hirashita T., Yamamura H., Kawai M.** Tetrahedron Lett. 1999, Vol. 40, p. 2331-2334.

132. **Aube J., Gawley R.E.** Principles of Asymmetric Synthesis. 2nd. ed., 2012.

133. **Z. Tu, M. Frohn, Z. Shi.** Organic Syntheses. 2003, Vol. 80, p. 1.

134. **Tian H., She X., Shi Y.** Org. Lett. 2001, Vol. 3, p. 715-718.

135. **Shi Y.** Acc. Chem. Res. 2004, Vol. 37, p. 488-496.

136. **Wang Z.X., Miller S.m., Anderson O.P., Shi Y.** J. Org. Chem. 201, Vol. 66, p. 521-530.

137. **Dennmark S.E., Forbes D.C., Hays D.S., De Pue J.S.** J. Org. Chem. 1995, Vol. 60, p. 1391-1407.

138. **Wang Z. X., Tu W, Frohn M., Yhang J-R., Shi Y.** J. Am. Chem. Soc. 1997, Vol. 119, p. 11224-11235.

139. **Tu Y., Wang Z. X., Shi Y.** J. Am. Chem. Soc. 1996, Vol. 118, p. 9806-9807.

140. **Zhu Y., Tu Y., Yu H., Shi Y.** Tetrahedron Lett. 1998, Vol. 39, p. 7819-7822.

141. **Tian H., She X., Yu H., Shu L., Shi Y.** J. Org. Chem. 2002, Vol. 67, p. 2435-2446.

142. **Payne G.B.** J. Org. Chem. 1962, Vol. 27, p. 3819.

143. **Fringuelli F., Pizzo F., Tortoioli S., Vaccaro L.** Green Chem. 2003, Vol. 5, p. 436.

144. **Masamune S., Choy W.** AldrichimicaACTA. 1982, Vol. 15, p. 47.

145. **Lee, A.W.M., Martin V.S., Masamune S., Sharpless K.B., Walker F.J.** J. Org. Chem. 1985, Vol. 50, p. 5687.

146. **Nicolaou K.C., Sorenses E.J.** Classics in Total Synthesis. 1996, p. 299-315.

147. **Carey F.A., Sundberg R.J.** Advanced Organic Chemistry, Part A. 5th ed., 2007.

148. **Kim E., Gordon D.M., Schmid W., Whitesides G.M.** J. Org. Chem. 1993, Vol. 58, p. 5500.

149. **Behrens C.H., Ko S.Y., Sharpless K.B.** J . Org. Chem. 1985, Vol. 50, p. 5687-5696.

150. **Behrens C.H., Ko S.Y., Sharpless K.B.,Walker F.J.** J. Org. Chem. 1985, Vol. 50, p. 5687.

151. **Smith L.H.S, Coote S.C., Sneddon H.F., Procter D.J.** Angew. Chem. Int. Ed. 2010, Vol. 49, p. 5832 – 5844.

152. **Hesse M., Meier H., Zeeh B.** Metodi spettroscopici in Chimica Organica, 2nd edition. 2010.

153. **R.M., Silverstein.** Identificazione Spettrometrica di Composto Organici, 2nd edition. 2006.

154. **Dobson C.M., Pain R.H.** Mechanism of Protein Folding. 2000, p. 1-28.

155. **Ohki S., Kainosho M.** Progress in Nuclear Magnetic Resonance Spectroscopy. 2008, Vol. 53, p. 208-226.

156. **Normann M., Dietmar K.** J. Label. Compd. Radiopharm. 2002, Vol. 45, p. 601-610.

Table of figures

List of tables

Appendix

Selected spectra

^{1}H-NMR of **(S)-2,2-dimethyl-1,3-dioxolane-4-carbaldehyde [1]**

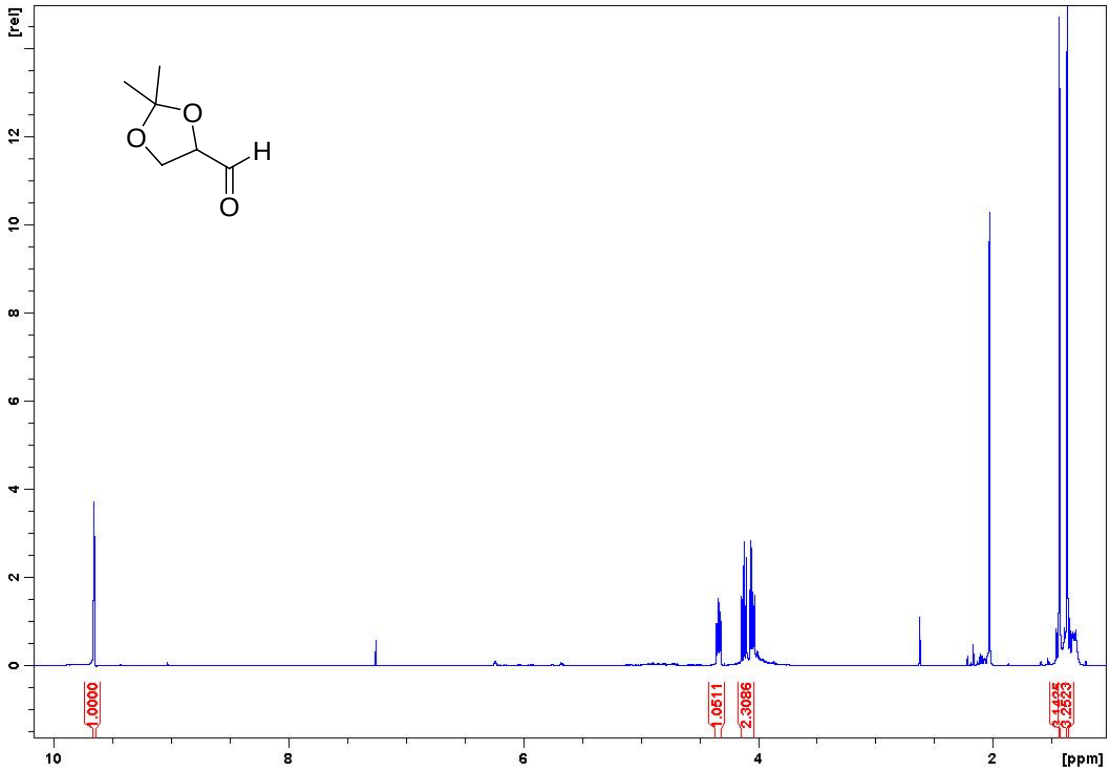

^{1}H-NMR of **1-((S)-2,2-dimethyl-1,3-dioxolan-4-yl)but-3-en-1-ol [2]**

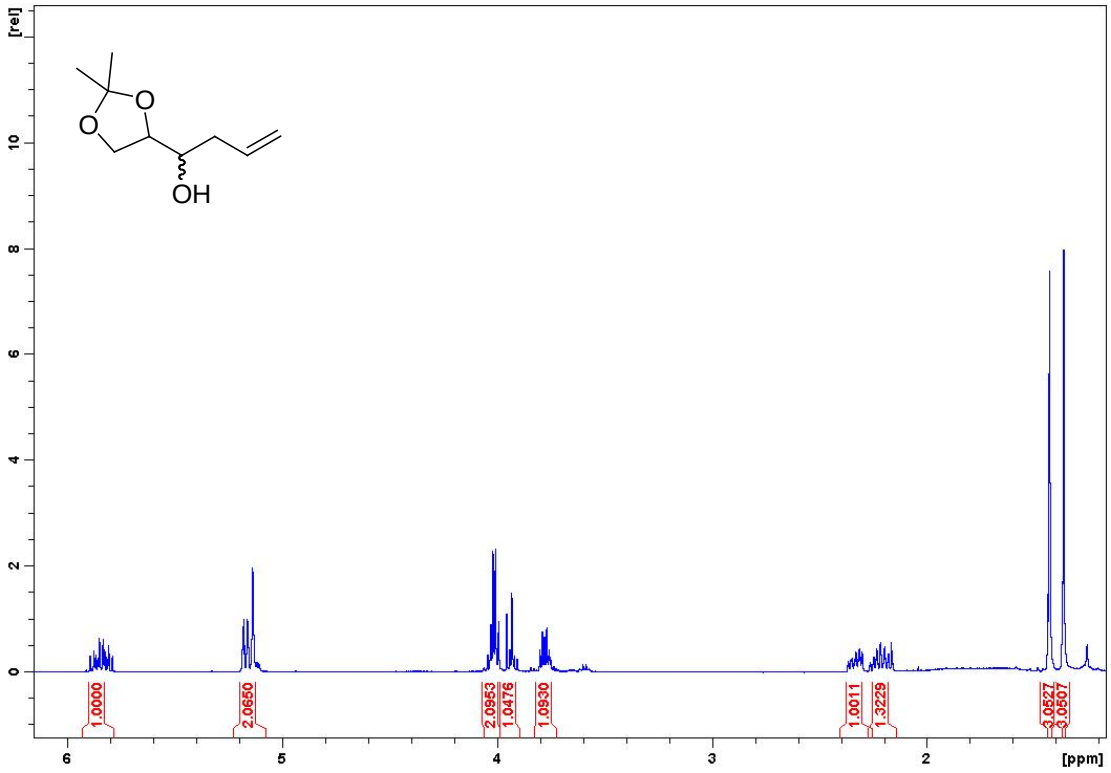

^{13}C-NMR of **1-((S)-2,2-dimethyl-1,3-dioxolan-4-yl)but-3-en-1-ol [2]**

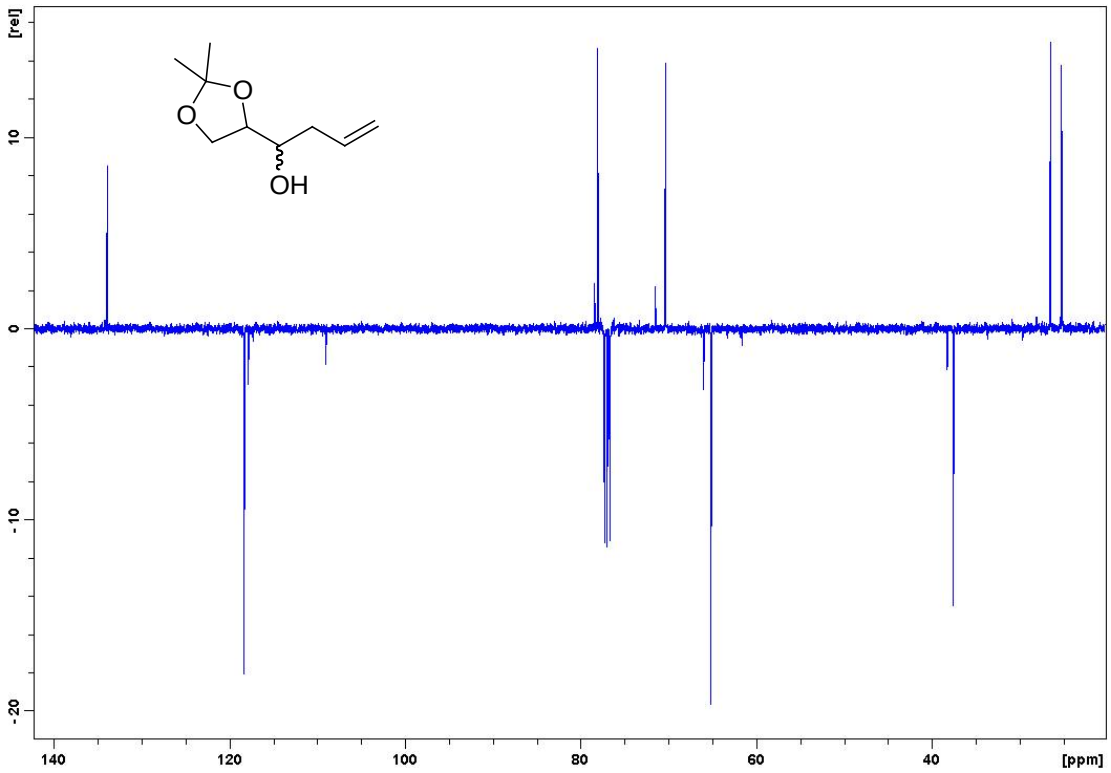

^{1}H-NMR of **1-((S)-2,2-dimethyl-1,3-dioxolan-4-yl)-2-(oxiran-2-yl)ethanol [3]**

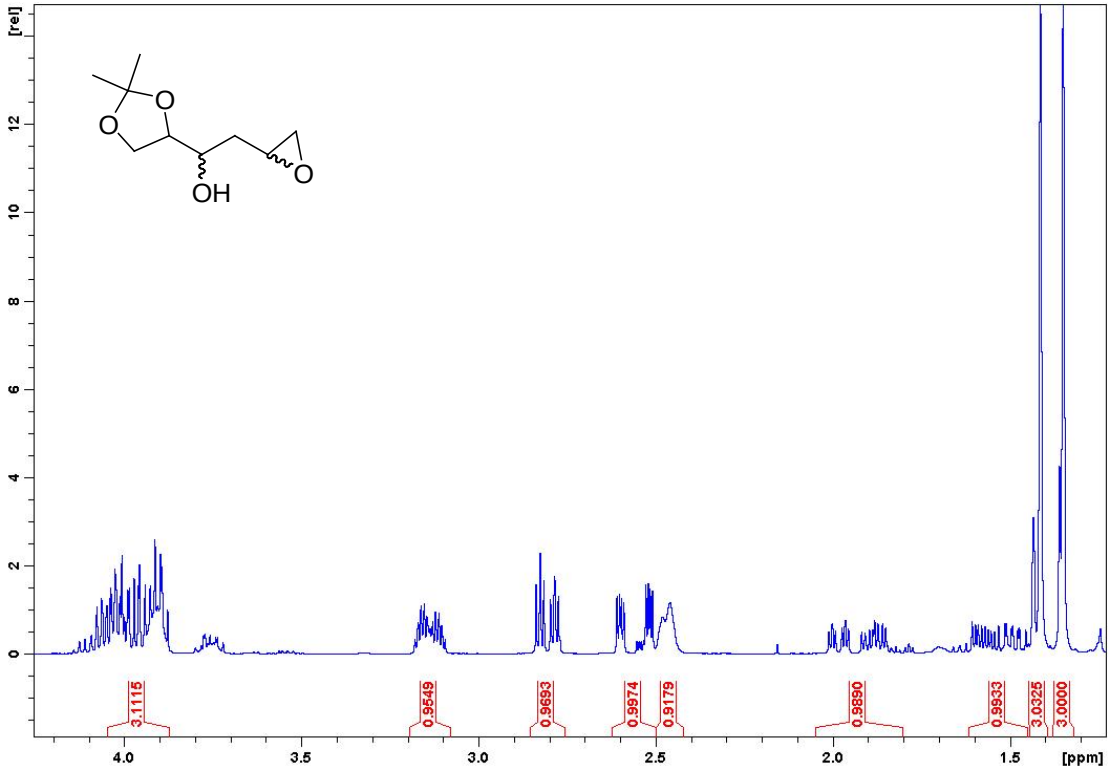

^{13}C-NMR of **1-((S)-2,2-dimethyl-1,3-dioxolan-4-yl)-2-(oxiran-2-yl)ethanol [3]**

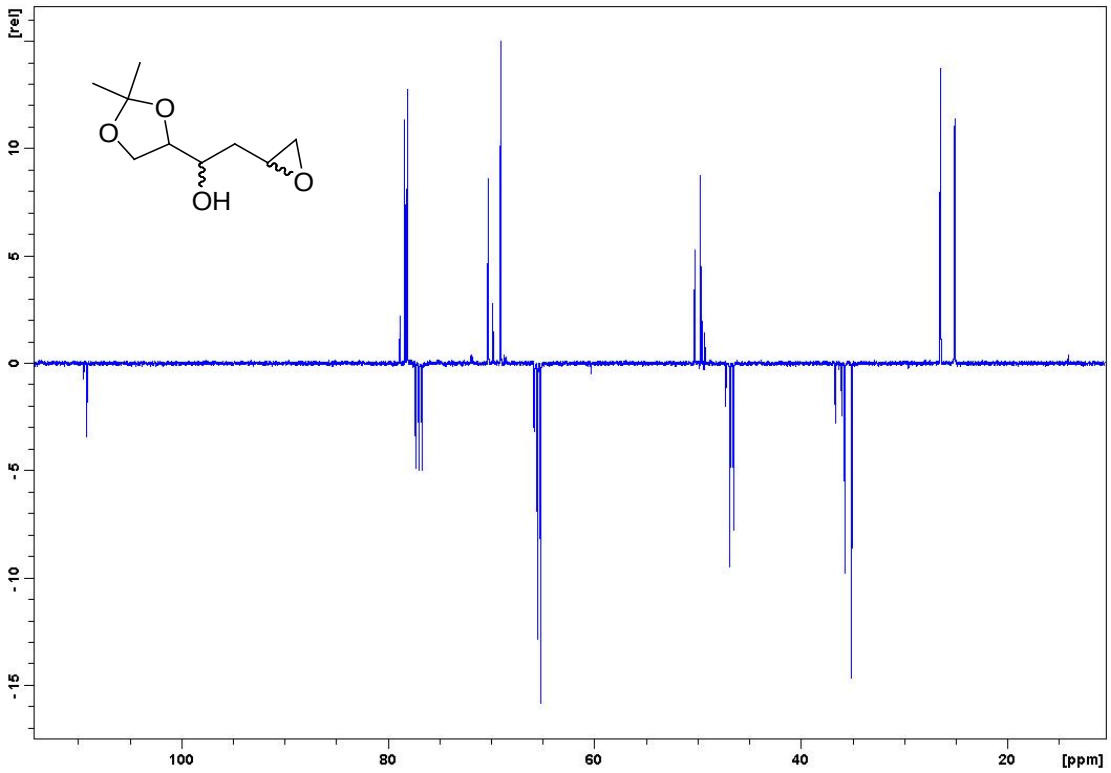

^{1}H-NMR of **1-((S)-2,2-dimethyl-1,3-dioxolan-4-yl)-4-(phenylthio)butane-1,3-diol [4]**

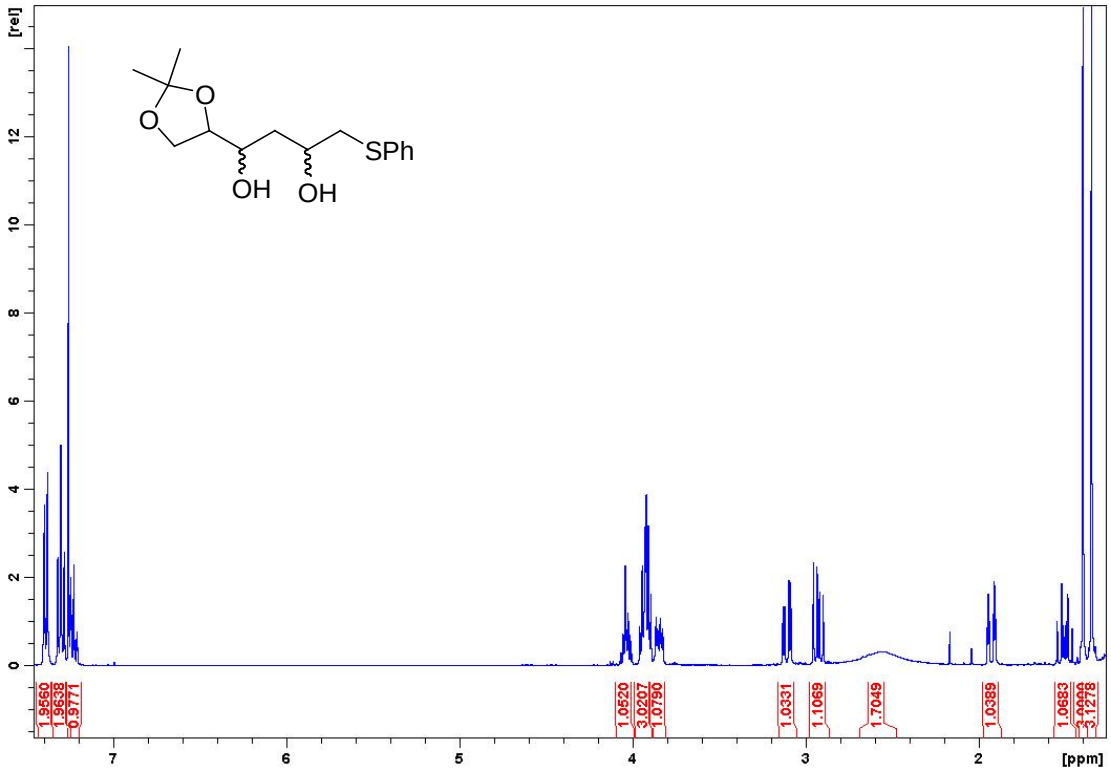

^{1}H-NMR of **1-((S)-2,2-dimethyl-1,3-dioxolan-4-yl)-4-(phenylsulfinyl)butane-1,3-diol [5]**

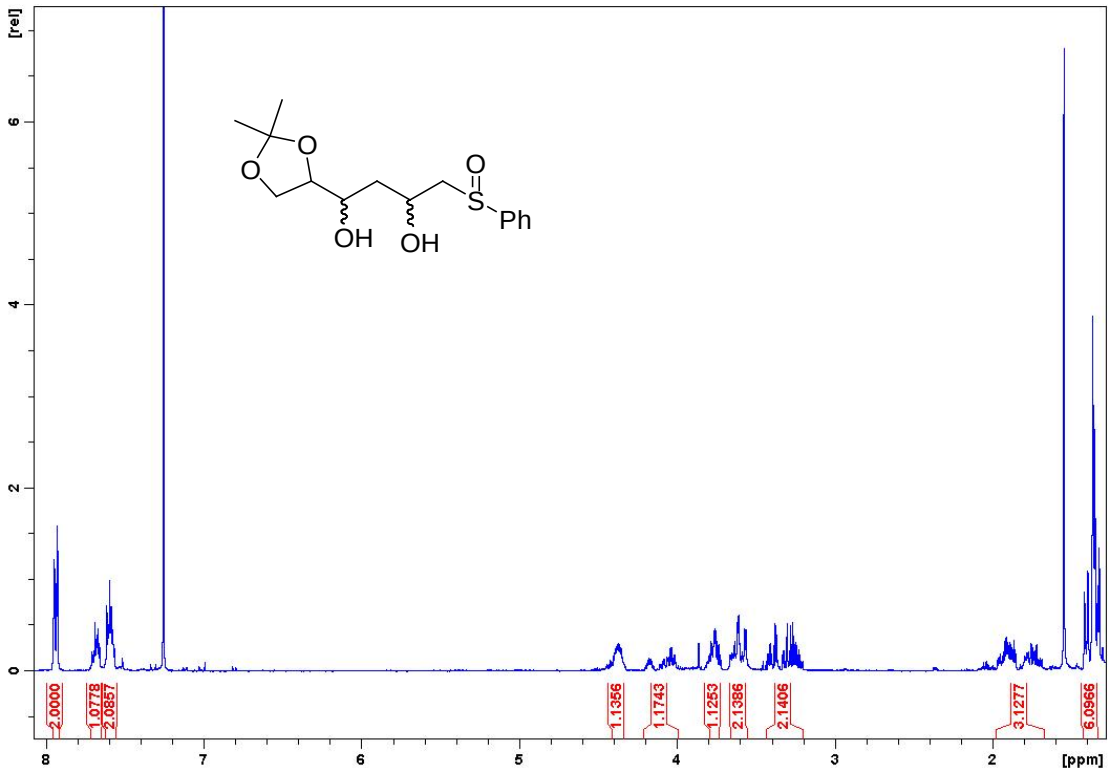

^{1}H-NMR of **1,3-Dioxolane, 2,2-dimethyl-4-[1-(phenylmethoxy)-3-butenyl] [11]**

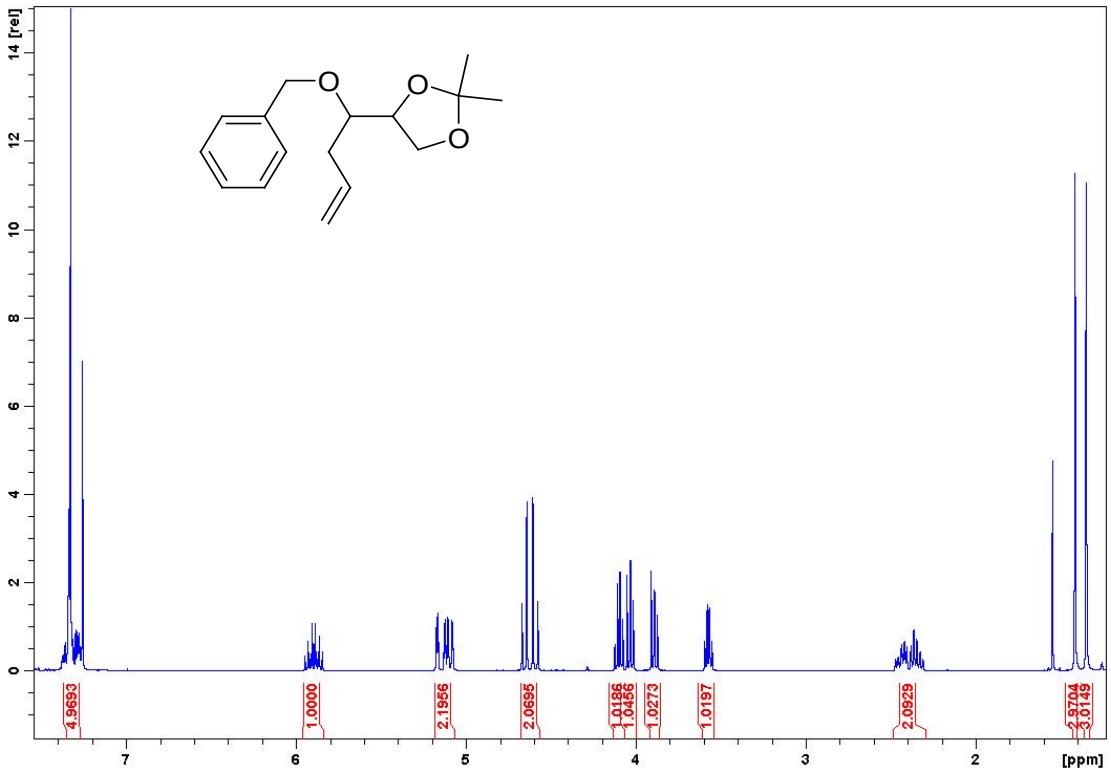

^{1}H-NMR of **5-Hexene-1,2-diol, 3-(phenylmethoxy) [12]**

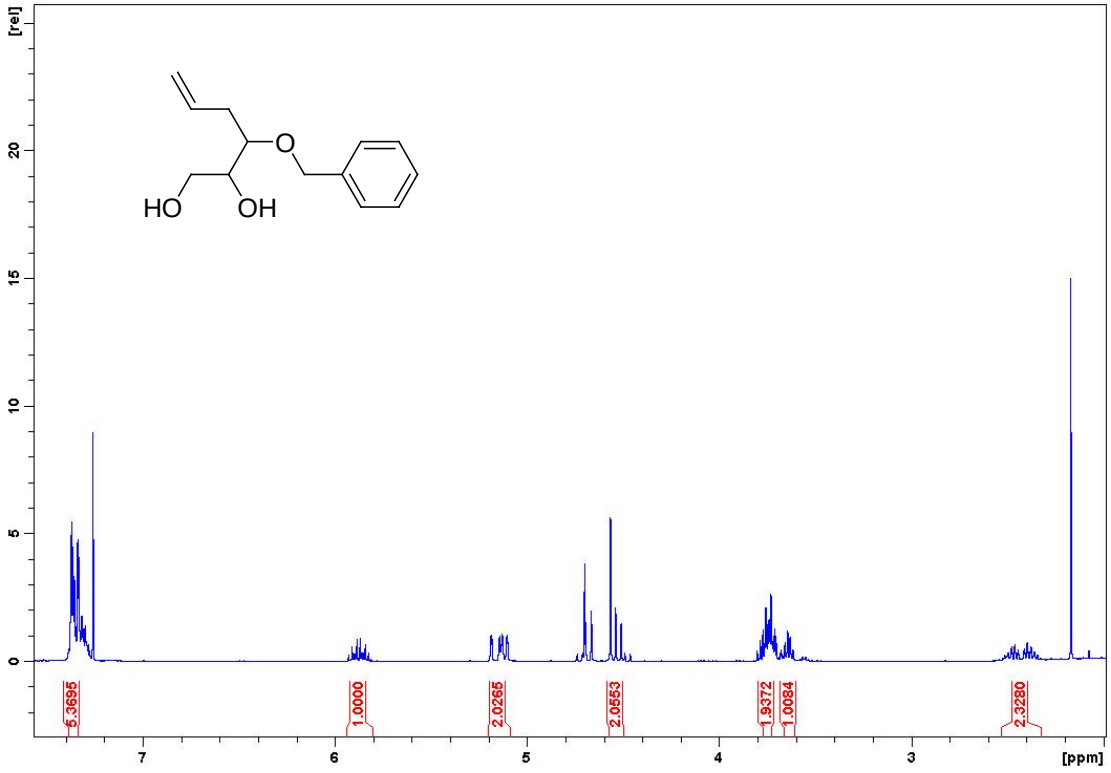

^{1}H-NMR of **4-Pentenal, 2-(phenylmethoxy) [13]**

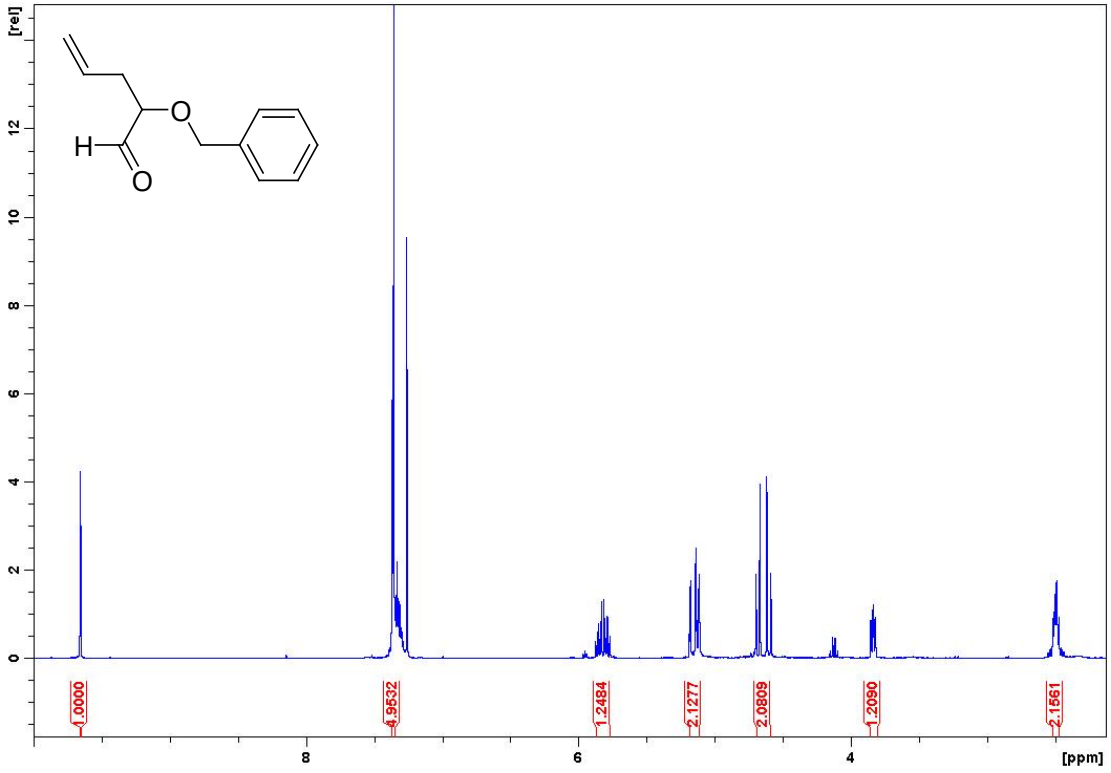

^{1}H-NMR of **ethyl 5-(benzyloxy)-4-hydroxy-2-methyleneoct-7-enoate [14]**

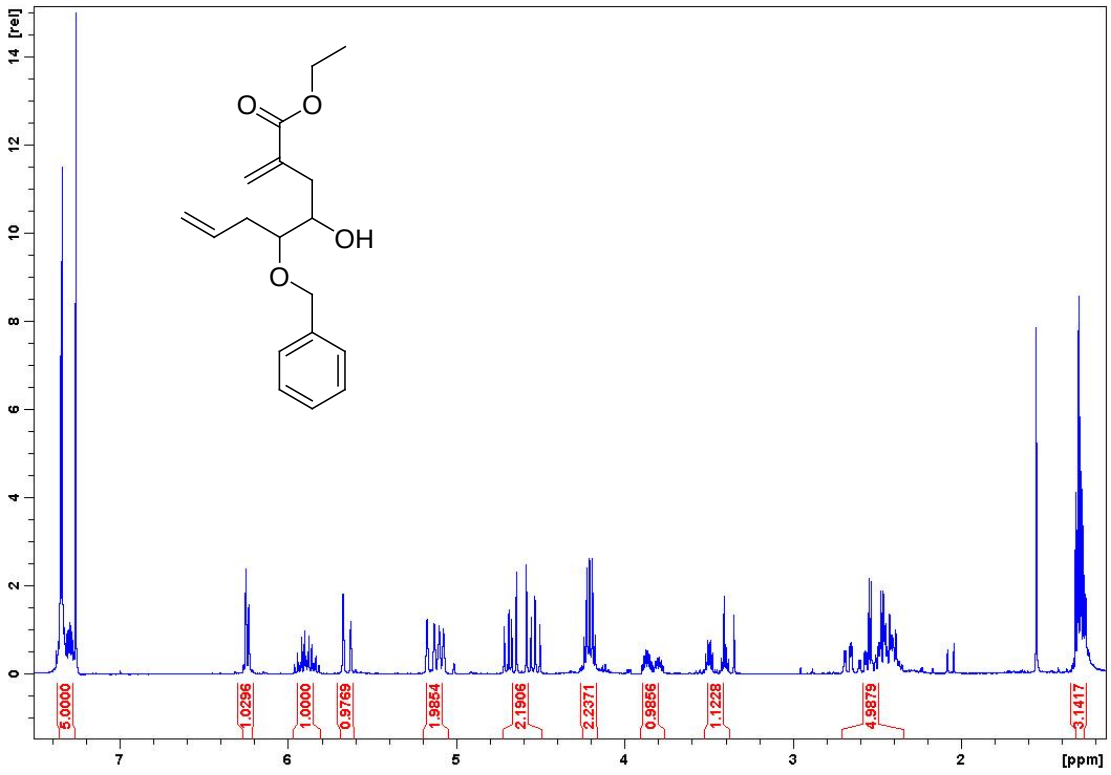

^{1}H-NMR of **ethyl 4-(benzyloxy)-5-hydroxycyclohex-1-enecarboxylate [15]**

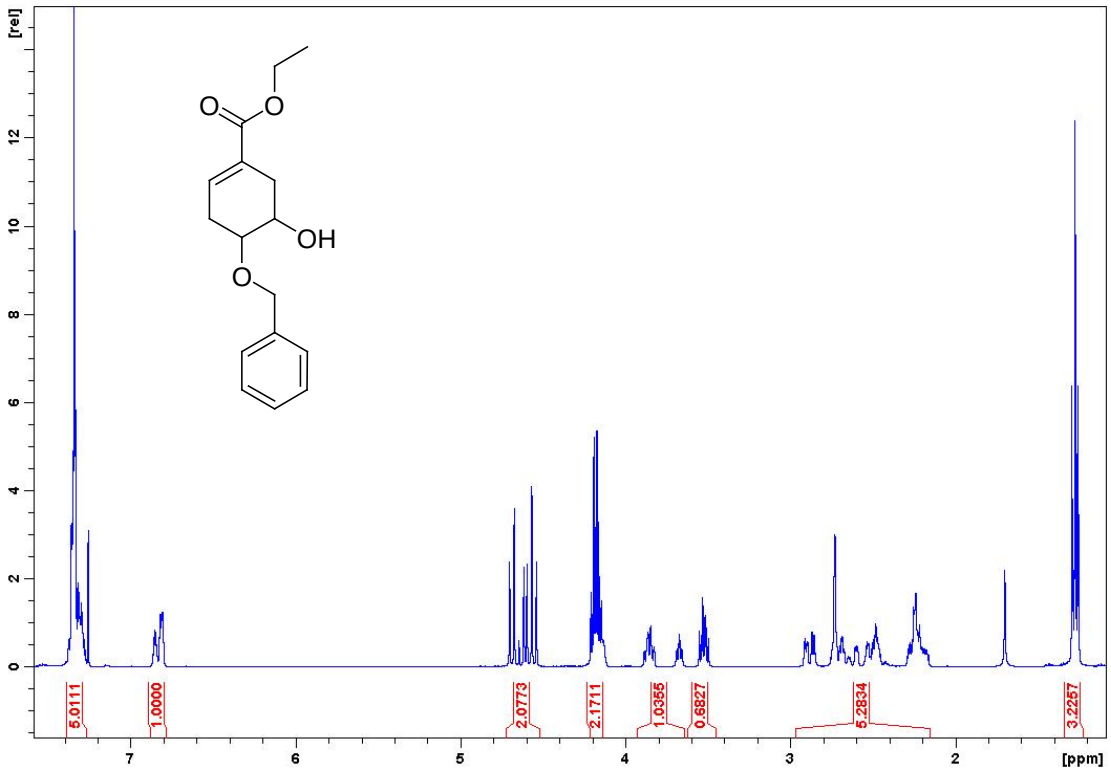

^{1}H-NMR of **4-(1-(4-methoxybenzyloxy)but-3-enyl)-2,2-dimethyl-1,3-dioxolane [16]**

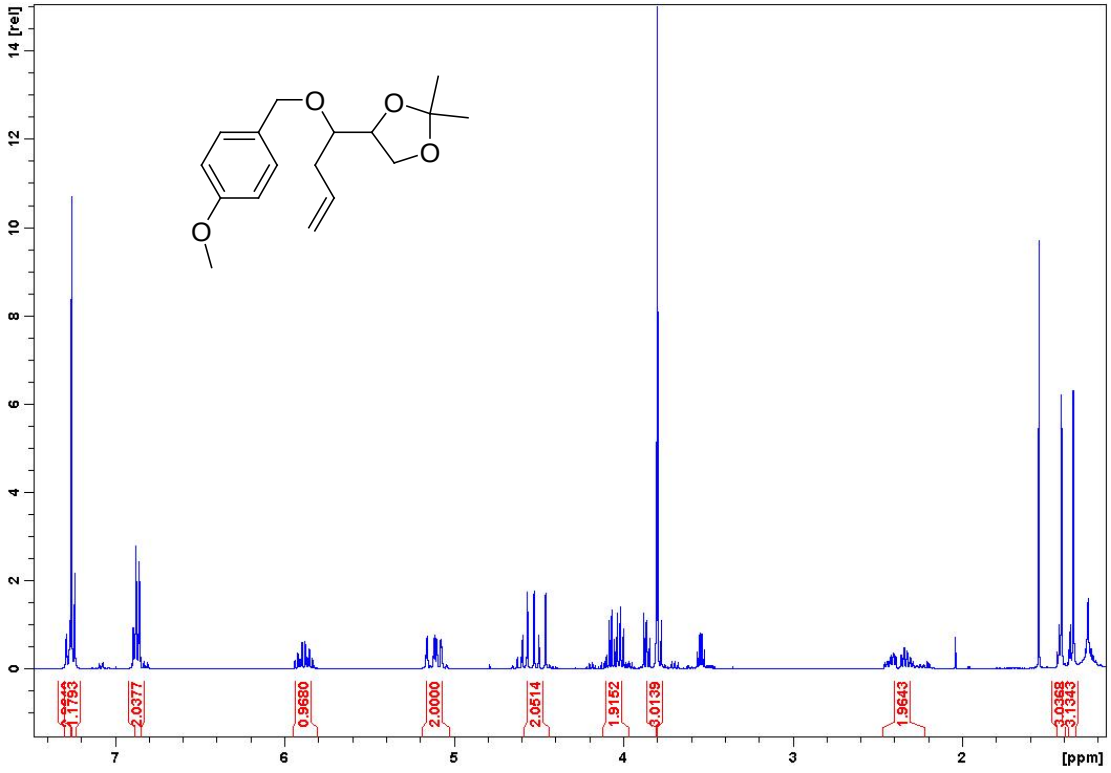

^{1}H-NMR of **3-(4-methoxybenzyloxy)hex-5-ene-1,2-diol [17]**

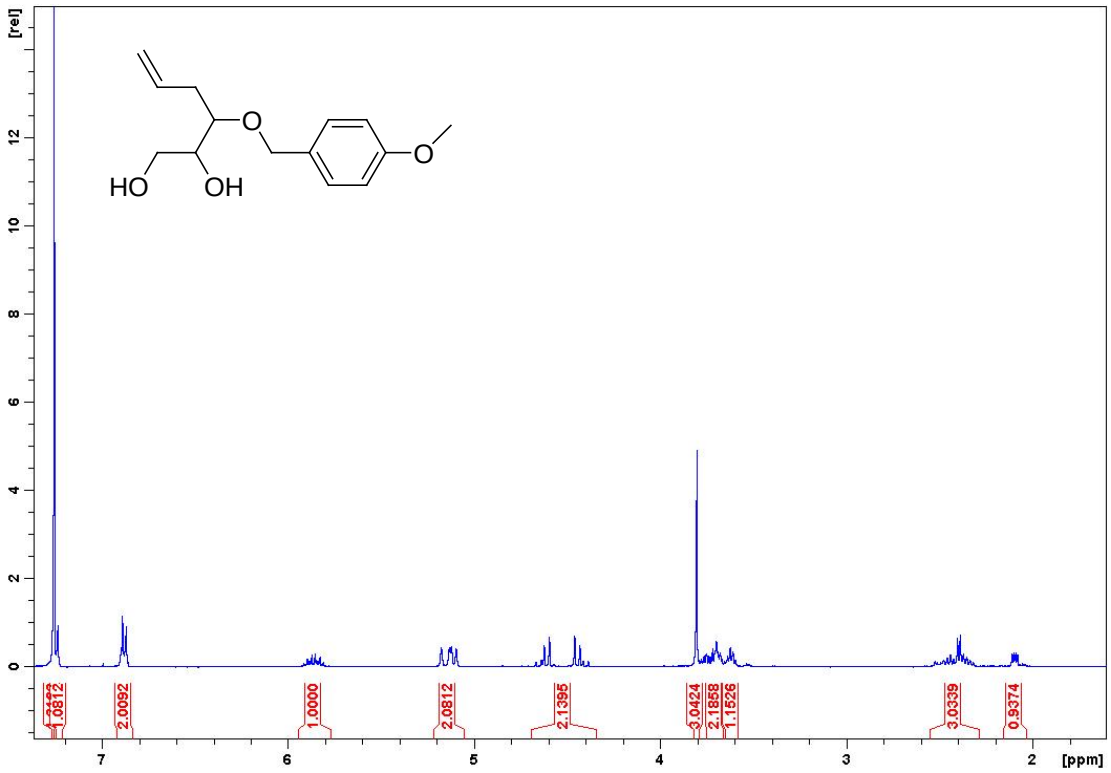

^{1}H-NMR of **Ethyl 2-(4-methoxybenzyloxy)acetate [19]**

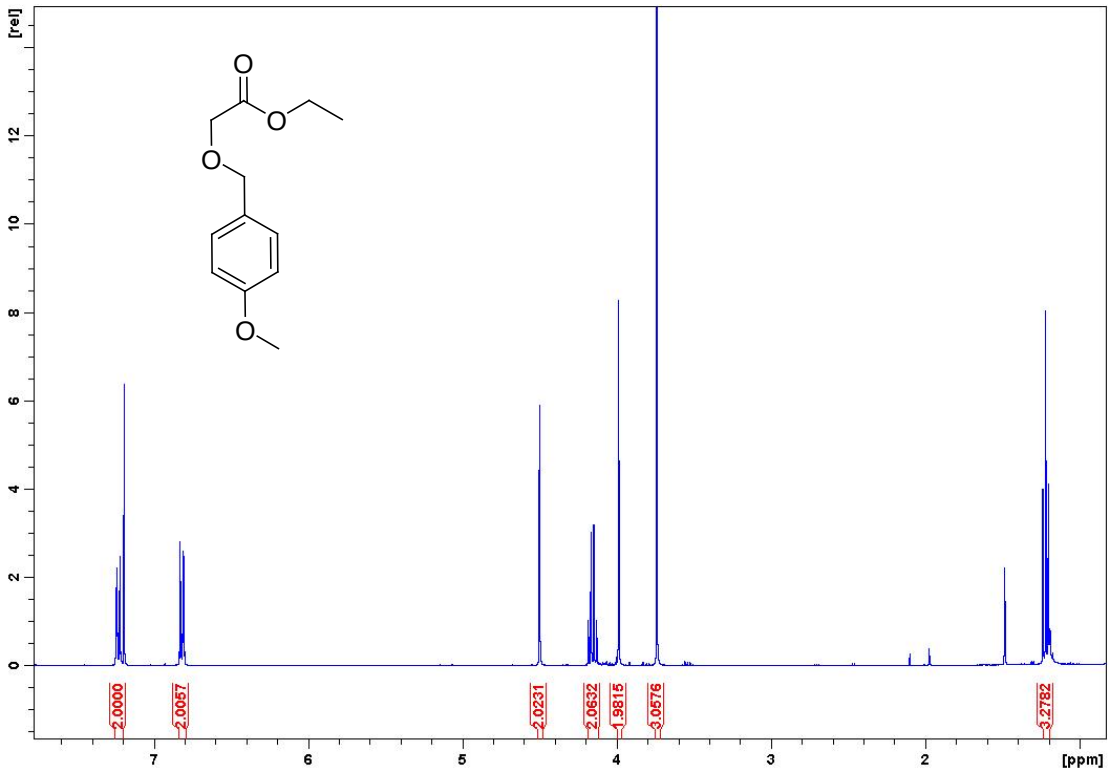

^{1}H-NMR of **ethyl 2-(4-methoxybenzyloxy)pent-4-enoate [20]**

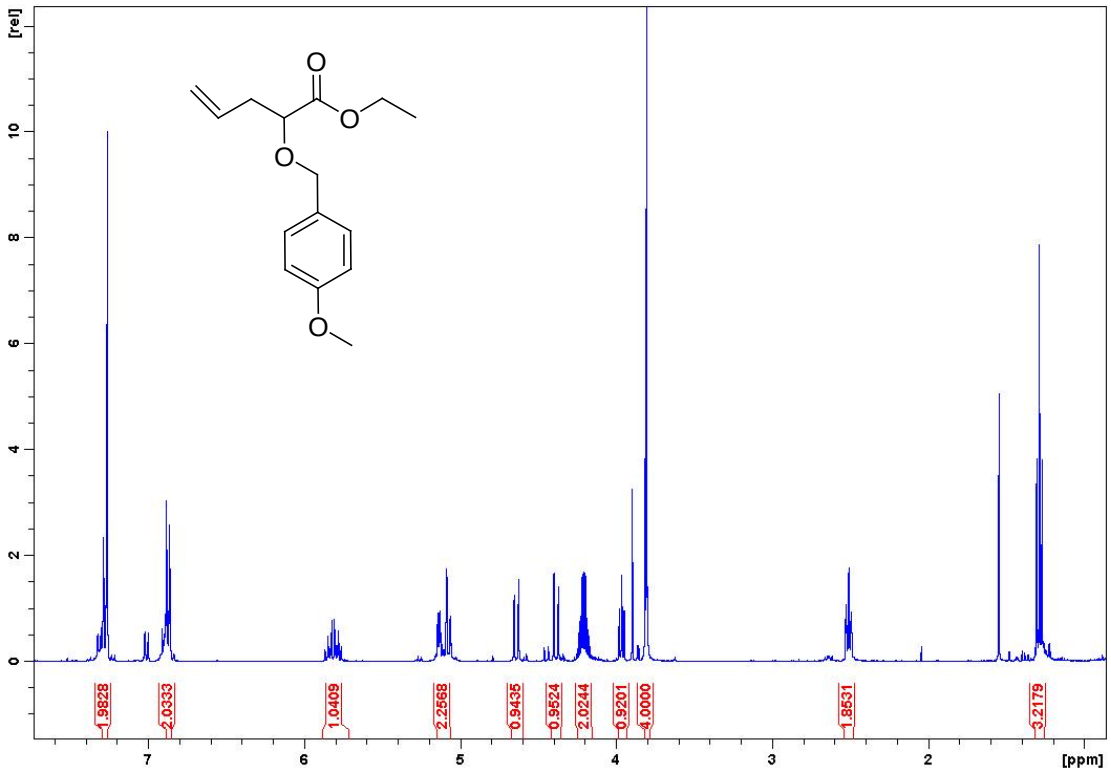

^{1}H-NMR of **2-(4-methoxybenzyloxy)acetic acid [22]**

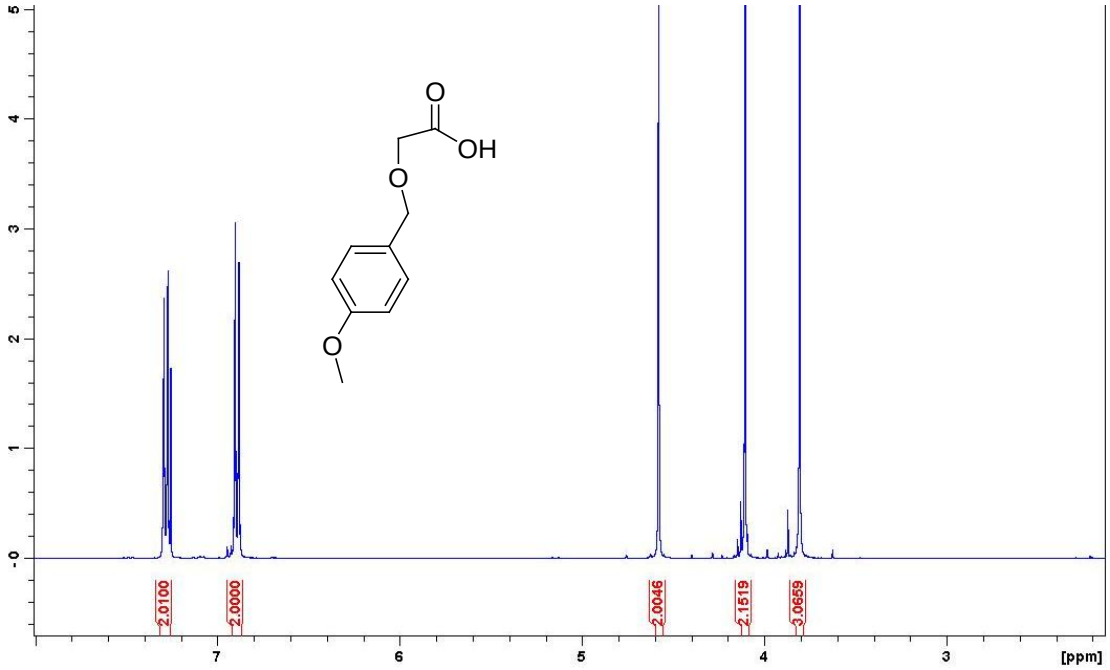

^{13}C-NMR of **2-(4-methoxybenzyloxy)acetic acid [22]**

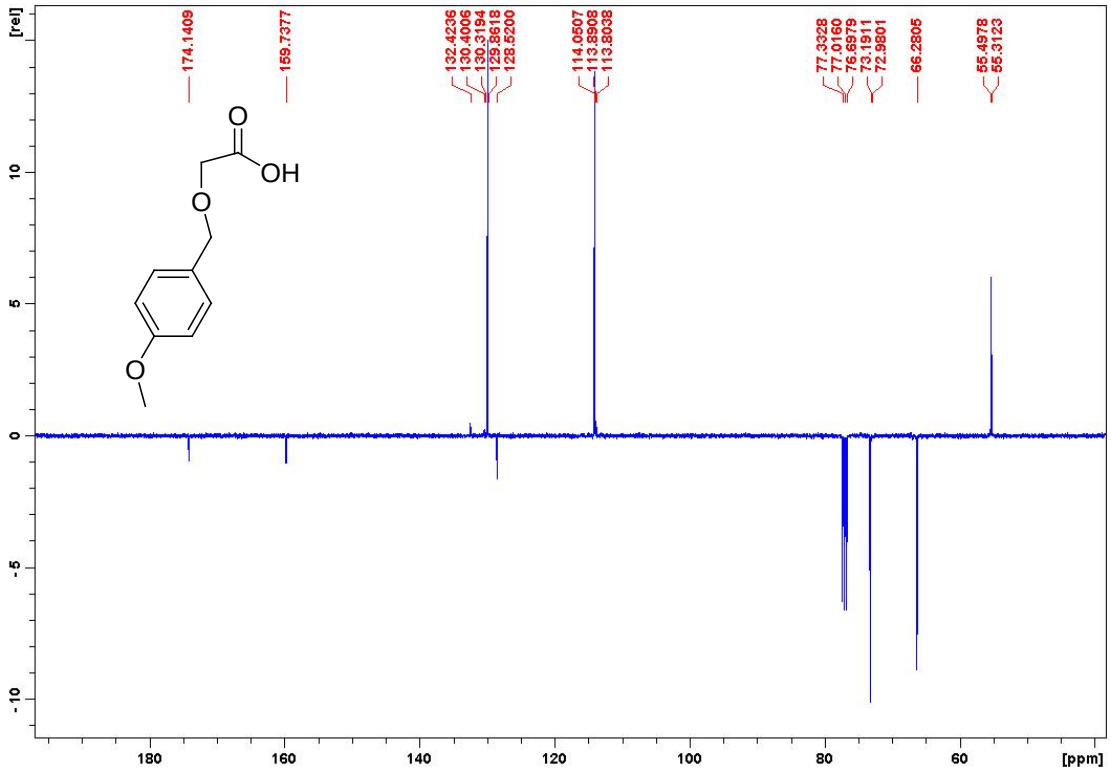

^{1}H-NMR of **allyl 2-(4-methoxybenzyloxy)acetate [23]**

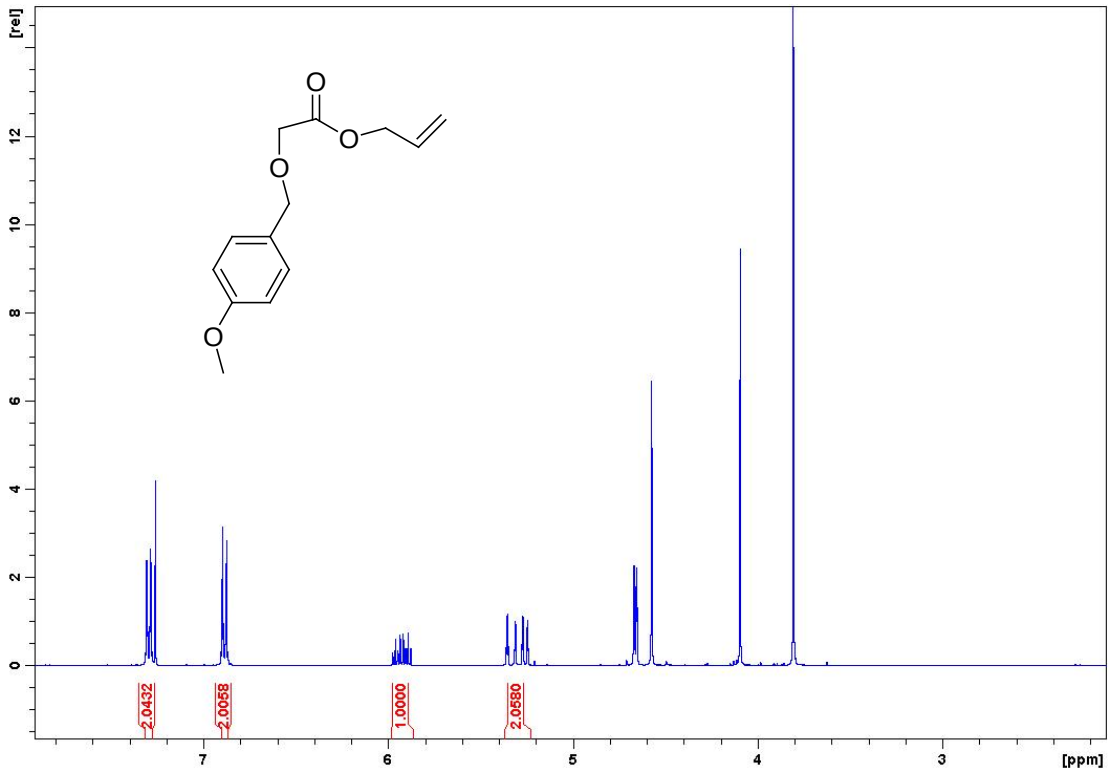

^{13}C-NMR of **allyl 2-(4-methoxybenzyloxy)acetate [23]**

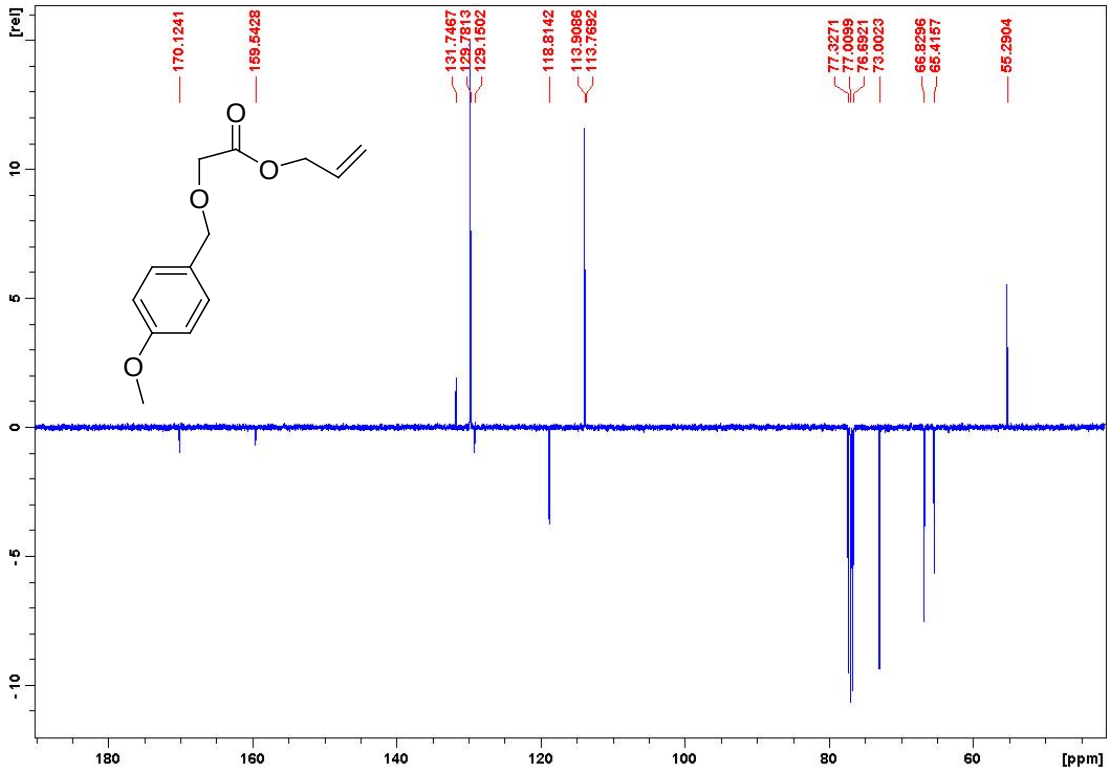

^{1}H-NMR of **2-(4-methoxybenzyloxy)pent-4-enoic acid [24]**

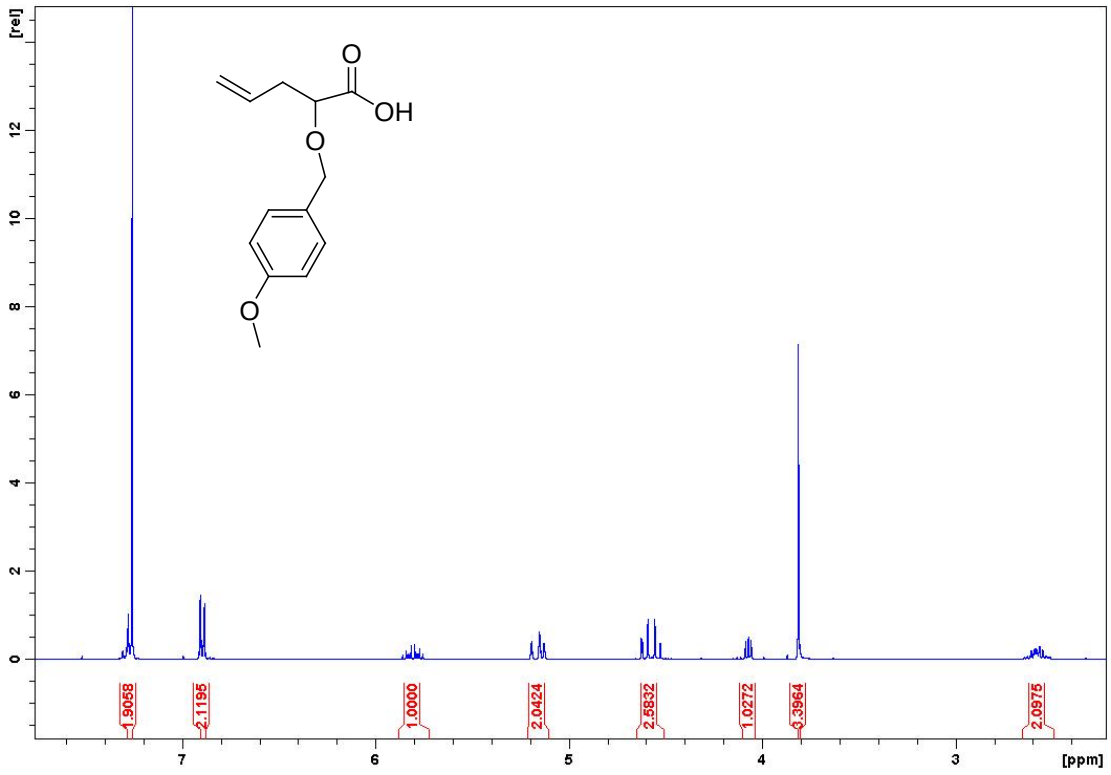

^{1}H-NMR of **methyl 2-(4-methoxybenzyloxy)pent-4-enoate [25]**

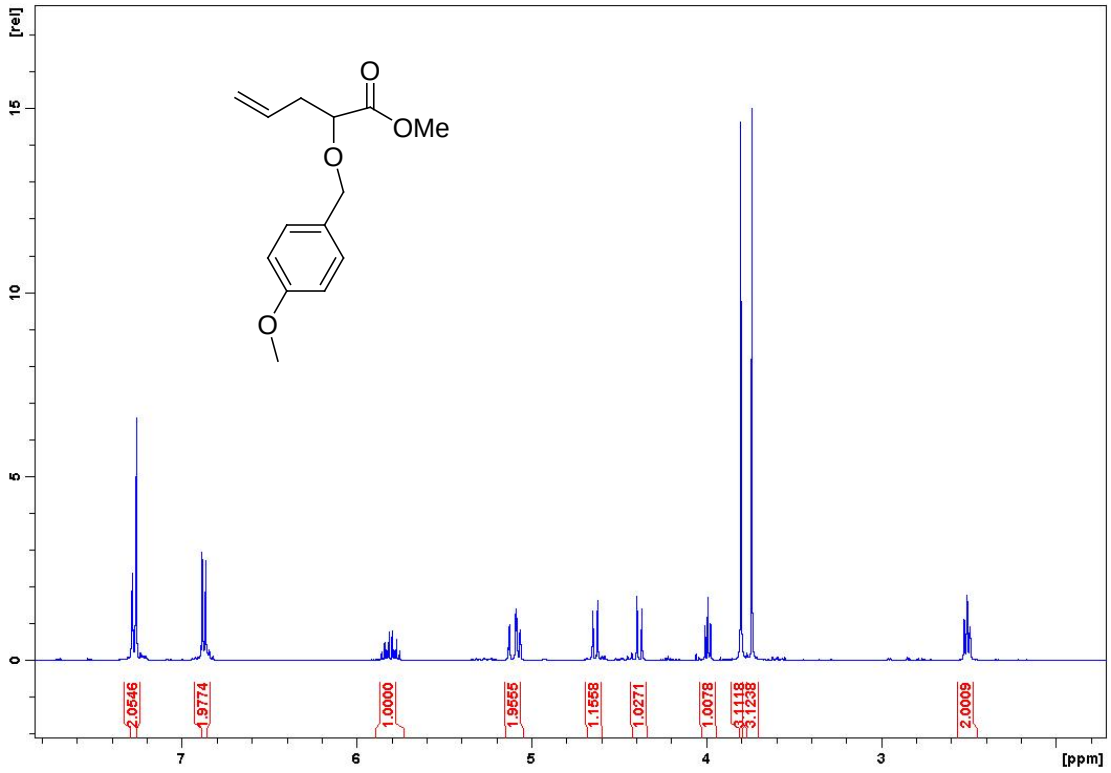

^{13}C-NMR of **methyl 2-(4-methoxybenzyloxy)pent-4-enoate [25]**

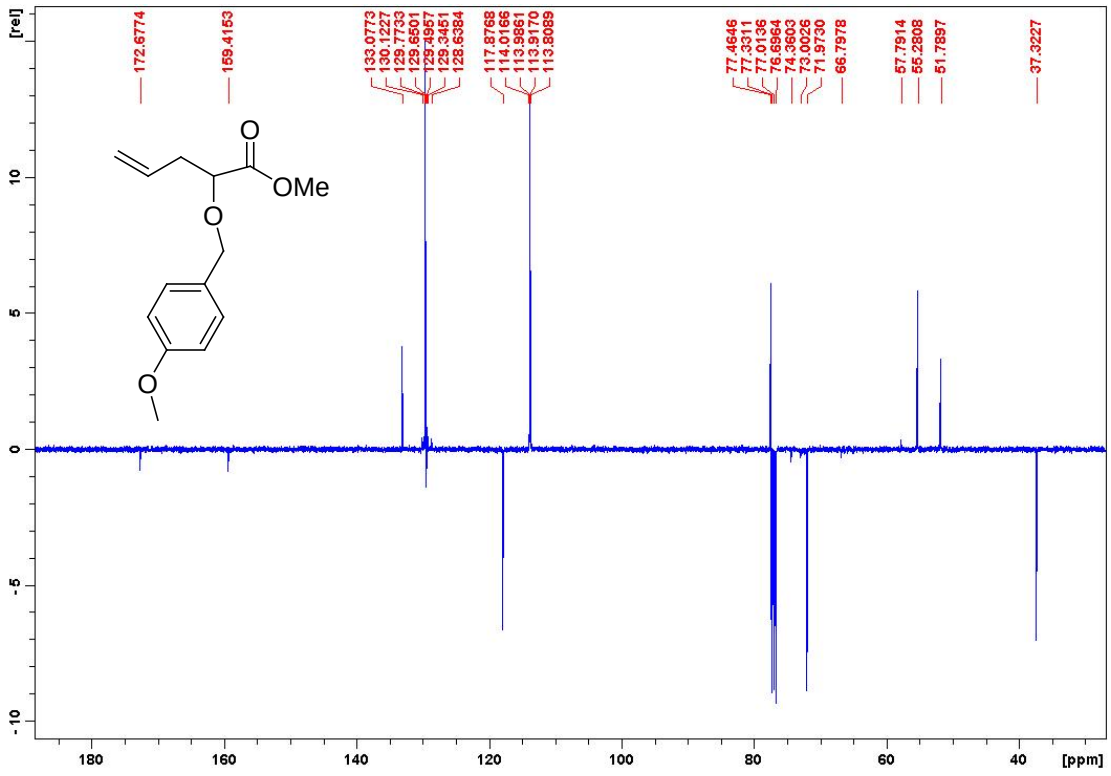

^{1}H-NMR of **2-(4-methoxybenzyloxy)pent-4-enal [26]**

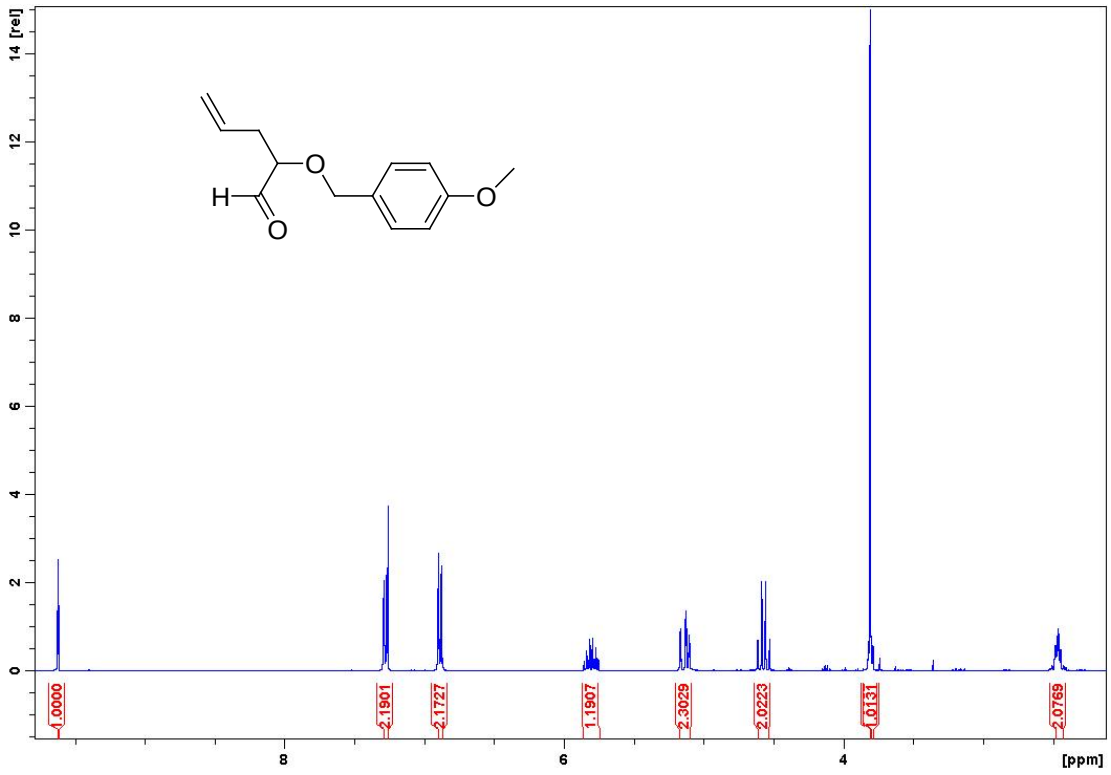

^{1}H-NMR of **ethyl 5-(4-methoxybenzyloxy)-4-hydroxy-2-methyleneoct-7-enoate [27]**

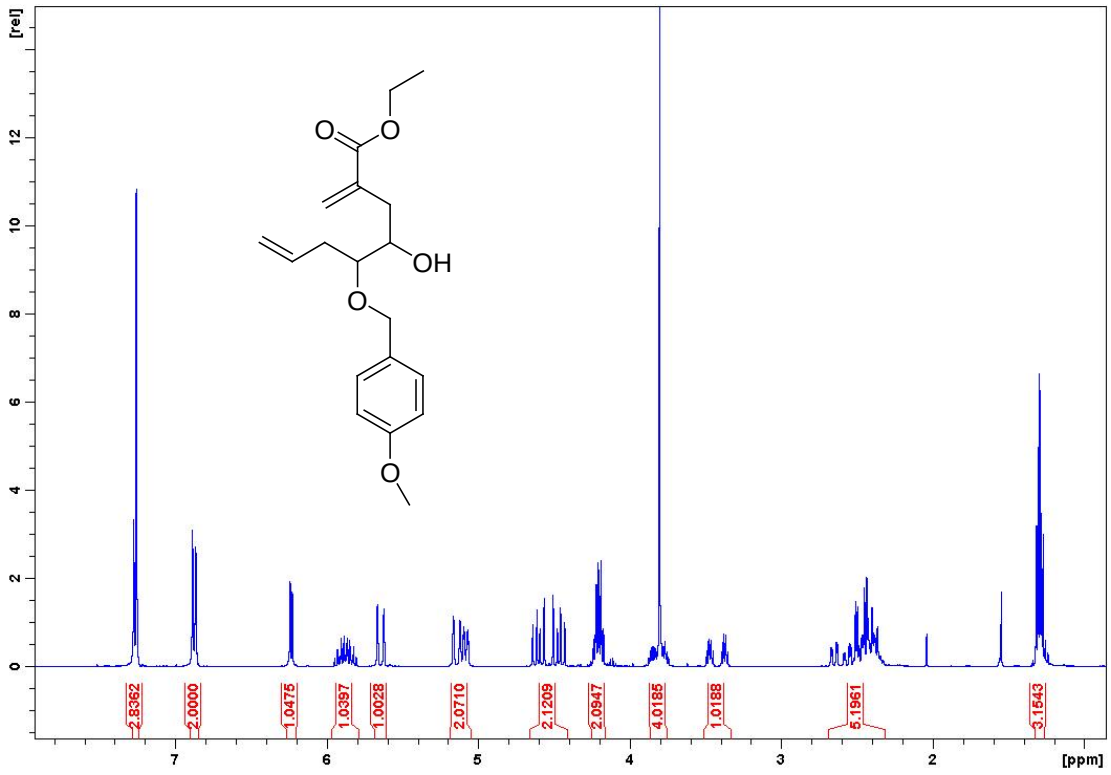

^{13}C-NMR of **ethyl 5-(4-methoxybenzyloxy)-4-hydroxy-2-methyleneoct-7-enoate[27]**

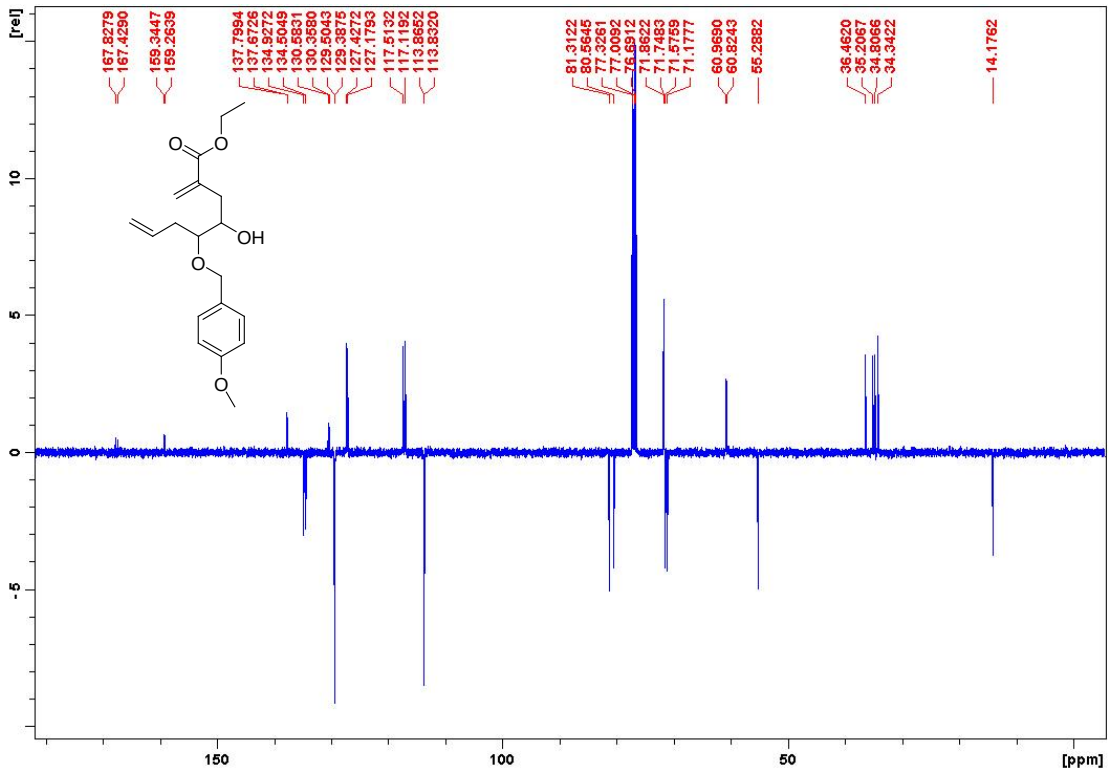

^{1}H-NMR of **ethyl 4-(4-methoxybenzyloxy)-5-hydroxycyclohex-1-enecarboxylate[28]**

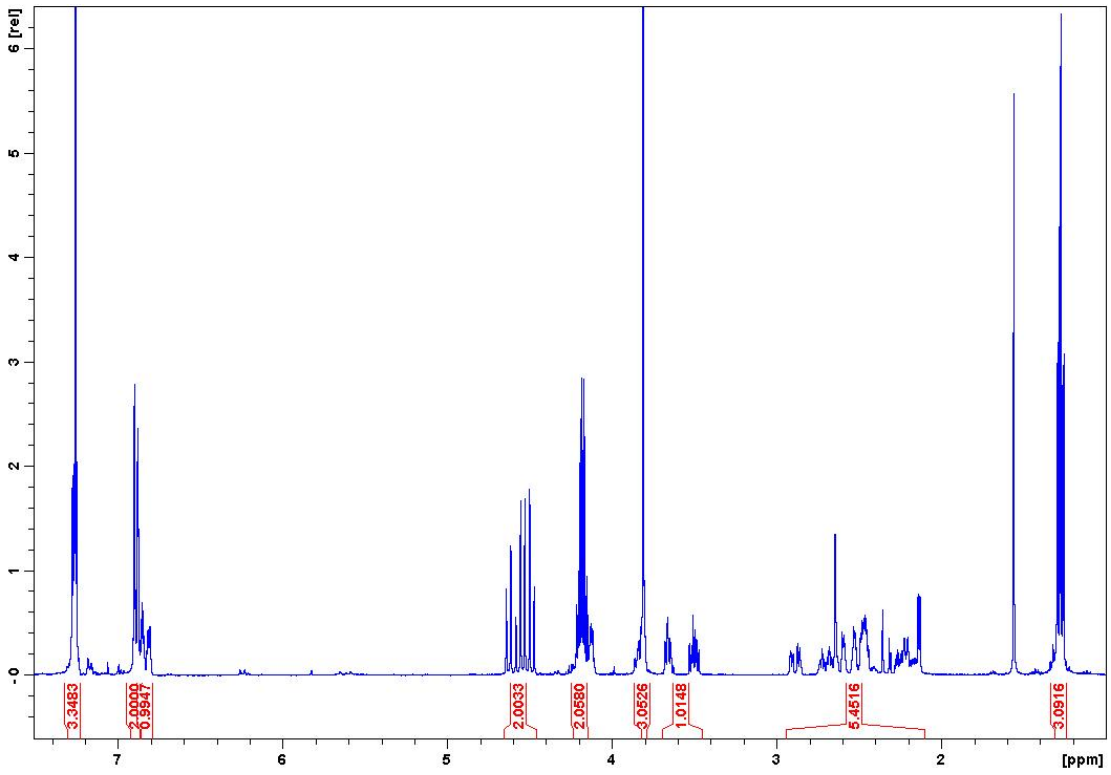

^{13}C-NMR of **ethyl 4-(4-methoxybenzyloxy)-5-hydroxycyclohex-1enecarboxylate[28]**

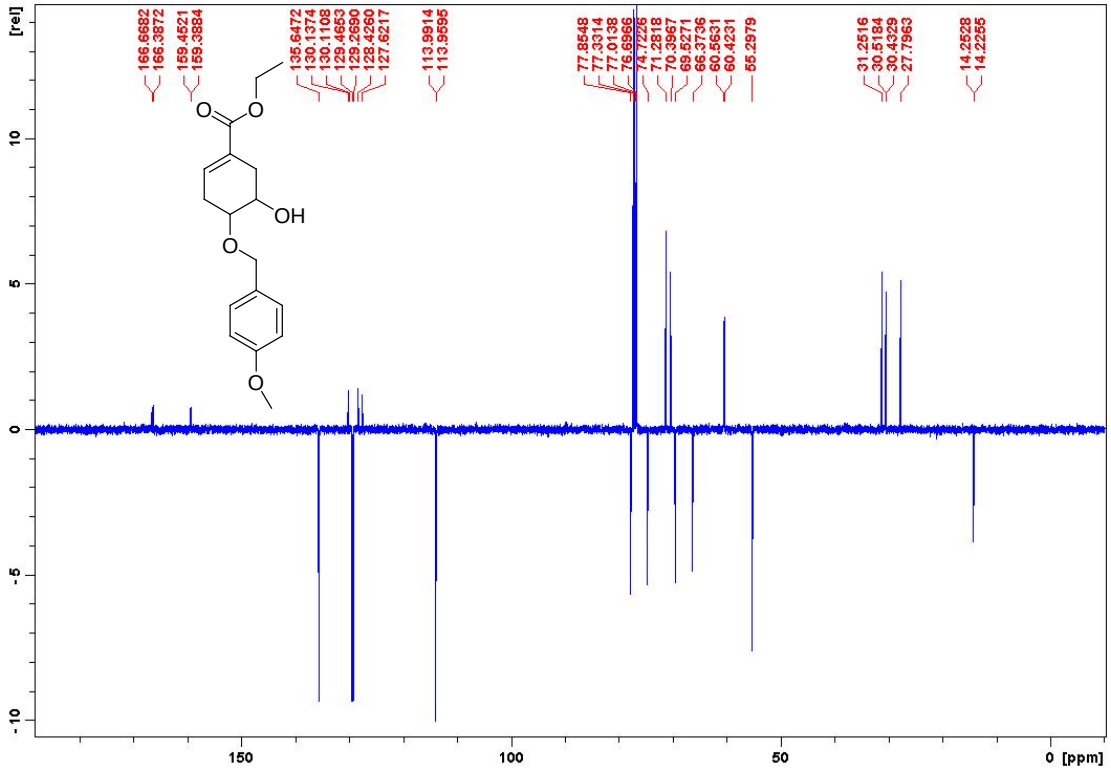

^{1}H-NMR of **ethyl 4,5-dihydroxycyclohex-1-enecarboxylate [29]**

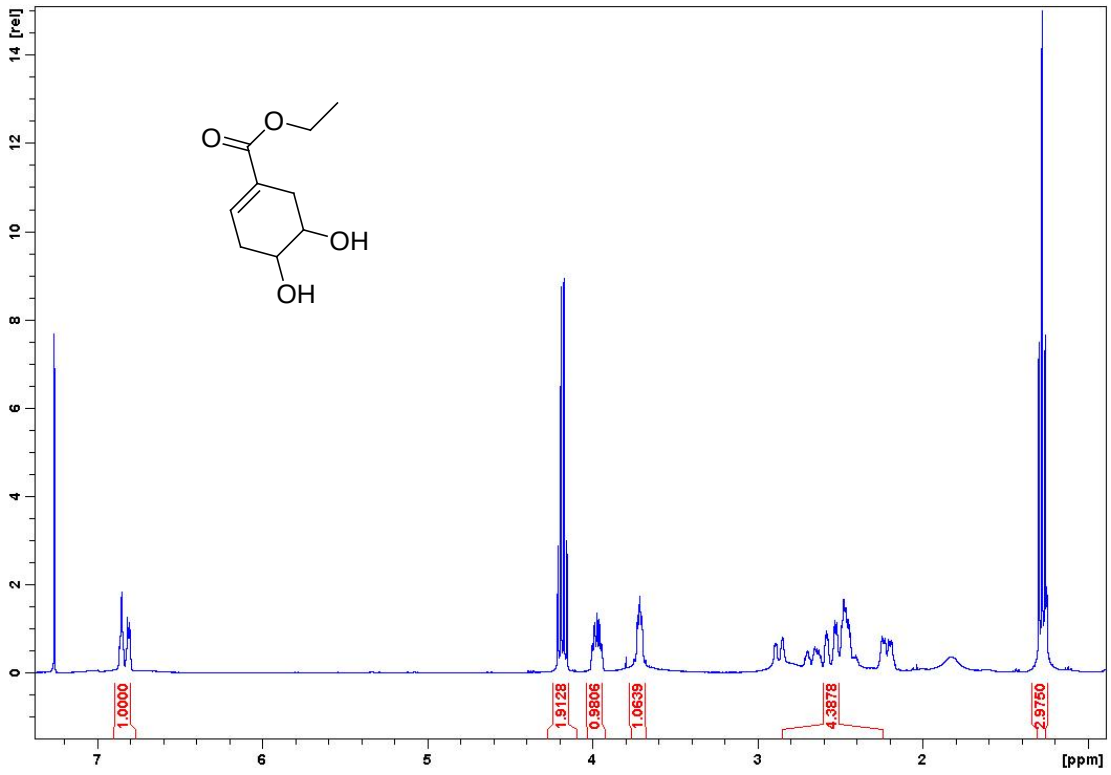

^{13}C-NMR of **ethyl 4,5-dihydroxycyclohex-1-enecarboxylate [29]**

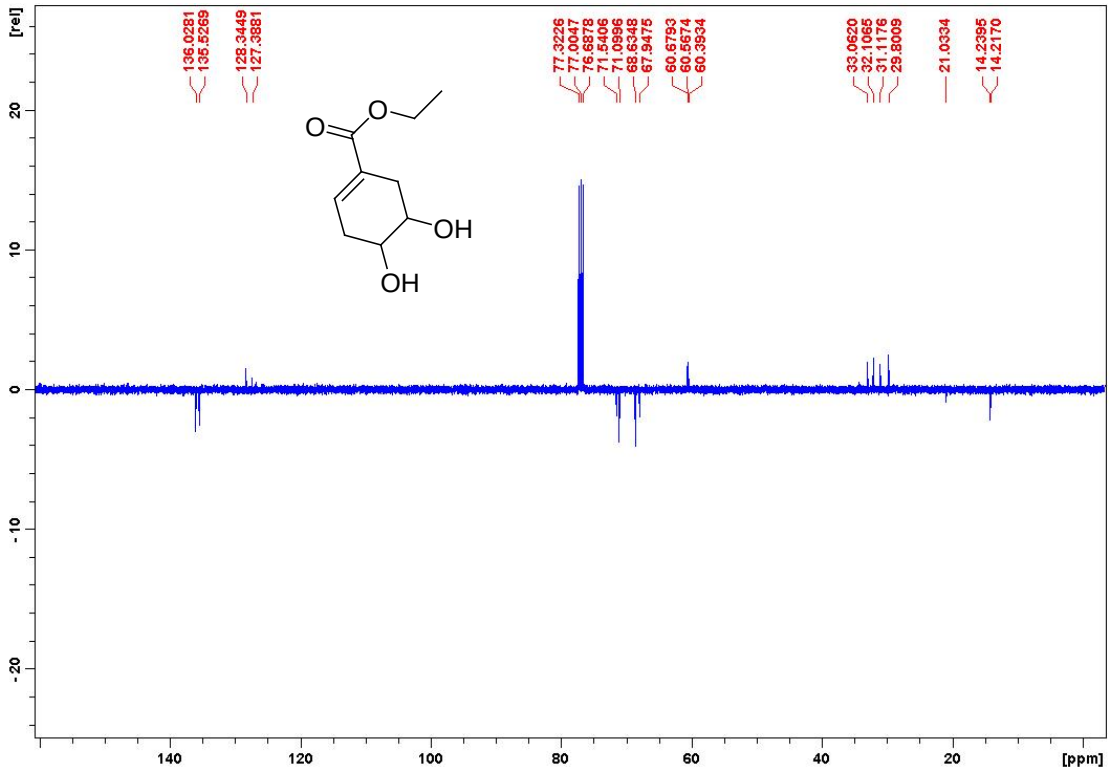

^{1}H-NMR of **benzoic acid [30]**

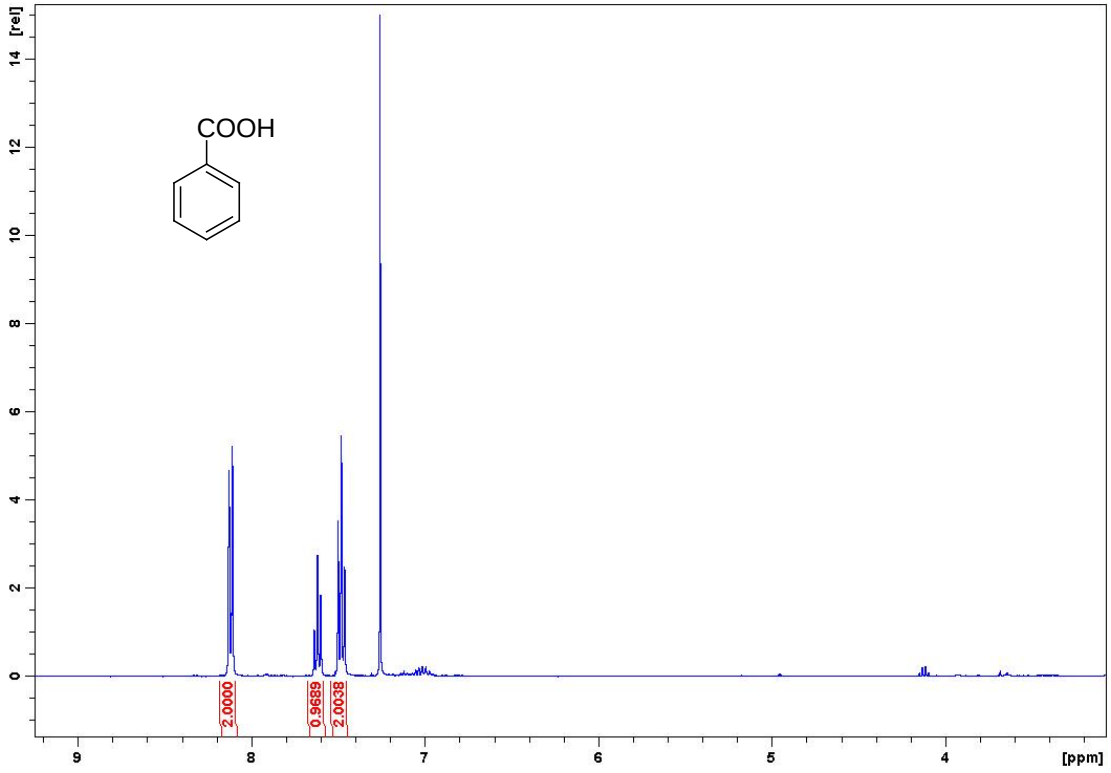

^{13}C-NMR of **benzoic acid [30]**

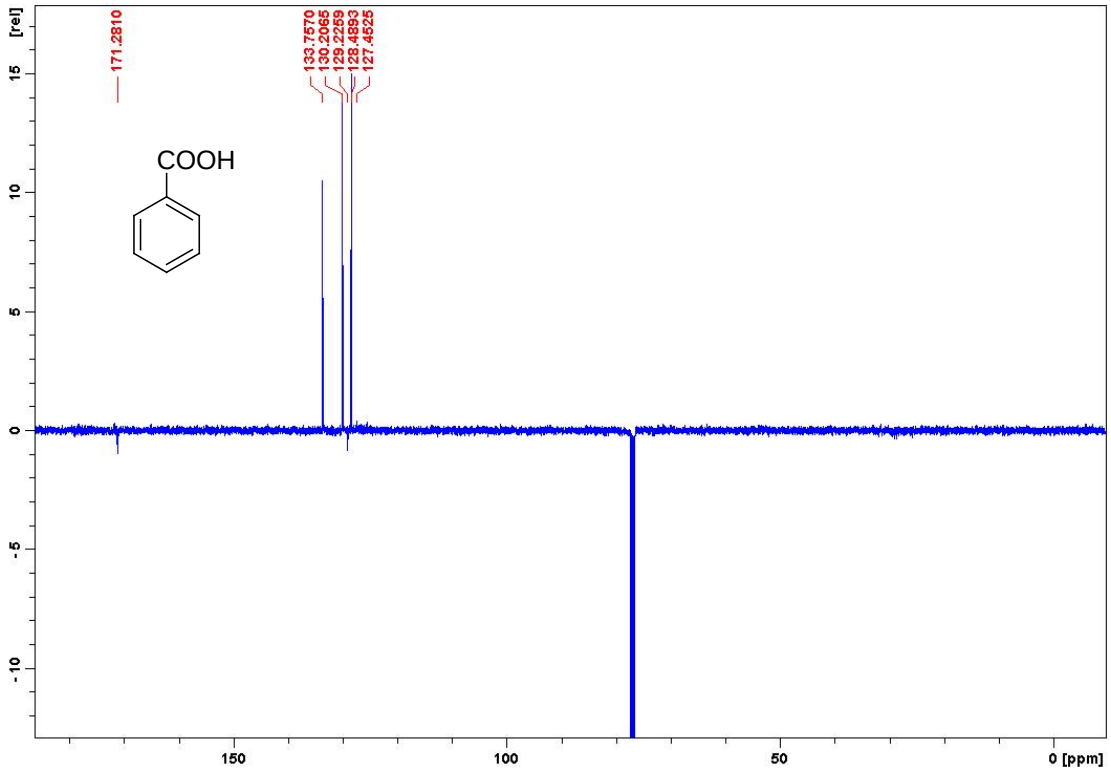

IR of **benzoic acid [30]**

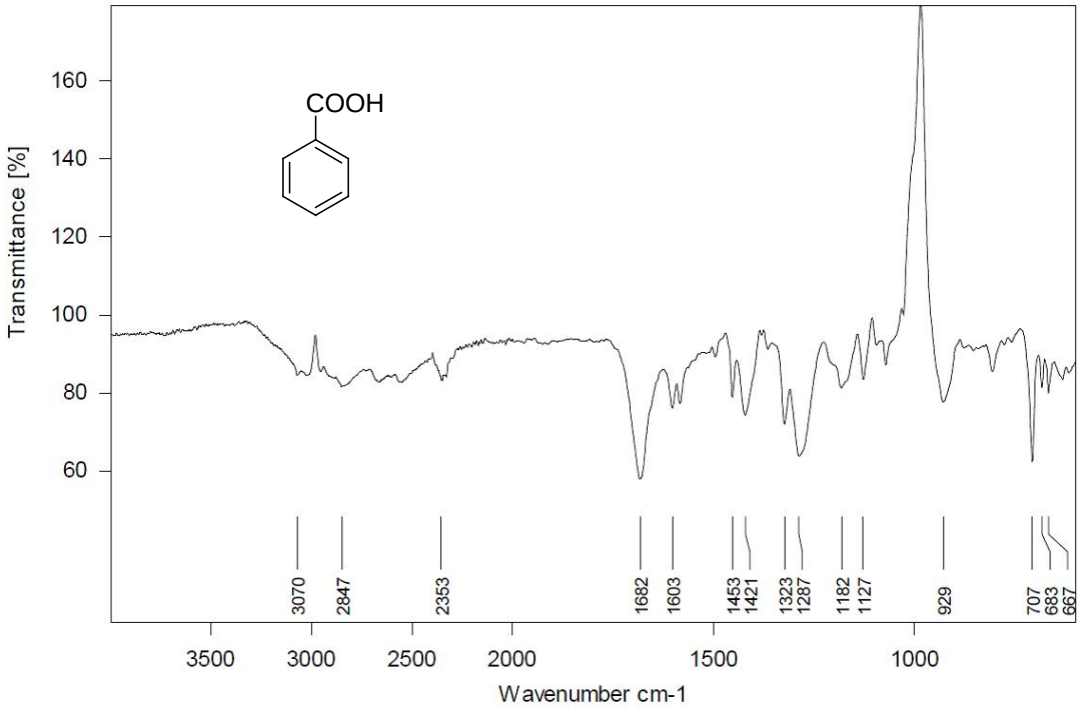

Curriculum Vitae

Name	**FEDERICA CAPPA MSC. BSC**

PERSONAL INFORMATIONS

E-mail	cappa.federica@gmail.com
Nationality	Italian
Date of birth	13.08.1984

EDUCATION AND TRAINING

Dates (from – to)	March 2010 – February2014 **University of Vienna, Faculty of Organic Chemistry**, Währingerstrasse 38, A-1190 Wien *http://www.univie.ac.at/*
Principal subjects	Organic Chemistry – Thesis title: "Synthesis of potentially bioactive compounds and tools for biological studies" -Synthetic organic chemistry, Purification methods, Interpretation of NMR, MS data.
Title of qualification awarded	**Doktorin der Naturwissenschaften (Dr. rer. nat.)**
Dates (from – to)	October 2006 – September 2009 **University of Pavia, Faculty of Physical Chemistry**, Viale Taramelli, 16 I-27100 PAVIA (ITALY) *Tel: 0382-987200 Fax: 0382-987575* *http://chifis.unipv.it/physchem.html*
Principal subjects	Thesis title: "Analysis of Roman Denarii of the 1st Century AD" Scanning Electron Microscopy (SEM) in combination with energy X-ray microanalysis (SEM/EDAX)" -Microscopy analysis, Analytical chemistry, Inorganic and Physical chemistry, Physical Techniques of investigation.
Title of qualification awarded	**Master degree of " Chemical Technologies "**

Dates (from – to)	September 2003 – July 2006
	University of Pavia, Faculty of Physical Chemistry, Viale Taramelli, 16 I-27100 PAVIA (ITALY) Tel: 0382-987200 Fax: 0382-987575 http://chifis.unipv.it/physchem.htm
Principal subjects	Thesis title: " Scanning Electron Microscopy Analysis associate with Microanalysis SEM-EDX of Natural and Synthetic Fibers "
	-Microscopy analysis, Analytical chemistry, Inorganic, Organic and Physical chemistry, Physical Techniques of investigation.
Title of qualification awarded	**Bachelor's Degree of " Chemical Technologies for Environment and Resources "**
Dates (from – to)	September 1998 – July 2003
	Istituto tecnico industriale statale (ITIS), G. Cardano Via Verdi , 9 -27100 PAVIA (ITALY)
Principal subjects	Chemistry: Analytical chemistry, Organic chemistry, Physical chemistry.
Title of qualification awarded	**High school diploma chemist**

ADDITIONAL COURSES/CONGRESSES

22.10.2008-24.10.2008	Synchrotron Radiation in Art and Archaeology. Barcelona, Spain.
15.02.2010-18.02.2010	VI Convegno Nazionale di Archeometria (AIAr). Pavia, Italy
01.09.2010-03.09.2010	Basisqualifizierung für EinsteigerInnen, Vienna
12.09.2010-17.09.2010	NMR-Summerschool „1D- and 2D-NMR Spectroscopy in Liquids" , Austria
20.05.2011-21.05.2011	VISOC, Vienna International Symposium on Organic Chemistry, Vienna
21.08.2011-26.08.2011	21st International Symposium on Glycoconjugates, Vienna
26.09.2011-29.09.2011	14. Österreichische Chemietage, Linz
16.02.2012	16. Kohlenhydratworkshop, Vienna

27.06.2012	Basics in Patent Law and Introduction to Patent Research
27.08.2012-30.08.2012	EuCheMS Chemistry Congress 2012, Prague

List of publications, posters and talks

Title of the poster: *"Scientific Investigations on Roman Coins of the Emperor Trajan (AD 98-117)"*. Marta Rodrigues, Federica Cappa, Manfred Schreiner, Paolo Ferloni, Martin Radtke, Uwe Reinholz, Bernhard Woytek, Michael Alram. Barcelona, 22-24 October 2008, Synchrotron Radiation in Art and Archaeology.

Title of the poster and talk: *"Physico-chemical measurements on Roman Silver Coins of the Nerva and Trajan consulates (AD 96 – 117)"*. Federica Cappa, Marta Rodrigues, Manfred Schreiner, Paolo Ferloni. Pavia, 15-18 February 2010, VI Convegno Nazionale di Archeometria (AIAr).

Title of publication: *"Further metallurgical analyses on silver coins of Trajan (AD 98–117)"*. Marta Rodrigues, Federica Cappa, Manfred Schreiner, Paolo Ferloni, Martin Radtke, Uwe Reinholz, Bernhard Woyteke and Michael Alram. *J. Anal. At. Spectrom.*, 2011, 26, 984-991

Title of talk: *"Towards the synthesis of potentially bioactive 3-Deoxy-sugars"*. Federica Cappa, Roman Lichtenecker, Walther Schmid. Vienna, 16. February 2012, 16. Kohlenhydratworkshop.

Title of poster: *"Towards the synthesis of specifically 13-C-ring labeled phenylalanine"*. Federica Cappa, Roman Lichtenecker, Christoph Lentsch,Walther Schmid. Prague, 27 – 30 August 2012, EuCheMS Chemistry Congress.